# Natural Product Reports

ROYAL SOCIETY
OF **CHEMISTRY**
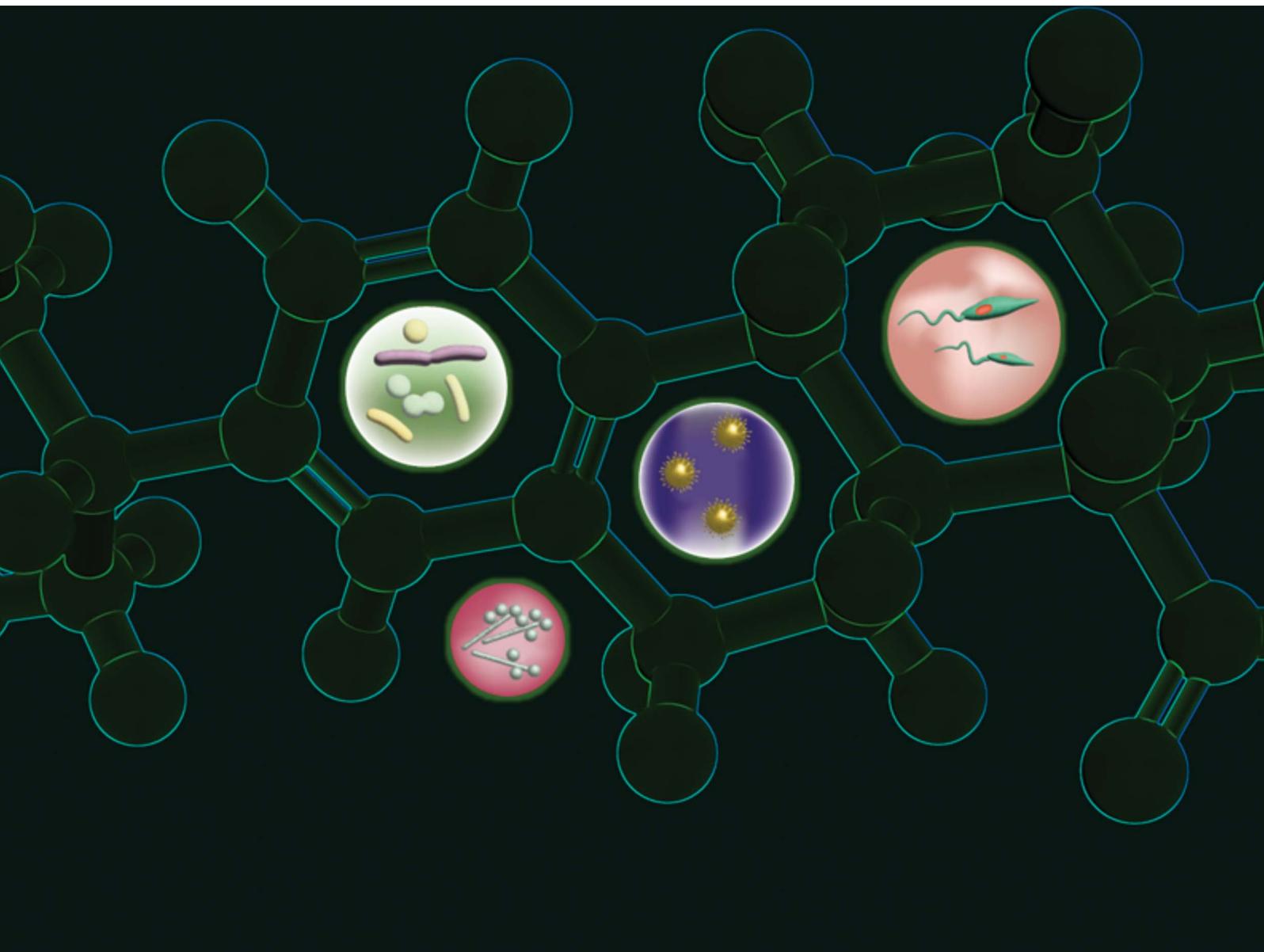
**REVIEW ARTICLE**
Vânia M. Moreira *et al.*
Bi- and tricyclic diterpenoids: landmarks from a decade
(2013–2023) in search of leads against infectious diseases

Check for updates

# Bi- and tricyclic diterpenoids: landmarks from a decade (2013–2023) in search of leads against infectious diseases

Olha Antoniuk, [abc] Ana Maranha, [bc] Jorge A. R. Salvador, [abc] Nuno Empadinhas [bc] and Vânia M. Moreira [*abcd]

Covering: 2013 to 2023

In an era where antimicrobial resistance severely threatens our ability to treat infections, the discovery of new drugs that belong to different chemical classes and/or bear original modes of action is urgently needed. In this case, diterpenoids comprise a productive field with a proven track record in providing new anti-infectives to tackle bacterial infections and malaria. This review highlights the potential of both naturally occurring and semi-synthetic bi- and tricyclic diterpenoids to become leads in search of new drugs to treat infections caused by bacteria, fungi, viruses and protozoan parasites. The literature from the last decade (2013–2023) is covered, focusing on naturally occurring and semi-synthetic bicyclic (labdanes and labdane-type) and tricyclic (all classes) diterpenoids, detailing their relevant biological activities in the context of infection, which are explained through structure–activity relationships.

*[a] Faculty of Pharmacy, University of Coimbra, Portugal. E-mail: vmoreira@ff.uc.pt*
*[b] Centre for Neuroscience and Cell Biology, University of Coimbra, Portugal*
*[c] Centre for Innovative Biomedicine and Biotechnology, University of Coimbra, Portugal*
*[d] Drug Research Program, Division of Pharmaceutical Chemistry and Technology, Faculty of Pharmacy, University of Helsinki, 00014 Helsinki, Finland*

# 1. Background and introduction

Naturally occurring and semi-synthetic bi- and tricyclic diterpenoids have been studied over the past years in the search for new leads to boost drug discovery. However, a comprehensive review of their potential interest in the field of infection has been missing. Among the bicyclic diterpenoids, both clerodanes[1] and halimanes[2] have been the topic of extensive reviews. However, in the case of labdanes, no literature review

1858 | *Nat. Prod. Rep.*, 2024, 41, 1858–1894

This journal is © The Royal Society of Chemistry 2024

has been published concerning their bioactivities since 2004.[3] Thus, prior reviews[4,5] are outdated, and a work dating 2010 (ref. 6) is solely dedicated to the chemistry of the labdane skeleton. A recently published work[7] accounts for naturally occurring antimicrobial diterpenoids but only covers the last 5 years and is devoid of semi-synthetic derivatives. Another review focused on natural diterpenes against tuberculosis,[8] and some reports are available on the bioactivities of the aromatic abietane dehydroabietic acid.[9,10] Herein, we cover the literature from the last decade (2013–2023) concerning naturally occurring and semi-synthetic bicyclic (labdanes and labdane-type) and tricyclic (all classes) diterpenoids, providing details of their relevant biological activities in the context of infections caused by bacteria, fungi, viruses and protozoan parasites. Furthermore, their anti-infective bioactivities are explained through structure–activity relationships (SARs), and directions for future research in this field are provided.

## 1.1 Infection and antimicrobial resistance

In 2019, infectious diseases were responsible for 24.2% of global mortality, resulting in 13.7 million deaths, with low-income countries bearing a disproportionate burden.[11,12] Lower respiratory tract infections and diarrhoeal diseases are ranked as the fourth and eighth leading causes of global mortality, respectively, while malaria, tuberculosis (TB), and HIV/AIDS remain among the top ten causes of mortality in low-income countries.[13] Among the deaths attributed to a single causative agent, bacterial infections account for 64.8% of the infectious disease mortality globally, followed by viruses (6.1%), fungi (2.4%), and parasites (1.0%).[14]

The discovery of antibiotics marked a significant milestone in modern medicine, shifting the burden of death from communicable to non-communicable diseases such as cardiovascular diseases, cancer, chronic respiratory diseases,

**Olha Antoniuk**

*Olha Antoniuk was born in Kyiv, Ukraine. She obtained her Pharmaceutical Sciences Degree in 2005 at the National University of Pharmacy (Ukraine) and her Master's Degree in Medicinal Chemistry and Biopharmaceutics in 2022 from the University of Lisbon, Portugal. She is currently a PhD student in Medicinal Chemistry at the University of Coimbra, and a member of the Centre for Neuroscience and Cell Biology (CIBB consortium). Her work is focused on the synthesis and development of antimicrobial drugs based on natural products (diterpenes).*

**Ana Maranha**

*Ana Maranha obtained her Biology Degree in 2008, her Masters in Molecular Cell Biology in 2010 and her PhD in Biosciences with a specialty in Microbiology in 2016, from the University of Coimbra (UC). Her PhD studies on the biosynthesis of mycobacterial polymethylated polysaccharides included a period at the University of Guelph, Canada. She is currently a researcher at the Molecular Microbiology and Microbiome Group at the Centre for Neuroscience and Cell Biology (CIBB consortium), and her work is focused on microbiome dysbiosis in chronic diseases, and natural products for antimicrobial drug discovery.*

**Jorge A. R. Salvador**

*Jorge Salvador has a PhD degree in Pharmacy-Pharmaceutical Chemistry, University of Coimbra (UC) in collaboration with the University of York, U.K. He spent one year as a Postdoctoral Student at the University of Sussex, UK, and has a postgraduation in Cancer Biology & Therapeutics-HICR from Harvard-Medical School, University of Harvard, USA. He has a position as a Full Professor at the Faculty of Pharmacy (UC) and is the group leader of the research group "Medicinal Chemistry & Drug Discovery" at the Centre for Innovative Biomedicine and Biotechnology (Portugal). His extensive work has been focused on studies of new anticancer compounds.*

**Nuno Empadinhas**

*Nuno Empadinhas holds a degree in Biology and a PhD in Biochemistry (2005) with specialty in Microbiology from the University of Coimbra (UC). He is a Principal Investigator at the Centre for Neuroscience and Cell Biology. He studied the physiology of microbes from extreme environments and elucidated the biogenesis of rare mycobacterial polysaccharides, discovering microbial genes/enzymes that were founding members of 17 new families in the IUBMB database. His transdisciplinary research has attracted ~2M€ funding and was awarded the Mizutani Glycoscience Grant (2012), Mantero Belard Award (2016), Thomé Villar Award (2017), Seed Project UC Award (2020), and Pfizer Prize for Basic Science (2023).*

This journal is © The Royal Society of Chemistry 2024

*Nat. Prod. Rep.*, 2024, **41**, 1858–1894 | 1859

diabetes, and neurological disorders. However, the increasing antimicrobial resistance (AMR) now threatens these advancements. With an estimated 4.95 million AMR-related deaths in 2019 alone, the urgency for new antimicrobials is critical.[15] The intrinsic or acquired resistance of certain pathogens, such as carbapenem-resistant *Acinetobacter* and Enterobacterales (CRE), methicillin-resistant *Staphylococcus aureus* (MRSA), drug-resistant *Mycobacterium tuberculosis* (DR-TB), and *Candida auris*, undermines conventional treatment approaches.[15,16] Presently, over 20% of bacterial infections are caused by drug-resistant strains, including pan-drug-resistant Gram-negative bacteria, which are non-susceptible to all agents in all antimicrobial categories and have been reported in over twenty countries worldwide.[17] In 2019, the average resistance to twelve priority antibiotic–bacterium combinations reached 30% in G20 countries and 20% in 17 Organization for Economic Co-operation and Development (OECD) countries, marking a 3% increase since 2009. Even with a deceleration trend, resistance to last-line antibiotics such as carbapenems can increase by 3.2 times, by 2035, when compared to 2005 levels.[17]

In 2019, eight pathogens including *Escherichia coli*, *Staphylococcus aureus*, *Klebsiella pneumoniae*, *Streptococcus pneumoniae*, *Acinetobacter baumannii*, *Pseudomonas aeruginosa*, *Mycobacterium tuberculosis* (Mtb) *and Enterococcus faecium* were responsible for 80% of AMR-associated deaths globally. In all cases except Mtb, over 60% of the deaths were linked to the AMR variant of the pathogen.[14,15] These organisms are prioritised on the WHO Priority Pathogens List (PPL) to guide the research and development of urgently needed effective drugs.[18] Additionally, the WHO has created the Fungal Priority Pathogen List (FPPL) to address the increasing threat of invasive fungal diseases. The critical pathogens in this list include *Cryptococcus neoformans*, *Candida auris*, *Aspergillus fumigatus*, and *Candida albicans*.[19,20] The emergence of drug resistance in neglected tropical diseases, such as human African trypanosomiasis[21] and leishmaniasis,[22] caused by protozoans also poses a significant global health challenge. These diseases disproportionately affect vulnerable populations, and the limited discovery of new agents exacerbates the problem.[23] Moreover, the spread of drug resistance to most of the available antimalarial drugs is also a major concern.[24]

Many pathogens can form biofilms, which are microbial communities that adhere to surfaces and are encased in a self-generated matrix.[25] Biofilms are a major virulence factor in various human infections, especially those linked to medical devices and chronic conditions such as chronic wounds and cystic fibrosis.[26] They shield microorganisms from environmental stresses, antimicrobials, and the immune system, making them highly resilient and hard to eliminate. Biofilm-related infections show inherent antibiotic tolerance, leading to additional treatment challenges and therapeutic failures. Their presence also promotes resistance evolution, as observed in pathogens such as *Staphylococcus aureus*, *Pseudomonas aeruginosa*, and nontuberculous mycobacteria (NTM), notably *Mycobacterium abscessus* in cystic fibrosis patients, as well as in Mtb in tuberculosis, where biofilms interfere with the efficacy of antibiotics.[27–29] AMR poses a risk not only to infectious disease treatment but also to the safety and efficacy of surgical procedures, immunosuppressive chemotherapy, sustainable food production, and the environment.[30] Factors such as antibiotic misuse, globalisation, natural disasters, and geopolitical instability contribute to AMR proliferation.[30] However, despite the dynamic preclinical research, the clinical pipeline for novel antimicrobials remains insufficient, primarily comprised of derivatives of existing antibiotic classes, with few new compounds entering the pipeline.[31,32] The need to safekeep new antibiotics for use in the case of a major sanitary crisis further detracts large pharmaceutical companies from antibiotic development, leaving academic institutions and smaller companies to bear the R&D burden.[33] However, despite new policy initiatives to improve the pipeline *via* push and pull incentives, overall it is believed that at present there is still insufficient targeted support and coordination for academia and small- and medium-sized companies, with drug discovery activities struggling to supply the necessary discovery and preclinical programmes.[33]

## 1.2 The impact of terpenoids in the discovery of novel anti-infective drugs

The historical value of natural products (NPs) and their derivatives as sources of new drugs is indisputable, as documented in the comprehensive work by Newman and Cragg.[34] In particular, the area of anti-infectives has remained totally dependent on NPs and their structures. About 48% of the total number of antibacterial drugs approved between 1981 and 2019 was either a NP or a NP derivative, and 22.2% was totally synthetic but based on the well-known quinolone scaffold. The pleuromutilins (**1–2**) (Fig. 1) and the resin acids (**3–5**) (Fig. 2) are example diterpenoids used for their antibacterial properties, as discussed in Section 2.4.

Only two antifungal drugs were approved in the same period, both NP-based, reflecting the dearth of research into this topic over the past few decades. Notably, one of the most recent

**Vânia M. Moreira**

*Vânia M. Moreira holds a PhD in Pharmacy-Pharmaceutical Chemistry, University of Coimbra (UC), in collaboration with the University of Maryland, USA. She holds the "Title of Docent" (*Dosentti*) in Medicinal Chemistry, University of Helsinki, Finland (2015), and is a Fellow of the Higher Education Academy (FHEA), UK (2018). She is an Associate Professor at the Faculty of Pharmacy, UC. Her work devoted to exploring the medicinal chemistry of terpenoid-based compounds has attracted funding from a panel of international sources, and she has received several distinctions and awards throughout her career, including a highlight by the EFMC as a "New Talent Europe 2016".*
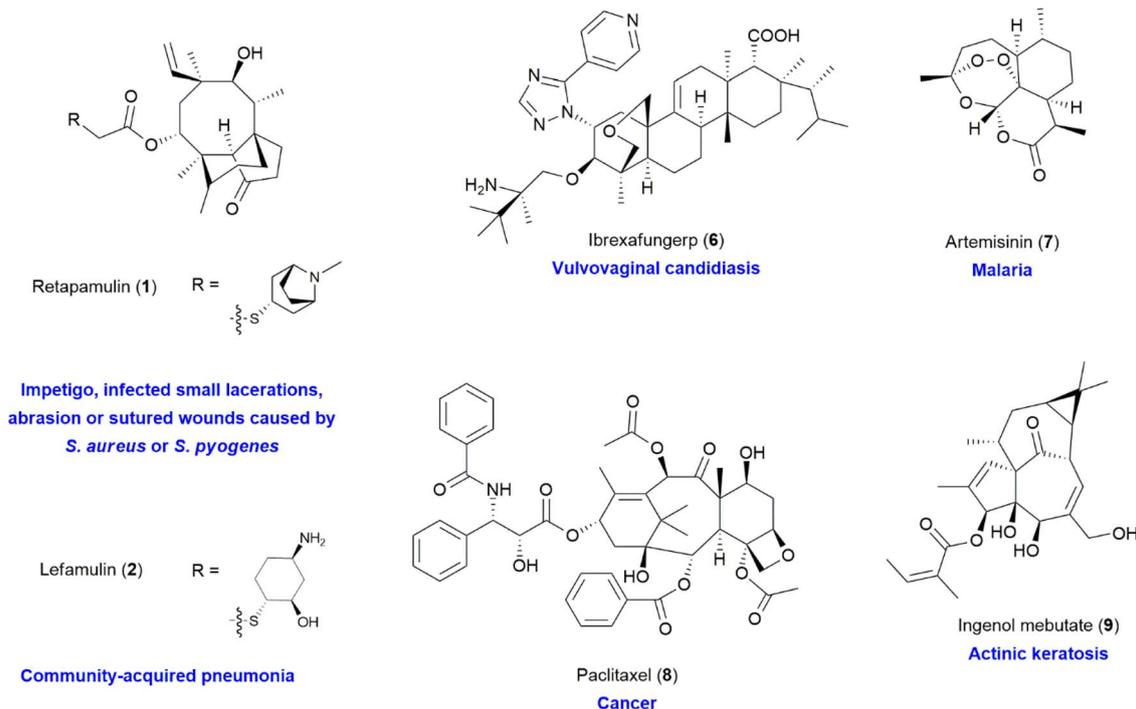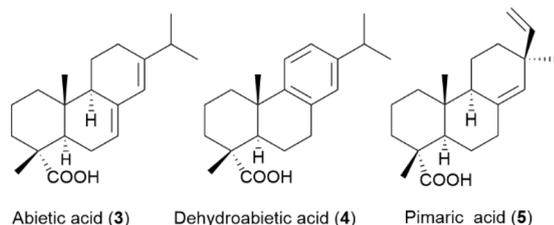
**Fig. 1** Terpenoids currently in clinics.



**Fig. 2** Main resin acids.

approvals in this field is the triterpene ibrexafungerp (**6**) (Fig. 1), for both the treatment and reduction of the incidence of vulvovaginal candidiasis.[35] Ibrexafungerp (**6**) is a glucan synthase inhibitor that is a derivative of the NP echinocandin enfumafungin, with a better bioavailability profile, which makes it suitable for oral administration. This compound interacts with the enzyme at a site that is distinct but partially shared with that of the echinocandins. Notably, ibrexafungerp (**6**) is active against several Candida strains including the multi-drug resistant *Candida auris*, which causes severe illness and spreads easily among patients in a nosocomial environment, as well as against *Candida glabrata* and *Aspergillus* species.[36] Finally, artemisinin (**7**) (Fig. 1), a sesquiterpene lactone isolated from *Artemisia annua*, with an unusual endoperoxide bridge, is still an important antimalarial agent to date, especially if used in combination regimens to treat drug-resistant malaria, and for helminth infections.[37] Its modes of action have been proposed to involve not only the parasite haemoglobin-digestion processes but also the mitochondria and the sarcoplasmic/endoplasmic reticulum $Ca^{2+}$-ATPase (SERCA).

## 2. The diterpenoids

### 2.1 Introduction to diterpenoids

Diterpenoids (C20), which are composed of four isoprene units, are members of a large super-family of >12 000 natural products, originating from (*E,E,E*)-geranylgeranyl diphosphate (GGPP) (Fig. 3A).[6,38] In plant plastids, the methylerythritol phosphate (MEP)-dependent pathway generates GGPP from isopentenyl diphosphate (IPP) and dimethylallyl diphosphate (DMAPP). In contrast, fungal diterpenoids are usually synthesised *via* the mevalonate (MVA) pathway.[39,40] Both plants and bacteria can use either pathway, but in plants, these pathways exist with a clear spatial separation, given that the MVA pathway operates only in the cytosol and peroxisomes.[38–41] Although the subcellular compartmentalization of the MVA and MEP pathways allows them to operate independently, metabolic exchange can occur between these two pathways.[39,40]

Diterpenoid biosynthesis can be initiated by two different types of reactions, both involving carbocationic cascades but triggered in different ways. The reactive allylic bond in GGPP invariably undergoes lysis/ionisation *via* a carbocationic cascade of reactions mediated by class I diterpene synthases (EC 4.2.3.*x*). However, this can be preceded by a protonation-initiated (bi)cyclisation reaction, catalysed by class II diterpene cyclases (EC 5.5.1.*x*), which leaves the allylic diphosphate ester bond of GGPP intact for the subsequent action of class I diterpene synthases (Fig. 3A).[38] The formed labda-13-en-8-yl cation intermediate (**I–IV**) can lead to four different isomers, with a fixed *trans* configuration across the decalin ring (Fig. 3A). The isomers are named "normal" or antipodal/enantiomeric "*ent*", depending on their absolute configuration compared to

This journal is © The Royal Society of Chemistry 2024

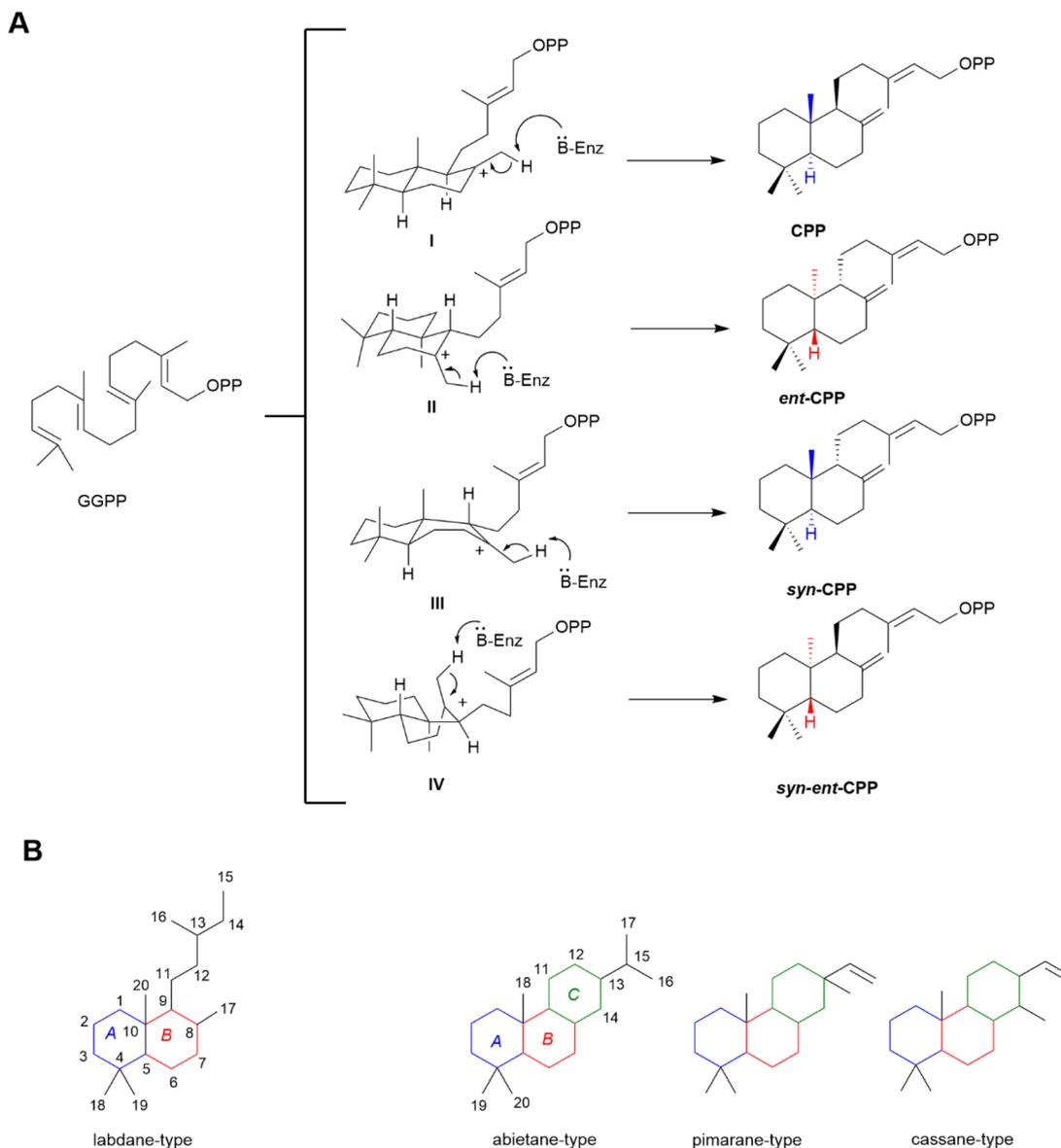*Nat. Prod. Rep.*, 2024, **41**, 1858–1894 | **1861**

Fig. 3  (A) Bicyclisation of GGPP to copalyl diphosphate (CPP) mediated by class II diterpene synthases. This reaction generally precedes that mediated by class I diterpene synthases. OPP = diphosphate group. (B) General structures of the bicyclic (labdane) and tricyclic (abietane, pimarane, and cassane) diterpenoids discussed in this work.

the stereochemistry of the analogous A/B rings in cholesterol, namely in copalyl diphosphate (CPP), *ent*-CPP, *syn*-CPP and *syn-ent*-CPP. The most observed isomers are *ent*-CPP and CPP, whereas the production of *syn-ent*-CPP has not been observed, with the *syn-ent* stereochemistry only recognized from plants of the *Calceolaria* genus.[6,42]

The most basic structures in the labdane-related diterpenoid super-family are the bicyclic labdane, clerodane and halimadane families formed by relevant class II diterpene cyclases, with relevant class I synthases presumably simply removing the diphosphate without catalysing cyclisation (Fig. 3B). The overwhelming majority of further cyclised labdane-related diterpenoids, including the tricyclic diterpenoids abietanes, and pimaranes, are derived from the action of relevant class I

diterpene synthases on the various stereoisomers of CPP (Fig. 3B).[6,38]

## 2.2 Structure and occurrence of the labdane-type diterpenoids

The labdane diterpenoids are secondary metabolites widely distributed in different parts of plants including their roots, barks, tubers, seeds and leaves, as well as in tissues of fungi, bacteria, insects and marine organisms.[5,43] A plethora of plant families can be listed as sources of labdanes including Asteraceae, Labiatae, Cistaceae, Pinaceae, Cupressaceae, Taxodiaceae, Acanthaceae, Annonaceae, Caprifoliaceae, Solanaceae, Apocynaceae, Verbenaceae and Zingiberaceae. Another important source of labdanes are coniferous plants.[5]

**1862** | *Nat. Prod. Rep.*, 2024, **41**, 1858–1894

This journal is © The Royal Society of Chemistry 2024

The scientific literature concerning diterpenoids and their natural terrestrial sources was regularly reviewed by Hanson from 1996 to 2019.† The general skeleton of labdane-type diterpenoids is depicted in Fig. 3B, which is comprised of a decalin core and a side chain at C9, consisting of six carbons and can be open or closed. Another common modification involves a furan ring on the side chain. Labdanes occur in nature in both the normal and antipodal series.[5]

### 2.3 Structure and occurrence of the tricyclic diterpenoids

Conifer resin is an abundant source of abietanes, as known as resin acids, among which the main compounds are abietic (**3**), dehydroabietic (**4**) and pimaric (**5**) acids (Fig. 2).[44] Rosin, *i.e.*, the solid portion of resin after the evaporation of volatiles, and its derivatives, have been widely used for industrial purposes in glues, inks, varnishes, adhesive plasters, soldering glues and sealing waxes.[44,45] Rosin has also been used as a glazing agent in medicines and chewing gum. Besides conifer resin, both abietanes and other tricyclic diterpenoids can be found in plant families including Lamiaceae, particularly in the genus *Salvia*, and in fungi, bacteria and marine organisms.[10,45] The general skeleton of the different classes of tricyclic diterpenoids is depicted in Fig. 3B. Abietanes bear an isopropyl side chain at C13, whereas that of the pimaranes and cassanes is unsaturated. The location of the ring C methyl substituent varies in the pimarane and cassane series.[46]

### 2.4 Diterpenoids in clinics

Diterpenoids have historically provided important drugs for the treatment of human illnesses. Among them, the diterpene taxane paclitaxel or Taxol® (**8**) (Fig. 1), which is present in the bark of the Pacific yew, is the best known, having widespread use as a broad-spectrum anticancer drug.[47] Its four-membered oxetane ring and complex ester side chain are both essential for its antitumoral activity, which occurs through inhibition of microtubule polymerisation, causing cell cycle arrest at the G2/M phase, and finally cell death.[47] Paclitaxel (**8**) is used to treat a variety of cancers including ovarian, lung, breast, head and neck, and melanoma.[47] Ingenol mebutate (Picato™) (**9**) is another relevant diterpenoid derivative that was approved for the treatment of actinic keratosis (a premalignant skin condition) in 2012, but was later discontinued.[48]

Regarding anti-infectives, the pleuromutilins (**1**–**2**) (Fig. 1) and resin acids (**3**–**5**) (Fig. 2) are significant examples.[49–51] The pleuromutilins have been known since the 1950s, when the compound that names the class, *i.e.*, pleuromutilin, was isolated from the mushroom *Pleurotus mutilus*.[49] The pleuromutilin scaffold is comprised of a unique annelation of five-, six-, and eight-membered rings and eight stable chiral centres, as well as a glycolic ester moiety as a side chain. The pleuromutilins inhibit bacterial protein synthesis by binding to the 50S ribosomal subunit at the peptidyl transferase centre, preventing the correct positioning of transfer ribonucleic acid

(tRNA) for peptide transfer and new bond formation.[49] Due to this mode of action, they exhibit a broad spectrum of action against Gram-positive, Gram-negative and atypical respiratory pathogens, and more importantly low potential for the development of resistance.[49] Topical retapamulin (**1**) (Fig. 1) was the first to be approved for the treatment of impetigo, infected small lacerations, abrasion or sutured wounds caused by *Staphylococcus aureus* or *Streptococcus pyogenes*.[49] In 2019, the FDA approved lefamulin (**2**) (Fig. 1) for the treatment of adults with community-acquired pneumonia.[52]

The antimicrobial properties of the tricyclic abietane-type diterpenoids known as resin acids have been known for several decades, especially in countries in Northern Europe such as Finland, where home-made spruce resin salve has long been used as traditional folk medicine for wound-healing.[51,53] Research has shown that the antimicrobial and wound-healing properties of the resin salve are due to the presence of resin acids, which comprise about 90–95% of its solid portion, with the most significant being abietic (**3**), dehydroabietic (**4**) and pimaric (**5**) acids.[44] At present, Norway spruce (*Picea abies*) resin salve is commercially available as Abilar® for the treatment of a plethora of conditions including wounds, scratches, bruises and abrasions, bite and puncture wounds, paronychia, burn injuries, chicken pox-related skin infections and impetigo (where *Staphylococcus aureus* is an important pathogen), infected and surgical wounds, and skin cracks.[51] Moreover, abietic acid (**3**) is an important component of dental filling materials such as Nishika Plast Seal Quick®, which is commercially available in Japan.[50]

## 3. Anti-infective labdane-type diterpenoids

The labdane-type diterpenoids portrayed in the literature over the past decade with significant anti-infective activity are detailed in the following sections. The structures of both naturally occurring and semi-synthetic compounds are depicted in Fig. 4–11, with that from natural sources categorised according to their side chain at C9. Section 3.6 is devoted to labdane-type diterpenoids produced by biotransformation. The data for all reported sources and biological activities for each compound are summarised in Tables 1 and 2. For consistency, we include values for the different reported biological activities only up to roughly 160–200 μM. At concentrations above these values, the compounds are generally too toxic or poorly soluble.

### 3.1 Naturally occurring labdane-type diterpenoids with an acyclic side chain at C9

The antibacterial activity of the labdane alcohol manool (**10**) (Fig. 4), which is present in *Salvia* species, has been extensively documented (Table 1, entry 1). Manool (**10**) is active against streptococci,[54] and notably against enterococci, with minimum inhibitory concentration (MIC) values ranging from 4 to 32 μg mL$^{-1}$.[55] Manool (**10**) was reported to inhibit both ATP production mediated by ATP synthase and ATP hydrolysis. Its ability to bind to this enzyme was further studied by docking and molecular dynamics simulations, which revealed that **10** forms lipophilic

---

† All the reviews on diterpenoids by James R. Hanson (1996–2019) are available from the *Nat. Prod. Rep.* online database.

This journal is © The Royal Society of Chemistry 2024

*Nat. Prod. Rep.*, 2024, **41**, 1858–1894 | **1863**

**Table 1** Biological activities of the naturally occurring labdane-type diterpenoids[a]

| Entry | Compound | Source | Reported biological activity[a] | Ref. |
|---|---|---|---|---|
| 1 | Manool (**10**) | *Sabvia sclarea*<br>*Sabvia tingitana* | MIC (*Enterococcus faecium* MB 2[b], *Enterococcus gallinarum*) = 4 µg mL⁻¹ (14 µM)<br>MIC (*Streptococcus agalactiae*, *Streptococcus dysgalactiae*) = 6.25 µg mL⁻¹ (22 µM)<br>MIC (*Enterococcus faecium* MB 152[c], *Enterococcus avium*) = 8 µg mL⁻¹ (28 µM)<br>MIC (*Enterococcus faecalis* MB 1[c], *Enterococcus casseliflavus*, *Enterococcus durans*) = 16 µg mL⁻¹ (55 µM)<br>MIC (*Enterococcus faecalis* MB 76[d], *) = 32 µg mL⁻¹ (110 µM) | 54–56 |
| 2 | Sclareol (**11**) | | MIC (*Staphylococcus aureus* MB 18[e], *Staphylococcus aureus* MB 188[f], *Staphylococcus saprophyticus* MB 41*,<br>*Staphylococcus capitis* MB 71*, *Staphylococcus warneri* MB 74[e], *Staphylococcus lugdunensis* MB 96*, *Staphylococcus hominis* MB 124[e], *Enterococcus faecalis* MB 1*, *Enterococcus faecium* MB 2[b], *Enterococcus durans*) = 32 µg mL⁻¹ (104 µM)<br>MIC (*Staphylococcus epidermidis* MB 165[d], *Staphylococcus epidermidis* MB 169[d], *Staphylococcus simulans* MB 94*,<br>*Staphylococcus haemolyticus* MB 115[e], *Enterococcus faecalis* MB 76[b], *Enterococcus faecium* MB 152[c], *Enterococcus avium* MB 119*, *Enterococcus casseliflavus* MB 159*, *Enterococcus gallinarum* MB 111*) = 64 µg mL⁻¹ (208 µM)<br>MIC (*Candida albicans, Candida auris, Candida parapsilosis*) = 50 µg mL⁻¹ (162 µM) | 55–57 |
| 3 | (**12**) | *Sabvia tingitana* | MIC (*Enterococcus faecalis* MB 1*, *Enterococcus avium* MB 119*, *Enterococcus gallinarum* MB 111*) = 32 µg mL⁻¹ (99 µM)<br>MIC (*Staphylococcus warneri* MB 74[e], *Staphylococcus lugdunensis* MB 96*, *Enterococcus faecalis* MB 76*, *Enterococcus faecium* MB 2[b], *Enterococcus faecium* MB 152[c], *Enterococcus casseliflavus* MB 159*, *Enterococcus durans* MB 113*) = 64 µg mL⁻¹ (197 µM) | 55 |
| 4 | Salvic acid (**13**) | *Eupatorium salvia* Colla | MIC (*Staphylococcus aureus*, *Bacillus cereus*) = 50 µg mL⁻¹ (155 µM) | 58 |
| 5 | *ent*-Copalic acid (**14**) | *Kaempferia pulchra* | MIC (*Streptococcus agalactiae*, *Streptococcus dysgalactiae*) = 1.56 µg mL⁻¹ (5.1 µM)<br>MIC (*Staphylococcus epidermidis*, *Staphylococcus aureus*) = 6.25 µg mL⁻¹ (21 µM)<br>MIC (*Trichophyton rubrum, Microsporum gypseum*) = 50 µg mL⁻¹ (164 µM) | 54, 59 and 60 |
| 6 | (**15**) | *Copaifera reticulata* | IC₅₀ (*Enterococcus faecium*) = 9.3 µg mL⁻¹ (28 µM)<br>IC₅₀ (MRSA*) = 10.7 µg mL⁻¹ (32 µM)<br>IC₅₀ (*Trichophyton mentagrophytes*) = 38 µg mL⁻¹ (113 µM)<br>IC₅₀ (*Trichophyton rubrum*) = 44.7 µg mL⁻¹ (133 µM) | 61 |
| 7 | (**16**) | | IC₅₀ (*Enterococcus faecium*) = 1.6 µg mL⁻¹ (5.3 µM)<br>IC₅₀ (MRSA*) = 2.5 µg mL⁻¹ (8.2 µM) | |
| 8 | (**17**) | *Caesalpinia decapetala* | MIC (MRSA*) = 12 µg mL⁻¹ (36 µM) | 62 |
| 9 | *ent*-Agathic acid (**18**) | *Copaifera reticulata* | IC₅₀ (*Trichophyton mentagrophytes*) = 30.2 µg mL⁻¹ (90 µM)<br>IC₅₀ (*Trichophyton rubrum*) = 41.7 µg mL⁻¹ (125 µM) | 61 |
| 10 | (**19**) | *Copaifera oleoresins* | MIC (*Candida tropicalis*) = 9.3 µg mL⁻¹<br>MIC (*Candida albicans*) = 74.3 µg mL⁻¹ | 63 |
| 11 | Anticopalic acid (**20**) | *Kaempferia elegans*<br>*Pinus pumila* | MIC (*Bacillus cereus*) = 3.13 µg mL⁻¹ (10 µM)<br>MIC (*Staphylococcus aureus*, *Enterococcus faecalis*) = 12.5 µg mL⁻¹ (41 µM)<br>MIC₉₀ (*Enterococcus faecalis*) = 50 µM | 64 and 65 |
| 12 | Anticopalol (**21**) | *Kaempferia elegans*<br>*Kaempferia pulchra* | MIC (*Enterococcus faecalis*, *Bacillus cereus*) = 6.25 µg mL⁻¹ (22 µM)<br>MIC (*Staphylococcus aureus*) = 12.5 µg mL⁻¹ (43 µM) | 64 |
| 13 | (**22**) | | MIC (*Bacillus cereus*) = 6.25 µg mL⁻¹ (21 µM) | 66 |
| 14 | Cuceolatin A (**23**) | *Cunninghamia lanceolata* | MIC (*Bacillus subtilis*) = 8.7 µM<br>MIC (*Staphylococcus aureus*) = 10.3 µM | |
| 15 | Cuceolatin B (**24**) | | MIC (*Staphylococcus aureus*) = 11.7 µM<br>MIC (*Bacillus subtilis*) = 18.6 µM | |

1864 | *Nat. Prod. Rep.*, 2024, **41**, 1858–1894

This journal is © The Royal Society of Chemistry 2024

Table 1 (Contd.)

| Entry | Compound | Source | Reported biological activity[a] | Ref. |
|---|---|---|---|---|
| 16 | Cuceolatin C (25) | | MIC (Bacillus subtilis*) = 24.6 μM | |
| 17 | (26) | | MIC (Staphylococcus aureus*) = 24.7 μM<br>MIC (Staphylococcus aureus*) = 5.9 μM | 67 |
| 18 | Pahangensin B (27) | Alpinia pahangensis | MIC (Bacillus subtilis*) = 12.3 μM<br>MIC (Bacillus cereus*) = 52.1 μg mL$^{-1}$ (157 μM) | 68 |
| 19 | (28) | Elytropappus rhinocerotis | MIC (Brevibacterium agri*) = 58 μg mL$^{-1}$ (179 μM) | 69 |
| 20 | Vitexolin B (29) | Vitex vestita | MIC (Bacillus cereus*$^f$) = 25–50 μM | 70 |
| 21 | (30) | Talaromyces scorteus | MIC (Vibrio parahaemolyticus**) = 8 μg mL$^{-1}$ (23 μM) | 71 |
| 22 | (31) | Leucas stelligera | IC$_{50}$ (Mycobacterium tuberculosis) = 5.95 μg mL$^{-1}$ (19 μM) | |
| 23 | (32) | | IC$_{50}$ (Mycobacterium tuberculosis) = 9.8 μg mL$^{-1}$ (30 μM) | 72 and 73 |
| 24 | (33) | Alpinia nigra<br>Etlingera coccinea<br>Etlingera sessilanthera | MIC (Bacillus subtilis*) = 4 μg mL$^{-1}$ (13 μM)<br>MIC (Staphylococcus aureus*$^f$, Bacillus cereus*) = 4–12.5 μg mL$^{-1}$ (13–41 μM)<br>MIC (Salmonella paratyphi**, Yersinia enterocolitica**) = 12.5 μg mL$^{-1}$ (41 μM) | |
| 25 | (34) | Alpinia nigra | MIC (Listeria monocytogenes *, Escherichia coli**) = 25 μg mL$^{-1}$ (83 μM)<br>MIC (Staphylococcus aureus*, Yersinia enterocolitica**) = 3.38 μg mL$^{-1}$ (11 μM)<br>MIC (Bacillus cereus*, Salmonella paratyphi**, Escherichia coli**) = 6.25 μg mL$^{-1}$ (20 μM)<br>MIC (Listeria monocytogenes*) = 12.5 μg mL$^{-1}$ (39 μM) | 72 |
| 26 | (35) | Salvia leriifolia | MIC (Staphylococcus aureus*) = 157 μM | 74 |
| 27 | (36) | Piliostigma thonningii | IC$_{50}$ (Trypanosoma brucei$^h$) = 3.84 μM<br>IC$_{50}$ (Leishmania donovani$^g$) = 7.82 μM | 75 |
| 28 | (37) | Psiadia arguta | IC$_{50}$ (Trypanosoma brucei$^h$) = 3.42 μM | |
| 29 | (38) | | IC$_{50}$ (Plasmodium falciparum) = 29.1 μM | 76 |
| 30 | (39) | | IC$_{50}$ (Plasmodium falciparum) = 33.2 μM | |
| 31 | (40) | | IC$_{50}$ (Plasmodium falciparum) = 36.6 μM | |
| 32 | (41) | | IC$_{50}$ (Plasmodium falciparum) = 22.2 μM | |
| 33 | Stachyonic acid A (42) | Basilicum polystachyon | IC$_{50}$ (WNV) = 1.2 μM<br>IC$_{50}$ (DENV) = 1.4 μM<br>IC$_{50}$ (H1N1) = 4.1 μM<br>IC$_{50}$ (H3N2) = 18 μM | 77 and 78 |
| 34 | Forspensin A (43) | Forsythia suspensa | EC$_{50}$ (RSV) = 14.6 μM<br>IC$_{50}$ (H1N1) = 21.8 μM | 79 |
| 35 | Forspensin B (44) | | EC$_{50}$ (RSV) = 15.4 μM<br>IC$_{50}$ (H1N1) = 23.2 μM | |
| 36 | Forspensin C (45) | | EC$_{50}$ (RSV) = 13.7 μM<br>IC$_{50}$ (H1N1) = 22.9 μM | |
| 37 | Forspensin D (46) | | EC$_{50}$ (RSV) = 11.8 μM<br>IC$_{50}$ (H1N1) = 27.4 μM | |
| 38 | Forspensin E (47) | | EC$_{50}$ (RSV) = 10.5 μM<br>IC$_{50}$ (H1N1) = 24.6 μM | |
| 39 | Forsyshiyanin A (48) | | EC$_{50}$ (RSV) = 10.5 μM<br>IC$_{50}$ (H1N1) = 18.4 μM | 80 |

This journal is © The Royal Society of Chemistry 2024

Nat. Prod. Rep., 2024, 41, 1858–1894 | 1865

**Table 1** (Contd.)

| Entry | Compound | Source | Reported biological activity[a] | Ref. |
|---|---|---|---|---|
| 40 | Forsyshiyanin B (49) | | $EC_{50}$ (RSV) = 13.2 µM<br>$IC_{50}$ (H1N1) = 26.2 µM | 61, 81–83, 84 and 85 |
| 41 | (50) | | $EC_{50}$ (RSV) = 14.4 µM<br>$IC_{50}$ (H1N1) = 19.9 µM | |
| 42 | (51) | | $EC_{50}$ (RSV) = 12.7 µM<br>$IC_{50}$ (H1N1) = 25.7 µM | |
| 43 | (52) | | $EC_{50}$ (RSV) = 10.5 µM<br>$IC_{50}$ (H1N1) = 24.1 µM | |
| 44 | (53) | | $EC_{50}$ (RSV) = 11.8 µM<br>$IC_{50}$ (H1N1) = 24.9 µM | |
| 45 | (54) | | $EC_{50}$ (RSV) = 12.0 µM<br>$IC_{50}$ (H1N1) = 23.5 µM | |
| 46 | (55) | | $EC_{50}$ (RSV) = 11.1 µM<br>$IC_{50}$ (H1N1) = 18.6 µM | |
| 47 | ent-Polyalthic acid (57) | Copaifera reticulata<br>Copaifera lucens<br>Copaifera duckei<br>Copaifera trapezifolia | MIC (Peptostreptococcus micros[i],*, Porphyromonas gingivalis**) = 6.25 µg mL$^{-1}$ (20 µM)<br>MIC (Lacticaseibacillus casei[i],*) = 12.5 µg mL$^{-1}$ (40 µM)<br>MIC (Streptococcus sobrinus*, Streptococcus mitis*, Streptococcus mutans*, Streptococcus salivarius[i],*, Streptococcus sanguinis*, Enterococcus faecalis*, Aggregatibacter actinomycetemcomitans**, Fusobacterium nucleatum**, Actinomyces naeslundii*) = 25 µg mL$^{-1}$ (80 µM)<br>MIC (Streptococcus salivarius*, Streptococcus sanguinis[i],*, Lacticaseibacillus casei*, Porphyromonas gingivalis[i],*, Fusobacterium nucleatum[i],**, Prevotella nigrescens**, Bacteroides fragilis**) = 50 µg mL$^{-1}$ (158 µM)<br>$IC_{50}$ (Enterococcus faecium*) = 8.5 µM<br>$IC_{50}$ (MRSA*) = 8.9 µM<br>$IC_{50}$ (Trichophyton mentagrophytes) = 4.3 µg mL$^{-1}$ (14 µM)<br>$IC_{50}$ (Trichophyton rubrum) = 6.8 µg mL$^{-1}$ (22 µM)<br>MIC (Candida glabrata) = 12.5 µg mL$^{-1}$ (40 µM)<br>MFC (Candida glabrata) = 25 µg mL$^{-1}$ (79 µM)<br>$IC_{50}$ (Trypanosoma brucei[b]) = 3.87 µg mL$^{-1}$ (12 µM)<br>$IC_{50}$ (Leishmania donovani[h]) = 8.68 µg mL$^{-1}$ (28 µM)<br>$IC_{50}$ (Toxoplasma gondii[i]) = 64 µg mL$^{-1}$ (202 µM) | 85 |
| 48 | Coronarin E (58) | Hedychium ellipticum | MIC (Mycobacterium tuberculosis) = 12.5 µg mL$^{-1}$ (44 µM) | 86 |
| 49 | Andrographolide (60) | Andrographis paniculata | $IC_{50}$ (Trypanosoma brucei[i]) = 8.3 µM, SI = 8.5<br>$IC_{50}$ (Leishmania martiniquensis[m]) = 4.04 µg mL$^{-1}$ (12 µM)<br>$EC_{50}$ (DENV[n]) = 21.3–22.7 µM<br>$IC_{50}$ (CHIKV[i]) = 77 µM | 77, 87–93 |
| 50 | Vitexolide A (61) | Vitex vestita | MIC (Bacillus cereus*,[i], Staphylococcus haemolyticus*) = 6 µg mL$^{-1}$ (18 µM)<br>MIC (Staphylococcus aureus[f],*) = 12–24 µg mL$^{-1}$ (36–72 µM)<br>MIC (Corynebacterium striatum*, Enterococcus durans*, Enterococcus faecalis*, Enterococcus gallinarum*, Staphylococcus lugdunensis*, Staphylococcus saprophyticus*, Enterococcus faecalis[i],*, Listeria monocytogenes[i],*) = 24 µg mL$^{-1}$ (72 µM)<br>MIC (Enterococcus avium*, Enterococcus faecium[i], Enterococcus gallinarum*, Listeria innocua[i], Staphylococcus sciuri[i],*) = 48 µg mL$^{-1}$ (144 µM) | 69 |
| 51 | (62) | | MIC (Bacillus cereus*,[f], Staphylococcus haemolyticus*, Staphylococcus intermedius*, Streptococcus agalactiae*) = 24 µg mL$^{-1}$ (72 µM)<br>MIC (Staphylococcus aureus[f],*, Staphylococcus epidermidis*, Staphylococcus lugdunensis*, Staphylococcus saprophyticus*) = 48 µg mL$^{-1}$ (144 µM) | |

1866 | Nat. Prod. Rep., 2024, 41, 1858–1894

This journal is © The Royal Society of Chemistry 2024

**Table 1** (*Contd.*)

| Entry | Compound | Source | Reported biological activity[a] | Ref. |
|---|---|---|---|---|
| 52 | Vitexolide D (**63**) | | MIC (*Bacillus subtilis*\*[f]) = 25 μg mL$^{-1}$ (79 μM)<br>MIC (*Bacillus cereus*\*[f]) = 25–50 μg mL$^{-1}$ (79–157 μM)<br>MIC (*Corynebacterium striatum*\*, *Enterococcus faecium*[i],\*, *Enterococcus gallinarum*[i],\*, *Listeria monocytogenes*[i],\*, *Staphylococcus aureus*\*[f], *Staphylococcus epidermidis*\*, *Staphylococcus intermedius*\*, *Streptococcus agalactiae*\*) = 50 μg mL$^{-1}$ (157 μM) | |
| 53 | Vitexolide E (**64**) | | MIC (*Enterococcus durans*\*, *Enterococcus faecalis*\*[f], *Enterococcus faecium*\*[f], *Streptococcus agalactiae*\*) = 50 μg mL$^{-1}$ (157 μM) | |
| 54 | (**65**) | *Leucas stelligera* | IC$_{50}$ (*Mycobacterium tuberculosis*) = 5.02 μg mL$^{-1}$ (16 μM) | 71 |
| 55 | (**66**) | *Hedychium ellipticum* | MIC (*Mycobacterium tuberculosis*) = 6.25 μg mL$^{-1}$ (20 μM) | 86 |
| 56 | (**67**) | *Colophospermum mopane* | MIC (*Klebsiella pneumoniae*\*\*, *Enterococcus faecalis*\*) = 62.5 μg mL$^{-1}$ (185 μM) | 94 |
| 57 | (**68**) | | MIC (*Klebsiella pneumoniae*\*\*, *Enterococcus faecalis*\*) = 62.5 μg mL$^{-1}$ (164 μM) | |
| 58 | (**69**) | | MIC (*Klebsiella pneumoniae*\*\*) = 62.5 μg mL$^{-1}$ (193 μM) | |
| 59 | (**70**) | | MIC (*Klebsiella pneumoniae*\*\*) = 46.9 μg mL$^{-1}$ (155 μM)<br>MIC (*Staphylococcus aureus*\*) = 62.5 μg mL$^{-1}$ (194 μM) | |
| 60 | Acuminolide (**71**) | *Vitex vestita* | MIC (*Bacillus cereus*\*) = 23 μM | 69 |
| 61 | (**72**) | *Leucas stelligera* | IC$_{50}$ (*Mycobacterium tuberculosis*) = 5.55 μg mL$^{-1}$ (17 μM) | 71 |
| 62 | Isoambreinolide (**73**) | *Vitex trifolia* | MIC (*Mycobacterium tuberculosis*) = 25 μg mL$^{-1}$ (95 μM) | 95 |
| 63 | Pahangensin A (**74**) | *Alpinia pahangensis* | MIC (*Bacillus cereus*\*, *Bacillus subtilis*\*) = 31.25 μg mL$^{-1}$ (52 μM)<br>MIC (*Staphylococcus aureus*\*) = 52.08 μg mL$^{-1}$ (87 μM) | 67 |
| 64 | Forsyqinlingine A (**75**) | *Forsythia suspensa* | EC$_{50}$ (RSV) = 5.0 μM<br>IC$_{50}$ (H1N1) = 6.9 μM | 96 |
| 65 | Forsyqinlingine B (**76**) | | EC$_{50}$ (RSV) = 4.8 μM<br>IC$_{50}$ (H1N1) = 7.7 μM | |

[a] Units reported according to the original reference. Conversion into micromolar is shown in brackets (μM). MIC = Minimum inhibitory concentration; MFC = Minimum fungicidal concentration; IC$_{50}$ = Concentration that inhibits the growth of a species by 50%; SI = Selectivity index; MRSA = Methicillin-resistant *Staphylococcus aureus*; DENV = Dengue virus; WNV = West Nile virus; H1N1 and H3N2 = Influenza A virus; RSV = Respiratory Syncytial virus; CHIKV = Chikungunya virus; \*Gram-positive; \*\*Gram-negative. [b] Vancomycin-sensitive. [c] Vancomycin-resistant. [d] Multidrug-resistant. [e] Methicillin-resistant. [f] Several strains. [g] Parasite residing inside cells. [h] Amastigotes. [i] Clinical isolates. [j] Tachyzoites. [k] Trypamastigotes. [l] Procyclic forms. [m] Promastigotes. [n] Virus residing inside cells.

This journal is © The Royal Society of Chemistry 2024

*Nat. Prod. Rep.*, 2024, **41**, 1858–1894 | 1867

Table 2   Biological activity of labdane-type diterpenoids produced *via* biotransformation

| Entry | Compound | Microorganism | Reported biological activity[a] | Ref. |
|---|---|---|---|---|
| 1 | **77** | *Cunninghamella elegans* | MIC (*Candida albicans*) = 1.1 μg mL$^{-1}$ (3.1 μM) | 63 |
|   |   |   | MIC (*Candida tropicalis*) = 4.4 μg mL$^{-1}$ (13 μM) |   |
| 2 | **78** |   | MIC (*Candida albicans*) = 1.1 μg mL$^{-1}$ (3.1 μM) |   |
|   |   |   | MIC (*Candida tropicalis*) = 4.4 μg mL$^{-1}$ (13 μM) |   |
| 3 | **79** | *Aspergillus brasiliensis* | MIC (*Candida glabrata*) = 12.5 μg mL$^{-1}$ (36 μM) | 84 |
| 4 | **80** |   | MIC (*Candida glabrata*) = 12.5 μg mL$^{-1}$ (34 μM) |   |
| 5 | **81** |   | MIC (*Candida glabrata*) = 12.5 μg mL$^{-1}$ (36 μM) |   |
| 6 | **82** |   | MIC (*Candida glabrata*) = 12.5 μg mL$^{-1}$ (36 μM) |   |

[a] Units reported according to the original reference. Conversion into micromolar is shown in brackets (μM). MIC = Minimum inhibitory concentration.

interactions with the binding site residues and its terminal vinyl group participates in a NH–π interaction with the backbone nitrogen of residue A278.[55] Although the hydroxy group is the only polar group in **10**, the simulation revealed that strong H-bonding to specific amino acid residues significantly contributes to the anchoring of this compound to its binding site in the enzyme, which was confirmed through experimental data.[55]

The diols sclareol (**11**) and 14α-epoxysclareol (**12**) (Fig. 4) were overall less active against bacteria than manool (**10**) (Table 1, entries 2 and 3).[55] Sclareol (**11**) and clindamycin displayed synergistic activity, *i.e.*, their fractional inhibitory concentration index (FIC) was lower than 0.5, against MRSA.[56] The antifungal activity of sclareol (**11**) against *Candida* spp was investigated.[57] This compound inhibited the growth of *Candida albicans*, *Candida auris* and *Candida parapsilosis* with an MIC value of 50 μg mL$^{-1}$ (Table 1, entry 2), inducing apoptosis-like cell death in *Candida albicans*, with depolarization of the mitochondrial membrane potential and increase in the reactive oxygen species (ROS) levels. Sclareol (**11**) was also able to inhibit biofilm formation in *Candida albicans* in a dose-dependent manner, with a decrease in biofilm-related factors including ZAP1, ADH5, CSH1, TPO4 and CAN2. Hyphal formation was inhibited by more than 50% at the MIC value of sclareol (**11**), both in yeast extract peptone dextrose (YPD) and spider medium.[57] Notably, the activity of sclareol (**11**) was synergistic with that of miconazole against *Candida albicans* (FIC value of 0.31), with the co-treatment resulting in a 4-fold increase in potency for miconazole.[57]

Salvic acid (**13**) (Fig. 4) isolated from the aerial parts of *Eupatorium salvia* Colla was only active against Gram-positive bacteria, namely *Staphylococcus aureus* and *Bacillus cereus* (Table 1, entry 4).[58] *ent*-Copalic acid (**14**) (Fig. 4), the most abundant diterpene in the oleoresin of *Copaifera* species, displays potent antimicrobial action against staphylococci and streptococci, including clinical isolates,[54] and against anaerobic pathogens associated with dental infections and dental biofilm formation (Table 1, entry 5).[59]

The antibacterial effects of **14** were potentiated by combination with chlorhexidine, a commonly used disinfectant. Significant reductions in the bacterial burden, *i.e.*, from 3 log units, were observed after the treatment of *Peptostreptococcus anaerobius* with 6.25 μg mL$^{-1}$ of (**14**) alone, after 48 h. More importantly, *ent*-copalic acid (**14**) could eradicate (3 log units) pre-formed biofilms of both *Peptostreptococcus anaerobius* and *Actinomyces naeslundii* at 62.5 and 1000 μg mL$^{-1}$, respectively. Another study reported that **14** is also active against dermatophytes including *Trichophyton rubrum* and *Microsporum gypseum* (Table 1, entry 5).[60] A significant reduction in *Trichophyton rubrum* hyphal growth was observed by fluorescence microscopy after treatment with *ent*-copalic acid (**14**) at sub-inhibitory concentrations. Scanning electron microscopy (SEM) revealed the inhibition of hyphal growth and an irregular growth pattern following treatment with the compound.

Notably, labdane-type di-acid **15** and compound **16** (Fig. 4), also present in *Copaifera* species, were both active against drug-resistant MRSA (Table 1, entries 6 and 7, respectively), with **15** displaying no cytotoxicity at concentrations of up to 100 μg mL$^{-1}$, in a panel of cell lines.[61] Good antibacterial activity against MRSA was also observed for triene di-acid **17** (Fig. 4), isolated from *Caesalpinia decapetala* (Table 1, entry 8).[62] However, *ent*-agathic acid (**18**) (Fig. 4) was not active against bacteria but it displayed antifungal activity against the dermatophytes *Trichophyton rubrum* and *Trichophyton mentagrophytes* (Table 1, entry 9).[61] Di-acid **19** (Fig. 4) inhibited the growth of *Candida tropicalis* and *Candida albicans* with MIC values of 9.3 and 74.3 μM, respectively (Table 1, entry 10).[63]

The activity of three labdane-type diterpenoids, including anticopalic acid (**20**), anticopalol (**21**) and 8(17)-ladben-15-ol (**22**) (Fig. 4), against the Gram-positive *Staphylococcus aureus*, *Enterococcus faecalis* and *Bacillus cereus* was reported (Table 1, entries 11–13, respectively).[64,65] The four labdane-type diterpenoids (**23–26**) (Fig. 4), isolated from *Cunninghamia lanceolata*, were active against *Staphylococcus aureus* and *Bacillus subtilis*, with IC$_{50}$ values below 25 μM (Table 1, entries 14–17, respectively).[66] Pahangensin B (**27**) (Fig. 4) was reported to have mild activity against *Bacillus cereus* (Table 1, entry 18),[67] whereas labdane (**28**) (Fig. 4), isolated from *Elytropappus rhinocerotis*, was active against *Brevibacterium agri* (Table 1, entry 19).[68]

Vitexolin B (**29**) (Fig. 4), from *Vitex vestita*, was active against *Bacillus cereus* standard environmental and clinical isolates, with MIC values ranging from 25 to 50 μM (Table 1, entry 20).[69] The 5,9-dihydroxylated derivative (**30**) of isocupressic acid (Fig. 4) was isolated from the fungus *Talaromyces scorteus* AS-242 and found to inhibit the activity of the Gram-negative *Vibrio*
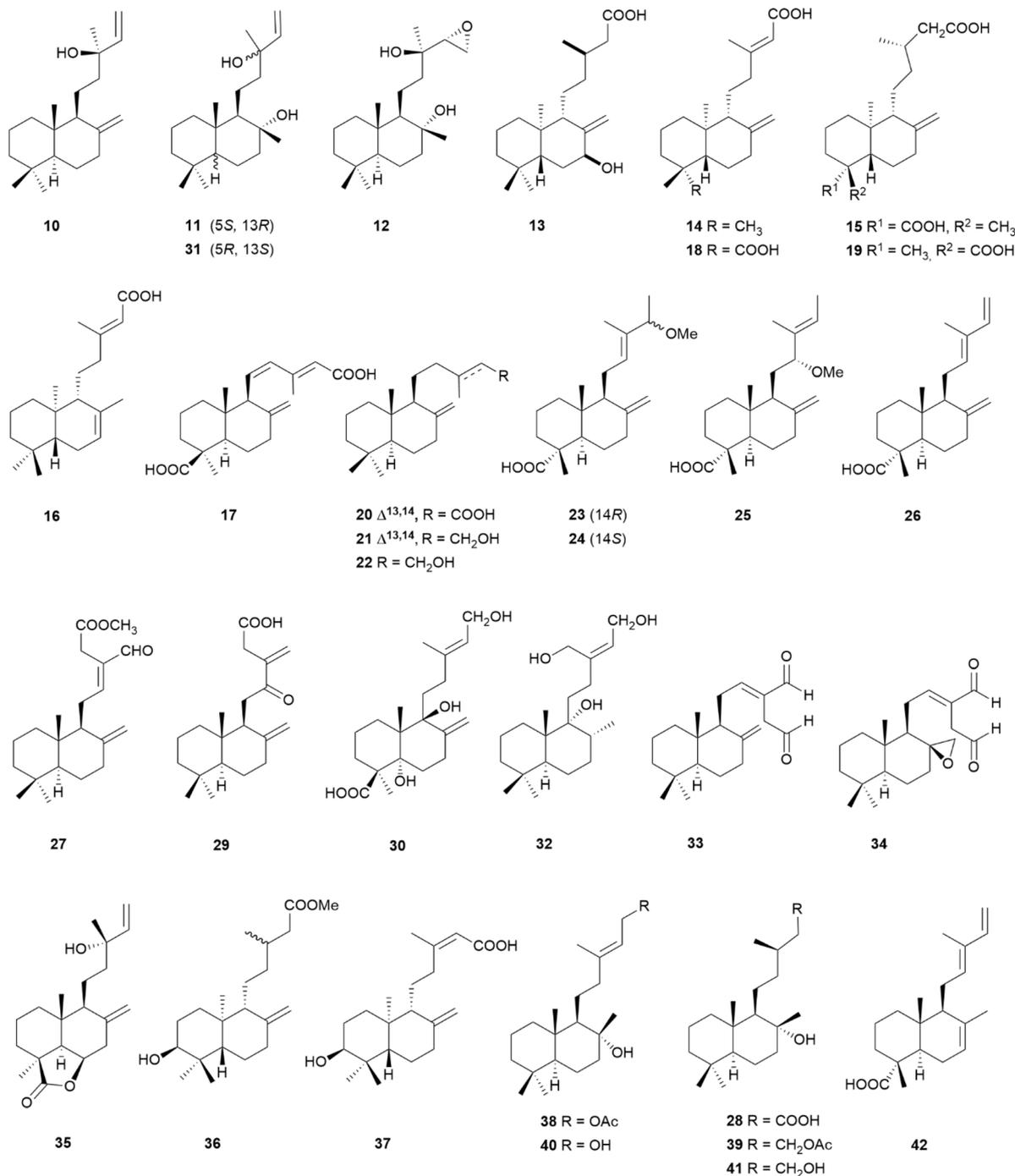
**1868** | *Nat. Prod. Rep.*, 2024, **41**, 1858–1894

This journal is © The Royal Society of Chemistry 2024

**Fig. 4** Naturally occurring labdane-type diterpenoids with an acyclic side chain at C9.

*parahaemolyticus*, which is responsible for gastroenteritis in humans, with an MIC value of 8 μg mL$^{-1}$ (Table 1, entry 21).[70]

The sclareol-type labdane (**31**) and the triol (**32**) (Fig. 4), isolated from *Leucas stelligera*, inhibited the growth of *Mycobacterium tuberculosis*, with IC$_{50}$ values of 5.95 and 8.94 μg mL$^{-1}$ (Table 1, entries 22 and 23, respectively), whereas no significant activity was observed against *Escherichia coli* or *Mycobacterium smegmatis*.[71] Compound (**32**) was particularly selective given that no significant cytotoxicity was observed in any of the cell

lines tested, namely MCF-7, Thp-1 and HepG2, at 100 μg mL$^{-1}$. The di-aldehyde labdane (**33**) and its epoxide analogue (**34**) (Fig. 4) have been isolated from diverse plant sources. Both compounds are active against a panel of bacteria, both Gram-positive and -negative (Table 1, entries 24 and 25, respectively).[72,73] The labdane-type diterpenoid (**35**) (Fig. 4), where lactonisation occurs at C6 and C19, was isolated from *Salvia leriifolia* and found to bear modest antibacterial activity against *Staphylococcus aureus* (Table 1, entry 26).[74]

This journal is © The Royal Society of Chemistry 2024

*Nat. Prod. Rep.*, 2024, **41**, 1858–1894 | **1869**

Labdane **36** and alepterolic acid (**37**) (Fig. 4), isolated from *Piliostigma thonningii*, were tested against the amastigotes of *Leishmania donovani* and *Trypanosoma brucei* (Table 1, entries 27 and 28, respectively).[75] The hydroxyl group at C3 was important for their antiprotozoal activity against *Trypanosoma brucei*. Several labdanes (**38–41**) (Fig. 4) were isolated from *Psiadia arg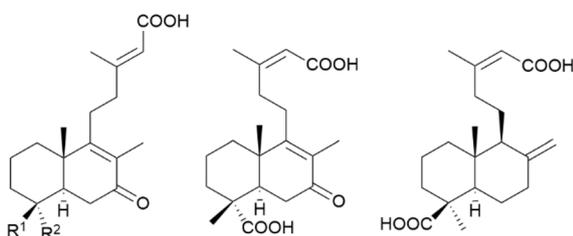uta* and evaluated for their antimalarial effects, with IC$_{50}$ values ranging from 22.2 to 36.6 μM against *Plasmodium falciparum* (Table 1, entries 29–32, respectively).[76]

On African green monkey kidney Vero cells, stachyonic acid A (**42**) (Fig. 4) was reported as an antiviral agent against Dengue virus, with an IC$_{50}$ value of 1.4 μM (Table 1, entry 33).[77] Another study reported that this compound is also active against the West Nile virus and human influenza viruses H1N1 and H3N2.[78]

Forsypensins A–E (**43–47**), forsyshiyanins A (**48**) and B (**49**), and other labdanes (**50–55**) (Fig. 5), isolated from *Forsythia suspensa*, were all active against the influenza (H1N1) and respiratory syncytial viruses (RSV) (Table 1, entries 34–46), respectively, but less potent than ribavirin, which was used as a positive control.[79,80]

Cyslabdane A (**56**) (Fig. 5), produced by *Streptomyces cyslabdanicus* K04-0144, although not an antibacterial compound itself, was reported to enhance the activity of β-lactam antibiotics against MRSA by 8–32-fold (penam), 4–32-fold (cephem), and 128 to over 1000-fold (carbapenem).[97]

## 3.2 Naturally occurring labdane-type diterpenoids bearing a furan ring on the side chain at C9

The activity of *ent*-polyalthic acid (**57**) (Fig. 6), present in the oleoresin of *Copaifera* species, was studied in a similar fashion to that of *ent*-copalic acid (**14**) (Fig. 4) against oral pathogens (Table 1, entry 47).[81,82] However, unlike **14**, synergy studies with chlorhexidine did not result in an improvement in activity. Compound (**57**) could inhibit biofilm formation in *Porphyromonas gingivalis* and in the clinical isolate *Peptostreptococcus micros* only by 50% at 6.5 μg mL$^{-1}$, but unable to eradicate established biofilms. *ent*-Polyalthic acid (**57**) was not toxic when tested on the *Caenorhabditis elegans* model, even after 72 h, at a high concentration of 1000 μg mL$^{-1}$.[82] The potential of *ent*-polyalthic acid (**57**) to affect the parasite *Toxoplasma gondii* residing inside BeWo cells and in human villous explants was also studied. This compound could inhibit the proliferation of *Toxoplasma gondii* tachyzoites at concentrations of 32 and 64 μg mL$^{-1}$ (BeWo cells) and 64 μg mL$^{-1}$ (villous explants), respectively.[82,83]

The authors observed that *ent*-polyalthic acid (**57**) could downregulate the levels of IL-6, IL-8 and TNF-α in villous explants regardless of *Toxoplasma gondii* infection and suggested that this immunomodulation of the placental microenvironment could be relevant for targeting the parasite.[83] Finally, *ent*-polyalthic acid (**57**) was also found to have a significant antifungal effect against the dermatophytes *Trichophyton rubrum* and *Trichophyton mentagrophytes*, with IC$_{50}$ values of 6.8 and 4.3 μg mL$^{-1}$, respectively (Table 1, entry 47).[61]

Coronarin E (**58**) (Fig. 6), isolated from *Hedychium ellipticum* Buch.-Ham. ex Sm., exhibits activity against *Mycobacterium tuberculosis* but with a low selectivity index (SI) (<10), as



**43** R$^1$ = R$^4$ = R$^5$ = H; R$^2$ = CH$_2$OH, R$^3$ = CH$_3$, R$^6$ = OH
**44** R$^1$ = OH, R$^2$ = CH$_2$OH, R$^3$ = CH$_3$, R$^4$ = R$^5$= R$^6$ = H
**45** R$^1$ = R$^4$ = R$^6$ = H, R$^2$ = COOH, R$^3$ = CH$_3$, R$^5$ = OH
**49** R$^1$ = R$^5$ = R$^6$ = H, R$^2$ = CH$_2$OH; R$^3$ = CH$_3$, R$^4$ = OH
**50** R$^1$ = OH, R$^2$ = R$^3$ = CH$_3$, R$^4$ = R$^5$ = R$^6$ = H
**51** R$^1$ = R$^4$ = R$^5$ = R$^6$ = H, R$^2$ = CH$_2$OH, R$^3$ = CH$_3$
**52** R$^1$ = R$^4$ = R$^5$ = R$^6$ = H, R$^2$ = COOH, R$^3$ = CH$_3$
**54** R$^1$ = R$^4$ = R$^5$ = R$^6$ = H, R$^2$ = CH$_3$, R$^3$ = COOH

**46** R$^1$ = CH$_2$OH, R$^2$ = CH$_3$
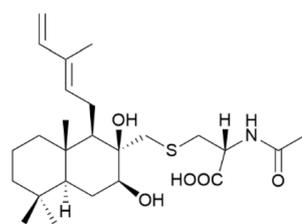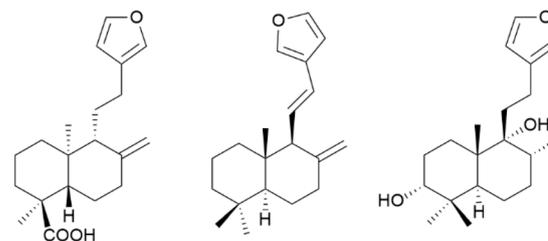**48** R$^1$ = COOH, R$^2$ = CH$_3$
**55** R$^1$ = CH$_3$, R$^2$ = CH$_2$OH

**47**

**53**

**56**

Fig. 5 Naturally occurring labdane-type diterpenoids with an acyclic side chain at C9 (Cont.).



**57**

**58**

**59**

Fig. 6 Naturally occurring labdane-type diterpenoids bearing a furan ring on the side chain at C9.

**1870** | *Nat. Prod. Rep.*, 2024, **41**, 1858–1894

This journal is © The Royal Society of Chemistry 2024

assessed on a panel of human cell lines (Table 1, entry 48).[86] Otostegindiol (59) (Fig. 6), isolated from the leaves of *Otostegia integrifolia* Benth, a plant used in Ethiopia for the treatment of malaria, could to induce the maximum decrease of 73% in parasite burden in mice infected with *Plasmodium berghei* at a dose of 100 mg kg$^{-1}$ per day.[98]

### 3.3 Naturally occurring labdane-type diterpenoids bearing a lactone on the side chain at C9

Andrographolide (60) (Fig. 7) is one of the most studied labdane-type diterpenoids. It is naturally occurring in *Andrographis paniculata*, a herbaceous plant of the Acanthaceae family, native to Asian countries and cultivated in Scandinavia and other parts of Europe.[88,89] This plant has traditionally been used for medicinal purposes since ancient times and its reported activities include antibacterial, antipyretic, antiviral and antioxidant. Andragrapholide (60) has been identified as its major component and its antiprotozoal and antiviral properties have been documented.[87–92] Andragrapholide (60) dose-dependently inhibited the growth of the procyclic (insect vector) forms of the parasite *Trypanosoma brucei*, with an IC$_{50}$ of 8.3 μM (Table 1, entry 49) and SI of 8.5.[88] Severe morphological alterations such as extensive swelling and disintegration of the cell membrane were observed after treatment with this compound. SEM showed swollen parasites with the loss of flagella, in comparison to the controls.

Cell cycle arrest at the sub-G$_o$/G$_1$ stage occurred, with externalisation of phosphatidylserine, conclusive of apoptotic-like cell death. In the parasite-treated cells, apoptotic nuclei were observed, with the accumulation of lipid-storage bodies in the cytoplasm, and oxidative stress was triggered by an increase in intracellular ROS. Further evidence of apoptotic-like cell death following treatment with 60 came from the induction of loss of membrane potential, depletion of the antioxidant thiol levels and increase in lipidic peroxidation. Andragrapholide (60) was also reported to be active against the promastigotes of *Leishmania martiniquensis*, with an IC$_{50}$ value of 4.04 μg mL$^{-1}$ (Table 1, entry 49), but its cytotoxicity was high in the same concentration range.[87] This compound was also active against the intracellular forms of the parasite.[87]

The antiviral effects of 60 were studied against *Chikungunya virus* (CHIKV), the causative agent of chikungunya fever, prevalent in Africa, India, Southeast Asia, and the Americas (Table 1, entry 49).[89] Its action was also studied against the hepatitis C (HCV)[90] and the Dengue[77,91,93] viruses. A study found that 60 caused a 3 log unit decrease in CHIKV burden within HepG2 cells, with an EC$_{50}$ of 77 μM (Table 1, entry 49) and without cytotoxicity.[89] Andrographolide (60) was suggested to act at the post-virus entry stages, given that the reduction of viral protein expression and virus titer was most significant immediately after the infection period of the cells.[89] Andrographolide (60) treatment of both Ava5cells, containing the HCV subgenomic replicon, and HCVcc-infected Huh-7 cells resulted in a decrease in viral protein and RNA, with EC$_{50}$ values of 6 and 5.1 μM, respectively, and without cytotoxicity.[90] Synergistic effects were observed with co-treatment of the infected cells with 60 and IFN-α, the HCV NS3/4A protease inhibitor telaprevir and the NS5B polymerase PSI-7977 inhibitor. Moreover, the antiviral effects of 60 were shown to involve the induction of the p38/MAPK/Nrf$_2$/HO-1 pathway.[90] The expression of haem oxygenase-1 (HO-1) was upregulated upon treatment with andrographolide (60), leading to increased levels of biliverdin, which suppressed HCV replication by promoting the antiviral responses mediated by IFN and inhibiting NS3/4A protease activity.[90] The antiviral effects of 60 were attenuated upon the use of either a HO-1 inhibitor or HO-1 gene knockdown, which evidenced its role in the mode of action of the compound.[90]

The phosphorylation of p38 mitogen-activated protein kinase (MAPK) was activated in the presence of (60), which resulted in the stimulation of nuclear factor erythroid-2 (Nrf$_2$)-mediated HO-1 expression.[90] The antiviral activity of andrographolide (60) against Dengue virus was somewhat less potent.[77,91] This compound inhibited the levels of viral infection in both HepG2 and HeLa cell lines, with EC$_{50}$ values of 21.3 and 22.7 μM, respectively, and reduction of viral proteins DENV E and NS3 in both cell lines.[91] In the case of CHIKV, the time of addition studies also showed that the activity of 60 is confined to the post-infection stage. A proteomic analysis of the anti-Dengue virus activity of 60 on HepG2 cells revealed that this activity can be cell-type dependent to a certain extent.[93] Andrographolide (60) treatment of infected cells impacts several processes, ultimately resulting in a reduction in viral replication. The authors proposed that the increase in phosphorylation of eukaryotic initiation factor 2 (eIF2α) in response to andrographolide (60) is indeed a major determinant of its anti-Dengue activity and that it occurs as a consequence of the
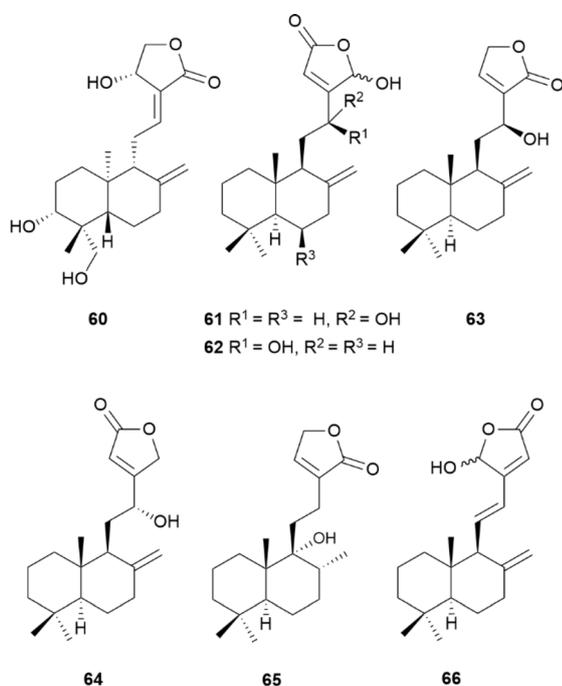


**Fig. 7** Naturally occurring labdane-type diterpenoids bearing a lactone on the side chain at C9.

This journal is © The Royal Society of Chemistry 2024

*Nat. Prod. Rep.*, 2024, **41**, 1858–1894 | 1871

effects of this compound, either direct or not, in the critical regulator of the unfolded protein response GRP78.[93]

The labdane-type lactones vitexolide A (**61**), 12-epivitexolide A (**62**), vitexolide D (**63**) and vitexolide E (**64**) (Fig. 7) were assessed against a panel of 46 Gram-positive bacteria species, including clinical isolates (Table 1, entries 50–53).[69] Among them, vitexolide A (**61**) was the most potent with MIC values ranging from 6 to 96 µM.[69]

Lactone **65** (Fig. 7) displayed selective activity against pathogenic *Mycobacterium tuberculosis*, with an $IC_{50}$ of 5.02 µg mL$^{-1}$, and no significant activity against non-pathogenic *Mycobacterium smegmatis* (Table 1, entry 54).[71] No significant cytotoxicity was observed for compound **65** against MCF-7, Thp-1 or HepG2 cells at a concentration of 100 µg mL$^{-1}$.[71]

Labdane **66** (Fig. 7), isolated from *Hedychium ellipticum* Buch.-Ham. ex Sm., also displayed antitubercular activity but with a low SI (<10) when assessed on a panel of human cell lines (Table 1, entry 55).[86]

### 3.4 Naturally occurring epoxy labdane-type diterpenoids

Labdanes **67–70** (Fig. 8), isolated from *Colophospermum mopane*, displayed MIC values ranging from 46.9 to 62.5 µg mL$^{-1}$ against a panel of bacterial strains (Table 1, entries 56–59, respectively).[94] Acuminolide (**71**) (Fig. 8), from *Vitex vestita*, was active against *Bacillus cereus* N190 with an MIC value of 23 µM (Table 1, entry 60).[69]

### 3.5 Other naturally occurring labdane-type diterpenoids

Spiro-tetrahydrofuran labdane derivative **72** (Fig. 9), isolated from *Leucas stelligera*, inhibited the growth of *Mycobacterium tuberculosis* (Table 1, entry 61). This compound also inhibited the growth of MCF-7 cells by roughly 40%, at 100 µg mL$^{-1}$, displaying moderate cytotoxicity.[71]

Isoambrenolide (**73**) (Fig. 9), isolated from *Vitex folia*, was also active against *Mycobacterium tuberculosis* H37Rv, with an MIC value of 100 µg mL$^{-1}$ (Table 1, entry 62).[95] The bis-lambda-triene lactone pahangensin A (**74**) (Fig. 9), isolated from *Alpinia pahangensis*, was moderately active against Gram-positive bacteria and devoid of activity against Gram-negative bacteria (Table 1, entry 63).[67] Two labdane-type alkaloids forsyqinlingines A (**75**) and B (**76**) (Fig. 9), from the ripe fruits of
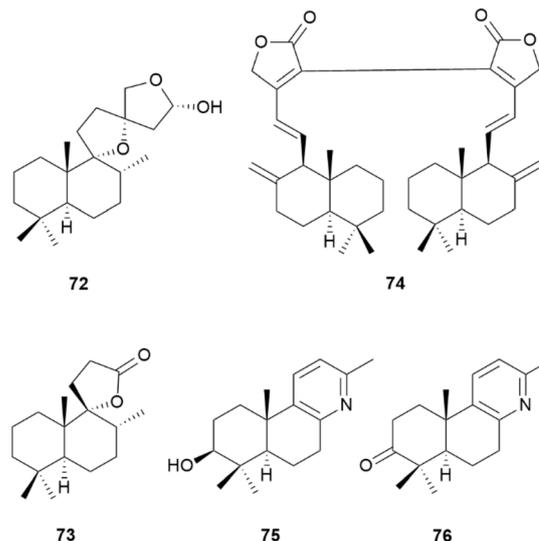
Fig. 9 Other naturally occurring labdane-type diterpenoids.

*Forsythia suspensa*, displayed antiviral activities against influenza A (H1N1) and respiratory syncytial viruses (RSV), with $IC_{50}$ values in the range of 6.9–7.7 µM and 4.8–5.0 µM (Table 1, entries 64 and 65), respectively.[96]

### 3.6 Labdane-type diterpenoids produced by biotransformation

Among the labdane-type diterpenoids, **77** and **78** (Fig. 10), produced by biotransformation with *Cunninghamella elegans*, displayed a significant improvement in antifungal activity against several *Candida* strains (Table 1, entries 1 and 2, respectively).[63] Compounds **77** and **78** were 40- and 2.5-fold more potent than the reference fluconazole against *Candida albicans* and *Candida tropicalis*, respectively. The microbial
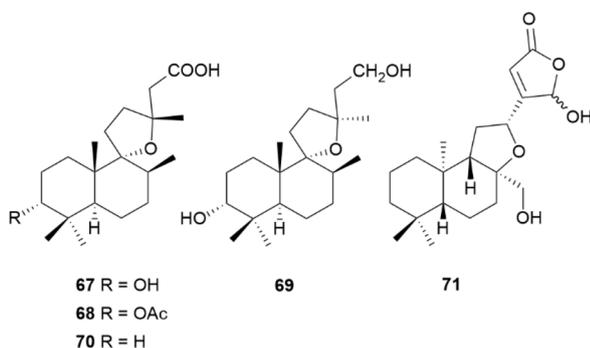
Fig. 8 Naturally occurring epoxy labdane-type diterpenoids.

Fig. 10 Labdane-type diterpenoids produced by biotransformation.

**1872** | *Nat. Prod. Rep.*, 2024, **41**, 1858–1894

This journal is © The Royal Society of Chemistry 2024

transformation of *ent*-polyalthic acid (**57**) (Fig. 6) with *Aspergillus brasiliensis* afforded compounds **79–82** (Fig. 10), with potent antifungal effects against *Candida glabrata* (Table 2, entries 3–6), being 4-fold more potent than fluconazole.[84]

### 3.7 Semi-synthetic labdane-type diterpenoids

A panel of salvic acid (**13**) (Fig. 4) esters was synthesised to probe the effect of increased lipophilicity on their antibacterial activity.[5] Similar to salvic acid (**13**), the presence of carboxylic acid at C15 was crucial for the antibacterial activity. T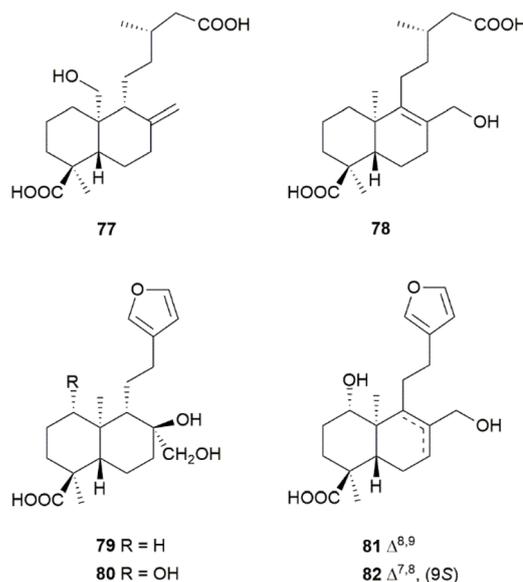he optimal length of the ester at C7 was achieved in compounds **83–89** (Fig. 11), with an 8- to 16-fold improvement in antibacterial potency, displaying MIC values ranging from 3.13 to 6.25 µg mL$^{-1}$. However, none of these compounds were active against Gram-negative bacteria.[58]

Among a panel of amide derivatives of *ent*-polyalthic acid (**57**) (Fig. 6), compounds **90** and **91** (Fig. 11) displayed the best

antileishmanial activity against *Leishmania donovani* axenic amastigotes, with IC$_{50}$ values of 6.73 and 3.84 µg mL$^{-1}$, respectively, and compound **90** was also active against *Trypanosoma brucei* trypomastigotes with an IC$_{50}$ of 2.54 µg mL$^{-1}$.[85] In the case of antileishmanicidal activity, bulky lipophilic groups were generally preferred as in **91**, **92** and **93**, with cyclic amides **94** and **95** not showing significant activity. All the amides were active against *Trypanosoma brucei*, with the exception of **96** and **97**, and also diols **98**, **99** and **100**. The parent *ent*-polyalthic acid (**57**) displayed IC$_{50}$ values of 8.86 and 3.87 µg mL$^{-1}$ against *Leishmania donovani* and *Trypanosoma brucei*, respectively, and neither **57** nor any of the compounds was more potent than pentamidine or amphotericin B, used as positive controls.[85]

Amides **95** and **97** and amines **101** and **102** (Fig. 11), produced from *ent*-polyalthic acid **57**, were also tested against the Gram-positive bacteria *Enterococcus faecalis*, *Enterococcus faecium*, *Staphylococcus epidermidis* and *Staphylococcus aureus*,
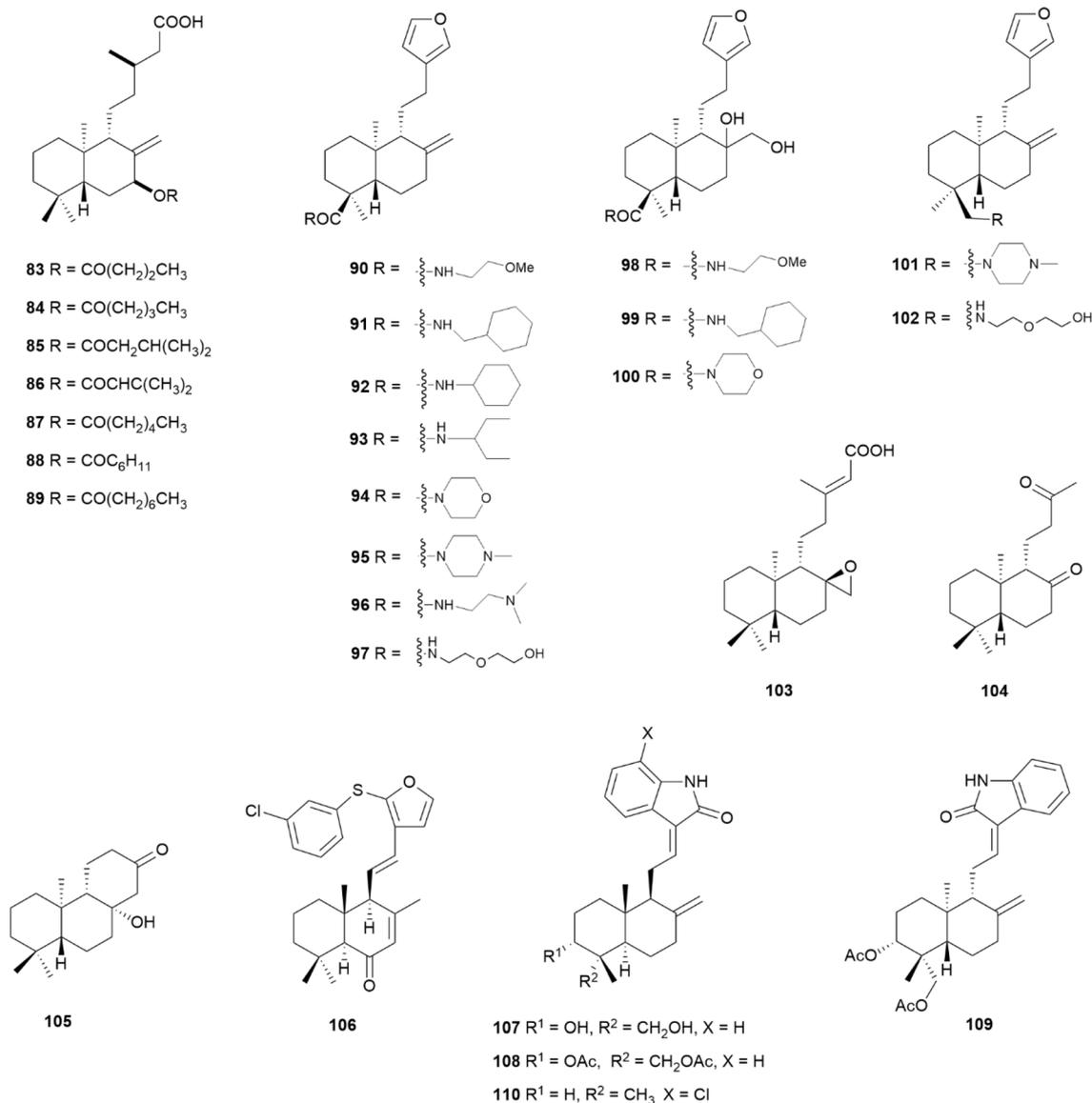


**Fig. 11** Semi-synthetic labdane-type diterpenoids.

This journal is © The Royal Society of Chemistry 2024

*Nat. Prod. Rep.*, 2024, **41**, 1858–1894 | **1873**

with MIC values ranging from 8 to 32 µg mL$^{-1}$.[99] The inhibition of *Staphylococcus epidermidis* biofilm formation was achieved in less than 1 log unit (~97%) with compounds **95** and **101** only, at a high concentration of 512 mg mL$^{-1}$.[99]

The derivatives of *ent*-copalic acid (**14**) (Fig. 4), compounds **103–105** (Fig. 11), prepared by oxidation and aldol condensation, displayed antitubercular activity with MIC values ranging from 6.25 to 25 µg mL$^{-1}$ against *Mycobacterium tuberculosis* H37Rv, and negligible cytotoxicity.[100] Among a panel of synthesised derivatives of hedychenone, compound **106** (Fig. 11) was the only one showing antibacterial activity against *Staphylococcus aureus*, as evaluated by the well diffusion assay.[101]

The synthesis of oxindole derivatives of andrographolide (**60**) (Fig. 7) led to the discovery of compound **107** (Fig. 11), where the NH-group of the oxindole moiety was crucial for its activity, considering that any derivative devoid of it, lost the antiviral potency against the CHIKV.[102] Diacetylated compounds **108** and **109** (Fig. 11) were only slightly less potent, suggesting that the hydroxyl groups on the decalin core were not relevant for the activity. The authors also ruled out that the *ent* series was not preferred, and that side chain (*E*) isomers performed better than their (*Z*) counterparts. Finally, compound **110** was observed to be a potent inhibitor against two isolates from human patients, with minimal cytotoxicity. This compound displayed both prophylactic and therapeutic effects on the host cells, where it was shown to interfere with viral replication.[102]

# 4. Anti-infective tricyclic diterpenoids

The tricyclic diterpenoids portrayed in the literature over the past decade, with significant anti-infective activity, are detailed in the following sections. The structures of both naturally occurring and semi-synthetic compounds are depicted in Fig. 12–20, with semi-synthetic compounds grouped according to their parent diterpenoid. The data for all the reported sources and biological activities for each compound are summarised in Tables 3 and 4 and follows the same inclusion criteria as described in Section 3.

## 4.1 Naturally occurring abietane-type diterpenoids

The activity of abietic acid (**3**) (Fig. 2) against a panel of bacterial strains has been well documented and found to be more significant against Gram-positive bacteria (Table 3, entry 1).[103–105] One study determined the susceptibility of standard American Type Culture Collection (ATCC) strains as well as that of multi-resistant *Staphylococcus aureus* and *Escherichia coli* strains to abietic acid (**3**), where this compound was consistently less active against Gram-negative and resistant strains.[103] However, in *Escherichia coli*, the combination of sub-inhibitory concentrations of abietic acid (**3**) with either the aminoglycoside gentamicin or the fluoroquinolone norfloxacin could decrease the MIC of both antibiotics. Combination regimens of ciprofloxacin or the pump inhibitor ethidium bromide with abietic acid (**3**) were also effective in inhibiting the growth of *Staphylococcus aureus* strains overexpressing NorA or MepA, two genes coding for efflux pumps in bacterial cells. Abietic acid (**3**) was

reported to significantly inhibit the growth of the cariogenic bacteria *Streptococcus mutans* and limit biofilm formation by this species by 2 log units at a concentration of 64 µg mL$^{-1}$.[105] The integrity of the bacterial membrane was compromised after treatment with this compound and under SEM, the bacterial surfaces appeared rough and irregular. Abietic acid (**3**) was mostly toxic to human cells at concentrations higher than 168 µg mL$^{-1}$, apart from monocytic cells, where toxicity was observed at 64 µg mL$^{-1}$, suggesting that oral rinse products will be more suitable for inclusion of abietic acid (**3**) to lessen its toxicity towards epithelial cells and fibroblasts.[105]

The ability of dehydroabietic acid (**4**) (Fig. 2) to limit biofilm formation in *Staphylococcus aureus* strains was first reported following the observation that two abietane-type diterpenoids, namely, 4-*epi*-pimaric acid and salvipisone, were bacterial biofilm inhibitors.[107] This compound was found to prevent biofilm formation in the low micromolar range, displaying a good cytocompatibility index, *i.e.*, being well tolerated by human cells (Table 3, entry 2). With an MIC value of 70 µM, dehydroabietic acid (**4**) could affect the viability and biomass of established biofilms at only 2- to 4-fold higher concentrations, an effect that could not be observed in the presence of antibiotics such as penicillin G and vancomycin, even at the impractical concentrations of 400 µM.[107,108,163] Other studies evaluated the antimicrobial and antibiofilm potential of dehydroabietic acid (**4**) against several Gram-positive and Gram-negative strains.[9,109–111,164] Overall, similar to abietic acid (**3**), dehydroabietic acid (**4**) was mostly active against Gram-positive bacteria.

Taxodone (**111**) (Fig. 12) was reported to be a moderate antistaphylococcal and antifungal agent, with MIC values of 31.25 and 62.5 µg mL$^{-1}$ against *Staphylococcus aureus* and *Candida albicans*, respectively (Table 3, entry 3).[113] Taxodione (**112**) displayed an IC$_{50}$ value of 0.05 µM against *Trypanosoma brucei rhodesiense* trypomastigotes, with very high selectivity, and was also active against *Trypanosoma cruzi* amastigotes and *Plasmodium falciparum*, but with low selectivity (Table 3, entry 4).[114] Taxodone (**111**) and 7-(2′-oxohexyl)-taxodione (**113**) were both less potent and selective than taxodione (**112**) (Table 3, entry 5). Taxodione (**112**) was also active against *Leishmania donovani*, *Leishmania amazonensis* and *Leishmania infantum* and exhibited antifungal and antimicrobial activities.[115–117] Horminones **114** and **115** (Fig. 12) displayed antistaphylococcal activity (Table 3, entries 6 and 7, respectively) and were synergistic (FIC value of 0.2) against MRSA when combined.[115,118] Horminone **115** displayed antimycobacterial activity, with MIC$_{90}$ values ranging from 11.93 to 44.19 µM, and was active against *Leishmania donovani* promastigotes.[115,118] Plectranthroyleanones B (**116**) and C (**117**) (Fig. 12) had moderate activity against the Gram-negative *Klebsiella pneumoniae*, with MIC values of 37.5 µg mL$^{-1}$ (Table 3, entries 8 and 9, respectively).[119] A paper disk test revealed that compounds **118–121** (Fig. 12) from *Caryopteris mongolica* were potentially active against Gram-positive bacteria including *Staphylococcus aureus*, *Enterococcus faecalis* and *Micrococcus luteus*.[165]

The presence of inhibition zones also indicated the potential antimicrobial activity of royleanones **122–125** (Fig. 12), isolated

1874 | *Nat. Prod. Rep.*, 2024, **41**, 1858–1894

This journal is © The Royal Society of Chemistry 2024

**Table 3** Biological activities of the naturally occurring tricyclic diterpenoids

| Entry | Compound | Source | Reported biological activity[a] | Ref. |
|---|---|---|---|---|
| 1 | Abietic acid (3) | Genus *Pinus* | MIC (*Cutibacterium acnes*\*) = 4 μg mL$^{-1}$ (13 μM)<br>MIC (*Staphylococcus epidermidis*\*) = 8 μg mL$^{-1}$ (27 μM)<br>MIC (*Streptococcus mitis*\*) = 16 μg mL$^{-1}$ (53 μM)<br>MIC (*Staphylococcus aureus*\*, *Pseudomonas fluorescens*\*\*) = 25 μg mL$^{-1}$ (83 μM)<br>MIC (*Salmonella typhimurium*\*\*, *Rothia mucilaginosa*\*) = 31 μg mL$^{-1}$ (103 μM)<br>MIC (*Bacillus subtilis*\*, *Escherichia coli*\*\*) = 50 μg mL$^{-1}$ (167 μM) | 103–105 and 106 |
| 2 | Dehydroabietic acid (4) | | IC$_{50}$ (pre$^b$, *Staphylococcus aureus*\*) = 27.8 μM; IC$_{50}$ (post$^c$, *Staphylococcus aureus*\*) = 112.8 μM; fold$^d$ = 2–4<br>MIC (*Staphylococcus aureus*\*) = 70 μM<br>MIC (*Staphylococcus aureus* Newman) = 12.5–25 μg mL$^{-1}$ (41–83 μM)<br>MIC (*Bacillus subtilis*\*, *Pseudomonas fluorescens*\*\*) = 50 μg mL$^{-1}$ (166 μM)<br>MIC (*Saccharomyces cerevisiae*) = 62.5 μg mL$^{-1}$ (207 μM) | 107, 108, 109–111, 106 and 112 |
| 3 | Taxodone (111) | *Salvia austriaca* | MIC (*Staphylococcus aureus*\*) = 31.25 μg mL$^{-1}$ (99 μM)<br>MIC (*Candida albicans*) = 62.5 μg mL$^{-1}$ (198 μM)<br>IC$_{50}$ (*Trypanosoma brucei rhodesiense$^f$*) = 1.67 μM, SI = 2.4<br>IC$_{50}$ (*Plasmodium falciparum*) = 3.66 μM, SI = 1.1<br>IC$_{50}$ (*Trypanosoma cruzi$^f$*) = 7.63 μM, SI < 1 | 113 and 114 |
| 4 | Taxodione (112) | *Salvia deserta*<br>*Salvia austriaca*<br>*Plectranthus barbatus*<br>*Taxodium distichum* | MIC (*Staphylococcus aureus*\*, MRSA\*) = 31.8 μM<br>MIC (*Candida glabrata, Cryptococcus neoformans*) = 15.9 μM<br>MIC (*Candida krusei*) = 31.8 μM<br>MIC (*Candida albicans*) = 63.6 μM<br>IC$_{50}$ (*Trypanosoma brucei rhodesiense$^f$*) = 0.05 μM, SI = 38<br>IC$_{50}$ (*Leishmania donovani$^g$*) = 1.46 μM<br>IC$_{50}$ (*Plasmodium falciparum*) = 1.9 μM, SI = 1<br>IC$_{50}$ (*Trypanosoma cruzi$^g$*) = 7.11 μM, SI < 1<br>IC$_{50}$ (*Trypanosoma brucei$^c$*) = 9.8 μM, SI = 2.3<br>IC$_{50}$ (*Leishmania amazonensis$^f$*) = 14.3 μM, SI < 1<br>IC$_{50}$ (*Leishmania infantum$^g$*, *Trypanosoma cruzi$^{jh}$*) = 25.7 μM | 114–117 |
| 5 | (113) | *Salvia austriaca* | IC$_{50}$ (*Trypanosoma brucei rhodesiense$^f$*) = 0.62 μM, SI = 5<br>IC$_{50}$ (*Plasmodium falciparum*) = 3.37 μM, SI < 1<br>IC$_{50}$ (*Trypanosoma cruzi$^f$*) = 7.76 μM, SI < 1 | 114 |
| 6 | Horminone (114) | *Plectranthus madagascariensis* | IC$_{50}$ (MRSA\*) = 29.7 μM<br>IC$_{50}$ (*Staphylococcus aureus*\*) = 38.7 μM | 115 |
| 7 | Horminone (115) | | IC$_{50}$ (MRSA\*) = 6.8 μM<br>IC$_{50}$ (*Staphylococcus aureus*\*) = 8.3 μM<br>IC$_{50}$ (*Mycobacterium tuberculosis*) = 11.93–44.19 μM<br>IC$_{50}$ (*Leishmania donovani$^f$*) = 29.43 μM | 115 and 118 |
| 8 | Plectranthroyleanone B (116) | *Plectranthus africanus* | MIC (*Klebsiella pneumoniae*\*\*) = 37.5 μg mL$^{-1}$ (80 μM) | 119 |
| 9 | Plectranthroyleanone C (117) | | MIC (*Klebsiella pneumoniae*\*\*) = 37.5 μg mL$^{-1}$ (83 μM) | |
| 10 | (126) | *Kaempferia roscoeana* | MIC (*Staphylococcus aureus*\*) = 25 μg mL$^{-1}$ (93 μM) | 120 |
| 11 | (127) | | MIC (*Staphylococcus epidermidis*\*, *Bacillus cereus*\*) = 25 μg mL$^{-1}$ (88 μM) | |
| 12 | (128) | *Plectranthus madagascariensis*<br>*Plectranthus grandidentatus* | MIC (*Enterococcus* spp.$^i$) = 7.81–15.63 μg mL$^{-1}$ (20–40 μM)<br>MIC (*Mycobacterium tuberculosis*) = 39.2–40.08 μM | 118 and 121 |

This journal is © The Royal Society of Chemistry 2024

*Nat. Prod. Rep.*, 2024, **41**, 1858–1894 | **1875**

**Table 3** (Contd.)

| Entry | Compound | Source | Reported biological activity[a] | Ref. |
|---|---|---|---|---|
| 13 | (129) | Plectranthus madagascariensis | MIC (Mycobacterium tuberculosis) = 1.93–15.62 µg mL$^{-1}$ (5.6–45 µM) | 118 |
| 14 | Torgranol E (130) | Torreya grandis | MIC (Mycobacterium tuberculosis) = 16 µg mL$^{-1}$ (47 µM) | 122 |
| 15 | (131) | | MIC (Mycobacterium tuberculosis) = 16 µg mL$^{-1}$ (51 µM) | |
| 16 | (132) | | MIC (Mycobacterium tuberculosis, Staphylococcus aureus*) = 16 µg mL$^{-1}$ (51 µM) | |
| 17 | Ferruginol (133) | Salvia deserta | MIC (MRSA*) = 17.5 µM | 115, 117, 123, 124 and 125 |
| | | Salvia hydrangea | MIC (Staphylococcus aureus*) = 34.9 µM | |
| | | Taxodium distichum | EC$_{50}$ (Plasmodium falciparum$^f$) = 0.20 µM | |
| | | Salvia sahendica | IC$_{50}$ (Plasmodium falciparum) = 2.9 µM | |
| | | Podocarpus ferruginea | IC$_{50}$ (Leishmania donovani$^f$) = 5.9 µM | |
| | | | IC$_{50}$ (Trypanosoma brucei rhodesiense$^h$) = 16.6 µM | |
| | | | IC$_{50}$ (Leishmania donovani$^e$) = 45.7 µM, SI < 1 | |
| | | | IC$_{50}$ (Leishmania amazonensis$^f$) = 4.4 µg mL$^{-1}$ (15 µM) | |
| | | | IC$_{50}$ (Leishmania major$^e$) = 12.1 µg mL$^{-1}$ (42 µM) | |
| 18 | (134) | Perowskia abrotanoides | IC$_{50}$ (Trypanosoma brucei rhodesiense$^h$) = 7.2 µM | 126 and 124 |
| | | Salvia sahendica | IC$_{50}$ (Plasmodium falciparum) = 9.6 µM | |
| | | | IC$_{50}$ (Leishmania donovani$^e$) = 11.6 µM | |
| 19 | Miltiodiol (135) | Perowskia abrotanoides | IC$_{50}$ (Trypanosoma brucei rhodesiense$^h$) = 0.5 µM | 126 |
| | | | IC$_{50}$ (Leishmania donovani$^h$) = 17 µM | |
| 20 | (136) | | IC$_{50}$ (Trypanosoma brucei rhodesiense$^f$) = 0.8 µM | |
| | | | IC$_{50}$ (Leishmania donovani$^e$) = 1.8 µM | |
| | | | IC$_{50}$ (Plasmodium falciparum) = 16.2 µM | |
| 21 | (137) | Torreya grandis | MIC (Staphylococcus aureus*) = 4 µg mL$^{-1}$ (13 µM) | 117 and 122 |
| | | | MIC (Mycobacterium tuberculosis) = 16 µg mL$^{-1}$ (51 µM) | |
| | | | IC$_{50}$ (Leishmania amazonensis$^f$) = 5.4 µg mL$^{-1}$ (17 µM) | |
| 22 | (138) | Taxodium distichum | IC$_{50}$ (Leishmania donovani$^e$) = 7.8 µg mL$^{-1}$ (25 µM) | 117 |
| | | | IC$_{50}$ (Leishmania amazonensis$^f$) = 0.52 µg mL$^{-1}$ (1.4 µM) | |
| 23 | (139) | Salvia repens | IC$_{50}$ (Leishmania donovani$^e$) = 2.5 µg mL$^{-1}$ (6.9 µM) | 127 |
| 24 | (143) | Salvia lerifolia | IC$_{50}$ (Leishmania donovani$^f$) = 0.75 µg mL$^{-1}$ (2.2 µM), SI = 23.8 | 128 |
| | | | IC$_{50}$ (Plasmodium falciparum) = 0.4 µM, SI = 84 | |
| | | | IC$_{50}$ (Trypanosoma brucei rhodesiense) = 19.7 µM | |
| | | | IC$_{50}$ (Trypanosoma cruzi$^h$) = 27.6 µM | |
| 25 | (144) | | IC$_{50}$ (Trypanosoma brucei rhodesiense$f$; Leishmania donovani$^f$) = 1.0 µM | |
| | | | IC$_{50}$ (Plasmodium falciparum) = 3.6 µM | |
| | | | IC$_{50}$ (Trypanosoma cruzi$^h$) = 4.6 µM | |
| 26 | Mangiolide (145) | Suregada zanzibariensis | IC$_{50}$ (MRSA*) = 3.9 µg mL$^{-1}$ (11 µM) | 129 |
| | | Suregada zanzibariensis | IC$_{50}$ (VRE*) = 7.2 µg mL$^{-1}$ (19 µM) | |
| | | | IC$_{50}$ (Cryptococcus neoformans) = 1.2 µg mL$^{-1}$ (3.2 µM) | |
| | | | IC$_{50}$ (Plasmodium falciparum) = 0.76 µg mL$^{-1}$ (2 µM), SI < 10 | |
| | | | IC$_{50}$ (Plasmodium falciparum$^j$) = 0.89 µg mL$^{-1}$ (2.4 µM), SI < 10 | |
| 27 | (146) | | IC$_{50}$ (Plasmodium falciparum$^f$) = 1.17 µg mL$^{-1}$ (3.5 µM), SI < 10 | |
| | | | IC$_{50}$ (Plasmodium falciparum) = 1.24 µg mL$^{-1}$ (3.8 µM), SI < 10 | |
| 28 | (147) | Plectranthus barbatus | IC$_{50}$ (Trypanosoma brucei$^h$) = 1.9 µM, SI = 50.5 | 116 |
| | | | IC$_{50}$ (Plasmodium falciparum) = 9.2 µM, SI = 10.4 | |
| | | | IC$_{50}$ (Leishmania infantum$^f$, Trypanosoma cruzi$^h$) = 25.7 µM, SI = 3.7 | |
| 29 | Clinopodiolide A (148) | Salvia clinopodioides | IC$_{50}$ (Entamoeba histolytica) = 43.0 µM | 130 |
| | | | IC$_{50}$ (Giardia lamblia) = 67.1 µM | |

1876 | Nat. Prod. Rep., 2024, 41, 1858–1894

This journal is © The Royal Society of Chemistry 2024

**Table 3** (*Contd.*)

| Entry | Compound | Source | Reported biological activity[a] | Ref. |
|---|---|---|---|---|
| 30 | Clinopodiolide B (149) | | $IC_{50}$ (*Entamoeba histolytica*) = 37.8 μM<br>$IC_{50}$ (*Giardia lamblia*) = 63 μM | |
| 31 | (150) | | $IC_{50}$ (*Entamoeba histolytica*) = 34.9 μM<br>$IC_{50}$ (*Giardia lamblia*) = 46.4 μM | |
| 32 | Triacetylclinopodiolide B (151) | | $IC_{50}$ (*Entamoeba histolytica*) = 39.5 μM<br>$IC_{50}$ (*Giardia lamblia*) = 47.7 μM | |
| 33 | Clinopodiolide C (152) | | $IC_{50}$ (*Entamoeba histolytica*) = 31.3 μM<br>$IC_{50}$ (*Giardia lamblia*) = 49.0 μM | |
| 34 | (153) | *Croton cascarilloide* | MIC (*Corynebacterium* spp.*) = 31 μg mL$^{-1}$ (103 μM)<br>MIC (*Enterococcus faecalis**) = 43 μg mL$^{-1}$ (142 μM)<br>MIC (*Enterococcus* spp.*) = 46 μg mL$^{-1}$ (152 μM) | 131 |
| 35 | (154) | | MIC (*Corynebacterium* spp.*) = 40 μg mL$^{-1}$ (119 μM)<br>MIC (*Enterococcus faecalis*, Enterococcus* spp.*) = 49 μg mL$^{-1}$ (147 μM) | |
| 36 | (155) | | MIC (*Corynebacterium* spp.*) = 35 μg mL$^{-1}$ (99 μM)<br>MIC (*Enterococcus faecalis**) = 41 μg mL$^{-1}$ (116 μM)<br>MIC (*Enterococcus* spp.*) = 47 μg mL$^{-1}$ (133 μM) | |
| 37 | Eupholide F (156) | *Euphorbia fischeriana* | MIC (*Mycobacterium tuberculosis*) = 50 μM | 132 |
| 38 | Eupholide G (157) | | MIC (*Mycobacterium tuberculosis*) = 50 μM | |
| 39 | Eupholide H (158) | | MIC (*Mycobacterium tuberculosis*) = 50 μM | |
| 40 | Jolkinolide B (159) | | MIC (*Mycobacterium smegmatis*) = 25 μg mL$^{-1}$ (77 μM) | 133 |
| 41 | 17-Hydroxyjolkinolide B (160) | | MIC (*Mycobacterium smegmatis*) = 1.5 μg mL$^{-1}$ (4.3 μM) | |
| 42 | (161) | *Euphorbia wallichii* | MIC (*Corynebacterium* spp.*) = 35 μg mL$^{-1}$ (107 μM)<br>MIC (*Enterococcus faecalis**) = 51 μg mL$^{-1}$ (155 μM)<br>MIC (*Enterococcus* spp.*) = 59 μg mL$^{-1}$ (180 μM) | 134 |
| 43 | (162) | | MIC (*Corynebacterium* spp.*) = 37 μg mL$^{-1}$ (108 μM)<br>MIC (*Enterococcus faecalis**) = 45 μg mL$^{-1}$ (131 μM)<br>MIC (*Enterococcus* spp.*) = 56 μg mL$^{-1}$ (163 μM) | |
| 44 | Icacinlactone H (163) | *Icacina trichantha* | MIC (*Helicobacter pylori*[1]**) = 8–16 μg mL$^{-1}$ (22–43 μM) | 135 |
| 45 | Icacinlactone B (164) | | MIC (*Helicobacter pylori*[1]**) = 8–16 μg mL$^{-1}$ (23–45 μM) | |
| 46 | Libertellenone A (165) | *Eutypella* spp. | MIC (*Escherichia coli**, Bacillus subtilis*, Vibrio vulnificus***) = 16 μg mL$^{-1}$ (48 μM)<br>MIC (*Staphylococcus aureus**) = 32 μg mL$^{-1}$ (96 μM) | 136 |
| 47 | Eutypellenoid B (166) | | MIC (*Escherichia coli**, Staphylococcus aureus**) = 8 μg mL$^{-1}$ (17 μM)<br>MIC (*Bacillus subtilis*, Vibrio alginolyticus**, Vibrio vulnificus**, Streptococcus agalactiae**) = 32 μg mL$^{-1}$ (68 μM)<br>MIC (*Candida parapsilosis, Candida albicans*) = 8 μg mL$^{-1}$ (17 μM)<br>MIC (*Candida glabrata*) = 16 μg mL$^{-1}$ (34 μM)<br>MIC (*Candida tropicalis*) = 32 μg mL$^{-1}$ (68 μM) | 137 |
| 48 | Eutypellenoid C (167) | | MIC (*Escherichia coli**, Staphylococcus aureus*, Bacillus subtilis**) = 32 μg mL$^{-1}$ (68 μM) | |
| 49 | Eutypenoid C (168) | *Azadirachta indica* | MIC (*Staphylococcus aureus**) = 32 μg mL$^{-1}$ (67 μM) | 138 |
| 50 | (169) | | MIC (*Pleomorphomonas oryzae***) = 32 μg mL$^{-1}$ (86 μM)<br>MIC (*Candida albicans*) = 64 μg mL$^{-1}$ (172 μM) | |
| 51 | (170) | | MIC (*Pleomorphomonas oryzae***) = 16 μg mL$^{-1}$ (40 μM)<br>MIC (*Candida albicans*) = 16 μg mL$^{-1}$ (40 μM)<br>MIC (*Aspergillus niger*) = 32 μg mL$^{-1}$ (80 μM) | |

This journal is © The Royal Society of Chemistry 2024

*Nat. Prod. Rep.*, 2024, **41**, 1858–1894 | **1877**

Table 3 (Contd.)

| Entry | Compound | Source | Reported biological activity[a] | Ref. |
|---|---|---|---|---|
| 52 | (171) | Aldama discolor | IC$_{50}$ (Plasmodium falciparum) = 3.8 μM, SI = 13<br>IC$_{50}$ (Trypanosoma cruzi[f]) = 15.4 μM, SI < 10<br>IC$_{50}$ (Leishmania donovani[f]) = 18.2 μM, SI < 10 | 139 |
| 53 | (172) | Aspergillus ochraceus | IC$_{50}$ (Trypanosoma brucei rhodesiense[h]) = 24.3 μM, SI < 10<br>MIC (Staphylococcus aureus[i,**]) = 8–10 μg mL$^{-1}$ (26–33 μM)<br>MIC (Staphylococcus capitis*, Staphylococcus haemolyticus*, Streptococcus pneumoniae*) = 9 μg mL$^{-1}$ (29 μM)<br>MIC (Staphylococcus epidermidis *) = 12 μg mL$^{-1}$ (39 μM)<br>MIC (Enterococcus faecalis *) = 25 μg mL$^{-1}$ (82 μM) | 140 |
| 54 | Talascortene C (173) | Talaromyces scorteus | MIC (Escherichia coli**) = 8 μg mL$^{-1}$ (23 μM) | 70 |
| 55 | Talascortene D (174) | | MIC (Escherichia coli**) = 16 μg mL$^{-1}$ (48 μM) | |
| 56 | Talascortene E (175) | | MIC (Escherichia coli**) = 1 μg mL$^{-1}$ (2.9 μM)<br>MIC (Micrococcus luteus*) = 8 μg mL$^{-1}$ (23 μM) | |
| 57 | Talascortene F (176) | | MIC (Escherichia coli**) = 8 μg mL$^{-1}$ (23 μM) | |
| 58 | Talascortene G (177) | | MIC (Vibrio parahaemolyticus**) = 8 μg mL$^{-1}$ (22 μM)<br>MIC (Pseudomonas aeruginosa**) = 32 μg mL$^{-1}$ (88 μM) | |
| 59 | (178) | Perowskia abrotanoides | IC$_{50}$ (Plasmodium falciparum) = 14.8 μM, SI = 5.2<br>IC$_{50}$ (Leishmania donovani[f]) = 27.7 μM, SI = 2.8 | 124 |
| 60 | (179) | Aldama discolor | IC$_{50}$ (Leishmania donovani[f]) = 13.8 μM, SI < 10<br>IC$_{50}$ (Plasmodium falciparum) = 16.5 μM<br>IC$_{50}$ (Trypanosoma cruzi[f]) = 19.4 μM, SI < 10 | 139 |
| 61 | (180) | | IC$_{50}$ (Plasmodium falciparum) = 16.1 μM<br>IC$_{50}$ (Leishmania donovani[f]) = 21.9 μM, SI < 10 | |
| 62 | (181) | Swartzia simplex | MIC (Candida albicans) = 32 μg mL$^{-1}$ (89 μM) | 141 |
| 63 | Simplexene D (182) | | MIC (Candida albicans) = 32 μg mL$^{-1}$ (92 μM) | |
| 64 | Bokkosin (183) | Calliandra portoricensis | EC$_{50}$ (Trypanosoma brucei[k,e]) = 0.33 μg mL$^{-1}$ (0.5 μM)<br>EC$_{50}$ (Trypanosoma brucei[e]) = 0.69 μg mL$^{-1}$ (1.1 μM), SI > 200<br>EC$_{50}$ (Leishmania mexicana[f]) = 5.8–9.2 μg mL$^{-1}$ (9.2–15 μM)<br>EC$_{50}$ (Trypanosoma congolense[e,t]) = 17.5 μg mL$^{-1}$ (28 μM)<br>EC$_{50}$ (Trypanosoma congolense[g]) = 21.6 μg mL$^{-1}$ (34 μM) | 142 |
| 65 | Caesalsappanin A (184) | Caesalpinia sappan | IC$_{50}$ (Plasmodium falciparum) = 7.4 μM, SI < 10 | 143 |
| 66 | Caesalsappanin E (185) | | IC$_{50}$ (Plasmodium falciparum) = 15.7 μM, SI > 10 | |
| 67 | Caesalsappanin G (186) | | IC$_{50}$ (Plasmodium falciparum) = 0.78 μM, SI > 10 | |
| 68 | Caesalsappanin H (187) | | IC$_{50}$ (Plasmodium falciparum) = 0.52 μM, SI > 10 | |
| 69 | Caesalsappanin I (188) | | IC$_{50}$ (Plasmodium falciparum) = 2.5 μM, SI > 10 | |
| 70 | (189) | Caesalpinia pulcherrima | IC$_{50}$ (Leishmania major[f]) = 30 μg mL$^{-1}$ (65 μM) | 144 |

[a] Units reported according to the original reference. Conversion into micromolar is shown in brackets (μM). MIC = Minimum inhibitory concentration; IC$_{50}$ = Concentration that inhibit the growth of a species by 50%; EC$_{50}$ = concentration corresponding to 50% growth inhibition of the parasite or cells; SI = Selectivity index; MRSA = Methicillin-resistant Staphylococcus aureus; VRE = Vancomycin-resistant Enterococcus; *Gram-positive; **Gram-negative. [b] Prior to biofilm establishment. [c] After biofilms are established. [d] IC$_{50}$(post)/IC$_{50}$(pre). [e] Promastigotes. [f] Amastigotes. [g] Parasite residing inside cells. [h] Trypomastigotes. [i] Several strains. [j] Chloroquine-resistant. [k] Pentamidine-resistant. [l] Diminazene-resistant.

1878 | Nat. Prod. Rep., 2024, 41, 1858–1894

This journal is © The Royal Society of Chemistry 2024

**Table 4** Biological activities of semi-synthetic tricyclic diterpenoids[a]

| Entry | Compound | Reported biological activity[b] | Ref. |
|---|---|---|---|
| 1 | **190** | MIC (*Staphylococcus epidermidis*\*) = 16 μg mL$^{-1}$ (40 μM) | 104 |
| | | MIC (*Rothia mucilaginosa*\*) = 31 μg mL$^{-1}$ (77 μM) | |
| 2 | **191** | MIC (*Staphylococcus aureus*\*) = 16 μg mL$^{-1}$ (35 μM) | 145 |
| | | MIC (*Cryptococcus neoformans* var. *grubii*) = 4 μg mL$^{-1}$ (8.8 μM) | |
| | | MIC (*Candida albicans*) = 8 μg mL$^{-1}$ (18 μM) | |
| 3 | **192** | MIC (*Candida albicans*) = 15.62 μg mL$^{-1}$ (23 μM) | 146 |
| 4 | **193** | MIC (*Staphylococcus aureus*[b],\*) = 1.56–3.13 μg mL$^{-1}$ (2.5–5 μM) | 110 |
| 5 | **194** | MIC (*Staphylococcus aureus*[b],\*) = 1.25–3.13 μg mL$^{-1}$ (2–5.1 μM) | |
| 6 | **195** | MIC (*Staphylococcus aureus*[b],\*) = 1.56–3.13 μg mL$^{-1}$ (2.9–5.8 μM) | |
| 7 | **196** | MIC (*Staphylococcus aureus*[b],\*) = 0.39–6.25 μg mL$^{-1}$ (0.8–13 μM) | 111 |
| 8 | **197** | MIC (*Staphylococcus aureus*[b],\*) = 1.25–3.13 μg mL$^{-1}$ (2.7–6.8 μM) | |
| 9 | **198** | MIC (*Staphylococcus aureus*[b],\*) = 1.56–3.13 μg mL$^{-1}$ (3.2–6.4 μM) | |
| 10 | **199** | MIC (*Staphylococcus aureus*[b],\*) = 1.56–6.25 μg mL$^{-1}$ (2.7–10 μM) | 147 |
| 11 | **200** | MIC (MRSA\*) = 7.8–31.2 μg mL$^{-1}$ (24–94 μM) | 153 |
| | | MIC (*Staphylococcus aureus*\*) = 15.6–31.2 μg mL$^{-1}$ (47–94 μM) | |
| 12 | **201** | MIC (MRSA\*) = 3.9–7.8 μg mL$^{-1}$ (11–23 μM) | |
| | | MIC (*Staphylococcus aureus*\*) = 7.8–15.6 μg mL$^{-1}$ (23–45 μM) | |
| 13 | **202** | MIC (MRSA\*) = 15.6–31.2 μg mL$^{-1}$ (43–87 μM) | |
| | | MIC (*Staphylococcus aureus*\*) = 31.2 μg mL$^{-1}$ (87 μM) | |
| 14 | **203** | MIC (MRSA\*) = 31.2–62.5 μg mL$^{-1}$ (83–167 μM) | |
| | | MIC (*Staphylococcus aureus*\*) = 62.5 μg mL$^{-1}$ (167 μM) | |
| 15 | **204** | MIC (*Staphylococcus aureus*\*, *Escherichia coli*\*\*) = 3.1 μg mL$^{-1}$ (6 μM) | 106 |
| | | MIC (*Pseudomonas fluorescens*\*\*) = 6.3 μg mL$^{-1}$ (12 μM) | |
| | | MIC (*Bacillus subtilis*\*) = 12.5 μg mL$^{-1}$ (24 μM) | |
| 16 | **205** | MIC (*Staphylococcus aureus*\*, *Escherichia coli*\*\*, *Pseudomonas fluorescens*\*\*) = 1.6 μg mL$^{-1}$ (3.1 μM) | |
| | | MIC (*Bacillus subtilis*\*) = 3.1 μg mL$^{-1}$ (6 μM) | |
| 17 | **206** | MIC (*Bacillus subtilis*\*) = 1.9 μg mL$^{-1}$ (4.1 μM) | 148 |
| | | MIC (*Escherichia coli*\*\*) = 3.9 μg mL$^{-1}$ (8.4 μM) | |
| | | MIC (*Staphylococcus aureus*\*) = 7.8 μg mL$^{-1}$ (17 μM) | |
| | | MIC (*Pseudomonas fluorescens*\*\*) = 15.6 μg mL$^{-1}$ (34 μM) | |
| | | MIC (*Candida albicans*) = 31.2 μg mL$^{-1}$ (67 μM) | |
| 18 | **207** | MIC (*Escherichia coli*\*\*, *Pseudomonas fluorescens*\*\*) = 7.8 μg mL$^{-1}$ (17 μM) | |
| | | MIC (*Bacillus subtilis*\*, *Staphylococcus aureus*\*) = 15.6 μg mL$^{-1}$ (34 μM) | |
| | | MIC (*Candida albicans*, *Candida tropicalis*) = 31.2 μg mL$^{-1}$ (69 μM) | |
| 19 | **208** | MIC (MRSA\*) = 31.2 μg mL$^{-1}$ (74 μM) | 149 |
| 20 | **209** | MIC (*Staphylococcus aureus*\*) = 1.9 μg mL$^{-1}$ (3.6 μM) | 150 |
| | | MIC (*Bacillus subtilis*\*) = 3.9 μg mL$^{-1}$ (7.4 μM) | |
| | | MIC (*Pseudomonas fluorescens*\*\*) = 7.8 μg mL$^{-1}$ (15 μM) | |
| | | MIC (*Escherichia coli*\*\*) = 15.6 μg mL$^{-1}$ (30 μM) | |
| | | MIC (*Candida albicans*, *Candida tropicalis*, *Aspergillus niger*) = 7.8 μg mL$^{-1}$ (15 μM) | |
| 21 | **210** | MIC (*Bacillus subtilis*\*) = 0.9 μg mL$^{-1}$ (1.6 μM) | |
| | | MIC (*Staphylococcus aureus*\*) = 1.9 μg mL$^{-1}$ (3.4 μM) | |
| | | MIC (*Escherichia coli*\*\*, *Pseudomonas fluorescens*\*\*) = 7.8 μg mL$^{-1}$ (14 μM) | |
| | | MIC (*Candida albicans*, *Candida tropicalis*) = 31.2 μg mL$^{-1}$ (56 μM) | |
| 22 | **211** | IC$_{50}$ (pre[c], *Staphylococcus aureus*\*) = 33.2 μM; IC$_{50}$ (post[d], *Staphylococcus aureus*\*) = 86.1 μM; fold[e] = 3 | 108 and 112 |
| | | MIC (*Staphylococcus aureus*\*) = 60 μM | |
| 23 | **212** | IC$_{50}$ (pre[c], *Staphylococcus aureus*\*) = 9.4 μM; IC$_{50}$ (post[d], *Staphylococcus aureus*\*) = 27.9 μM; fold[e] = 3 | |
| | | MIC (*Staphylococcus aureus*\*) = 15 μM | |
| | | IC$_{50}$ (*Leishmania donovani*[f]) = 5 μM, SI = 24 | |
| 24 | **213** | MIC (*Staphylococcus epidermidis*\*, *Streptococcus mitis*\*) = 8 μg mL$^{-1}$ (20 μM) | 104 |
| | | MIC (*Cutibacterium acnes*\*) = 16 μg mL$^{-1}$ (40 μM) | |
| | | MIC (*Rothia mucilaginosa*\*, *Salmonella typhimurium*\*\*) = 31 μg mL$^{-1}$ (77 μM) | |
| 25 | **214** | MIC (MRSA\*) = 7.4 μM | 151 |
| | | MIC (*Staphylococcus aureus*\*) = 15 μM | |
| 26 | **215** | IC$_{50}$ (*Trypanosoma cruzi*[f]) = 4.2 μM, SI = 8 | 152 |
| | | IC$_{50}$ (*Leishmania donovani*[f]) = 6.6 μM, SI = 14 | |
| 27 | **216** | IC$_{50}$ (*Trypanosoma cruzi*[f]) = 3.9 μM, SI = 20 | |
| | | IC$_{50}$ (*Leishmania donovani*[f]) = 2.3 μM, SI = 15 | |
| 28 | **217** | IC$_{50}$ (*Leishmania donovani*[f]) = 9 μM, SI = 33 | |
| 29 | **218** | IC$_{50}$ (*Trypanosoma cruzi*[f]) = 1.4 μM, SI = 17 | |
| 30 | **219** | IC$_{50}$ (*Trypanosoma cruzi*[f]) = 7.1 μM, SI = 31.4 | 153 |
| 31 | **220** | IC$_{50}$ (*Leishmania infantum*[g]) = 2.5 μM, SI = 51.8 | 154 |
| | | IC$_{50}$ (*Leishmania amazonensis*[g]) = 11.6 μM, SI = 11.2 | |
| | | IC$_{50}$ (*Leishmania guyanensis*[g]) = 14.2 μM, SI = 9.1 | |

**Table 4** (Contd.)

| Entry | Compound | Reported biological activity[b] | Ref. |
|---|---|---|---|
| 32 | 221 | $IC_{50}$ (*Leishmania donovani*[g]) = 14.8 μM, SI = 8.8 | |
| | | $IC_{50}$ (*Leishmania infantum*[h]) = 37.2 μM, SI = 3.5 | |
| | | $IC_{50}$ (*Leishmania amazonensis*[i]) = 31.4 μM, SI = 4.1 | |
| | | $IC_{50}$ (*Leishmania amazonensis*[g]) = 3.9 μM, SI = 8.7 | |
| | | $IC_{50}$ (*Leishmania infantum*[g]) = 5.0 μM, SI = 6.8 | |
| | | $IC_{50}$ (*Leishmania guyanensis*[g]) = 5.9 μM, SI = 5.8 | |
| | | $IC_{50}$ (*Leishmania donovani*[g]) = 9.21 μM, SI = 3.7 | |
| 33 | 222 | MIC (*Aspergillus fumigatus*, *Aspergillus terreus*) = 25 μg mL⁻¹ (83 μM) | 155 |
| | | MIC (*Aspergillus niger*) = 50 μg mL⁻¹ (165 μM) | |
| 34 | 223 | $EC_{50}$ (DENV-2[i]) = 1.4 μM, SI = 57.7 | 156 and 157 |
| | | $EC_{50}$ (ZIKV[i]) = 6.3 μM | |
| | | $EC_{50}$ (Brazilian ZIKV[i]) = 7.7 μM | |
| | | $EC_{50}$ (Colombian CHIKV[i]) = 9.8 μM | |
| | | $EC_{50}$ (HHV-2[i]) = 19.2 μM | |
| 35 | 226 | MIC (*Staphylococcus aureus**, *Escherichia coli***) = 30 μM | 158 |
| 36 | 227 | $IC_{50}$ (*Leishmania donovani*[f]) = 0.06 μM | 159 |
| | | $IC_{50}$ (*Leishmania donovani*[h]) = 0.37 μM, SI = 63 | |
| | | $IC_{50}$ (*Trypanosoma cruzi*[f]) = 0.6 μM, SI = 58 | |
| 37 | 228 | $IC_{50}$ (*Leishmania donovani*[g]) = 2.2 μM, SI > 90 | 160 |
| | | $IC_{50}$ (*Leishmania infantum*[g]) = 3.1 μM, SI > 64 | |
| | | $IC_{50}$ (*Leishmania amazonensis*[g]) = 3.7 μM, SI > 54 | |
| | | $IC_{50}$ (*Leishmania infantum*[h]) = 4.7 μM, SI > 42 | |
| | | $IC_{50}$ (*Leishmania amazonensis*[h]) = 5.0 μM, SI > 40 | |
| | | $IC_{50}$ (*Leishmania guyanensis*[g]) = 20.4 μM, SI > 10 | |
| 38 | 229 | $IC_{50}$ (*Leishmania donovani*[g]) = 3.2 μM, SI > 62 | |
| | | $IC_{50}$ (*Leishmania infantum*[g]) = 3.3 μM, SI > 18 | |
| | | $IC_{50}$ (*Leishmania infantum*[h]) = 3.3 μM, SI > 61 | |
| | | $IC_{50}$ (*Leishmania amazonensis*[h]) = 3.5 μM, SI > 57 | |
| | | $IC_{50}$ (*Leishmania amazonensis*[g]) = 20.7 μM, SI > 100 | |
| 39 | 230 | $IC_{50}$ (*Leishmania amazonensis*[h]) = 3.7 μM, SI > 54 | |
| | | $IC_{50}$ (*Leishmania donovani*[g]) = 5.4 μM, SI > 37 | |
| | | $IC_{50}$ (*Leishmania amazonensis*[g]) = 12.2 μM, SI > 16 | |
| | | $IC_{50}$ (*Leishmania infantum*[h]) = 17.5 μM, SI > 11 | |
| | | $IC_{50}$ (*Leishmania infantum*[g]) = 23.9 μM, SI > 8 | |
| | | $IC_{50}$ (*Leishmania guyanensis*[g]) = 38.5 μM, SI > 5 | |
| 40 | 231 | $IC_{50}$ (*Leishmania infantum*[h]) = 2.5 μM, SI > 80 | |
| | | $IC_{50}$ (*Leishmania amazonensis*[h]) = 3.0 μM, SI > 67 | |
| | | $IC_{50}$ (*Leishmania donovani*[g]) = 4.0 μM, SI > 50 | |
| | | $IC_{50}$ (*Leishmania amazonensis*[g]) = 4.9 μM, SI > 41 | |
| | | $IC_{50}$ (*Leishmania guyanensis*[g]) = 8.6 μM, SI > 23 | |
| | | $IC_{50}$ (*Leishmania infantum*[g]) = 8.7 μM, SI > 23 | |
| 41 | 232 | $IC_{50}$ (*Plasmodium falciparum*) = 0.086 μM, SI > 290 | 125 |
| | | $IC_{50}$ (*Plasmodium falciparum*[j]) = 0.20 μM, SI > 124 | |
| 42 | 233 | MIC (*Enterococcus casseliflavus**) = 0.98 μg mL⁻¹ (1.9 μM) | 121 |
| | | MIC (*Enterococcus faecium**) = 1.95 μg mL⁻¹ (3.7 μM) | |
| | | MIC (*Enterococcus faecalis*[b],*) = 1.95–3.91 μg mL⁻¹ (3.7–7.4 μM) | |
| | | MIC (MRSA*)[b] = 3.91–7.81 μg mL⁻¹ (7.4–15 μM) | |
| | | MIC (*Staphylococcus aureus*[b],*) = 3.91–15.63 μg mL⁻¹ (7.4–30 μM) | |
| 43 | 234 | MIC (*Enterococcus faecium**) = 0.98 μg mL⁻¹ (1.9 μM) | |
| | | MIC (*Enterococcus faecalis*[b],*) = 0.98–1.95 μg mL⁻¹ (1.9–3.7 μM) | |
| | | MIC (MRSA*,[b], *Enterococcus casseliflavus**) = 3.91 μg mL⁻¹ (7.5 μM) | |
| | | MIC (*Staphylococcus aureus*[b],*) = 3.91–62.5 μg mL⁻¹ (7.5–119 μM) | |
| 44 | 235 | MIC (*Cryptococcus neoformans* var. *grubii*) = 16 μg mL⁻¹ (29 μM) | 161 |
| | | MIC (*Candida albicans*) = 32 μg mL⁻¹ (58 μM) | |
| 45 | 236 | MIC (*Cryptococcus neoformans* var. *grubii*) = 16 μg mL⁻¹ (29 μM) | |
| | | MIC (*Candida albicans*) = 32 μg mL⁻¹ (58 μM) | |
| 46 | 237 | $IC_{50}$ (*Leishmania major*[g]) = 23.32 μg mL⁻¹ (47 μM) | 157 |
| 47 | 238 | $IC_{50}$ (*Leishmania major*[g]) = 9.8 μg mL⁻¹ (18 μM) | |
| 48 | 239 | $IC_{50}$ (H1N1) = 3.5 μM, SI = 200 | 162 |

[a] Units reported according to the original reference. Conversion into micromolar is shown in brackets (μM). MIC = Minimum inhibitory concentration; $IC_{50}$ = Concentration that inhibit the growth of a species by 50%; $EC_{50}$ = concentration corresponding to 50% growth inhibition of the parasite or cells; SI = Selectivity index; MRSA = Methicillin-resistant *Staphylococcus aureus*; DENV = Dengue virus; ZIKV = Colombina Zika virus; CHIKV = *Chikungunya virus*; HHV = Herpes virus; H1N1 = Influenza A virus; *Gram-positive; **Gram-negative. [b] Several strains. [c] Prior to biofilm establishment. [d] After biofilms are established. [e] $IC_{50}$(post)/$IC_{50}$(pre). [f] Parasites residing inside cells. [g] Promastigotes. [h] Amastigotes. [i] Post-infection stage. [j] Chloroquine-resistant.

1880 | Nat. Prod. Rep., 2024, 41, 1858–1894

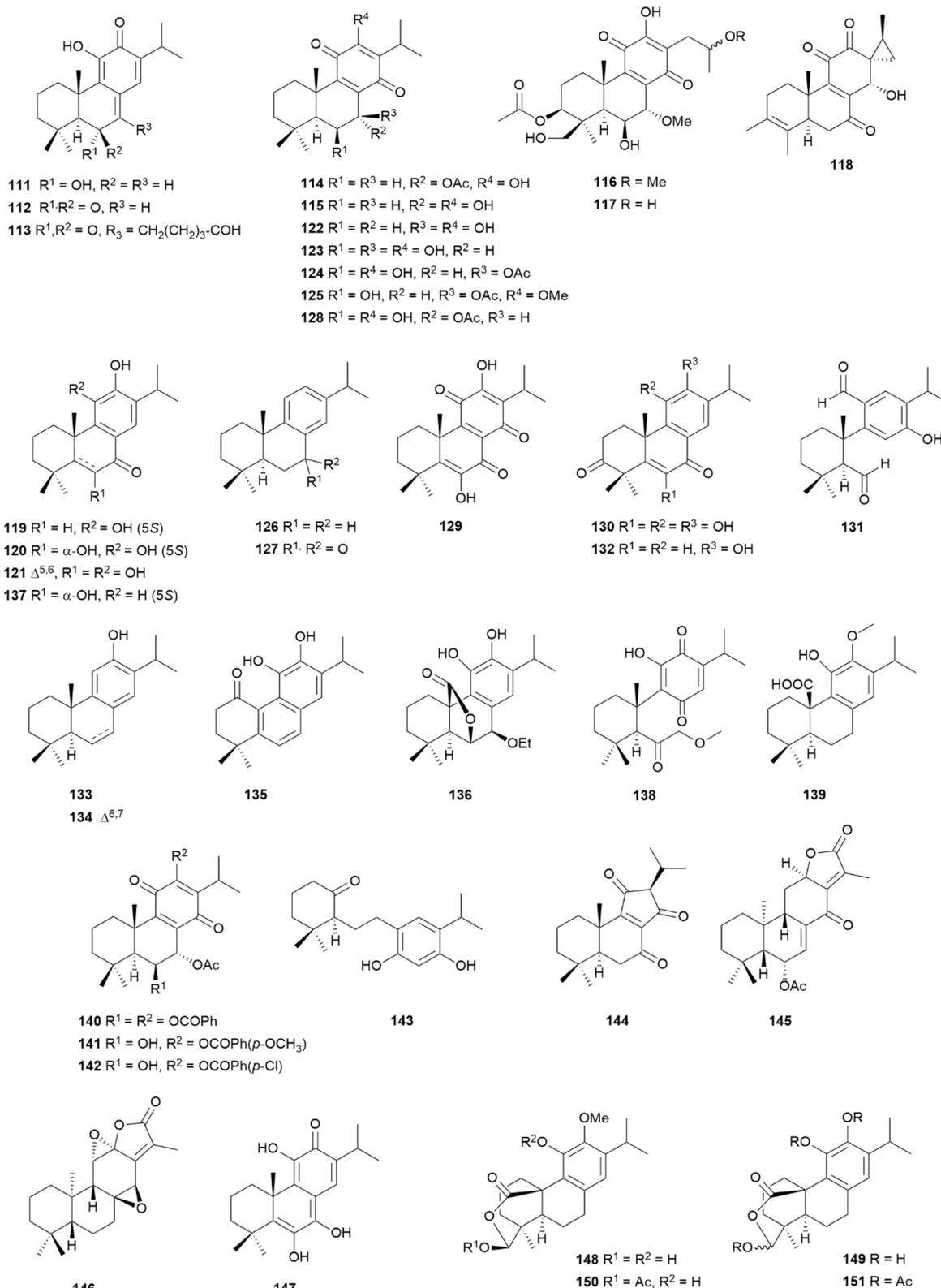This journal is © The Royal Society of Chemistry 2024

**Fig. 12** Naturally occurring abietane-type diterpenoids.

from *Plectranthus punctatus*, against *Escherichia coli*, *Bacillus subtilis*, *Micrococcus luteus*, *Pseudomonas agarici* and *Staphylococcus warneri*.[166] Compound (**126**) (Fig. 12), isolated from

*Kaempferia roscoeana*, displayed an MIC value of 25 μg mL$^{-1}$ against both *Staphylococcus epidermidis* and *Bacillus cereus*, whereas **127** (Fig. 12) was only active against *Staphylococcus*

This journal is © The Royal Society of Chemistry 2024

*Nat. Prod. Rep.*, 2024, **41**, 1858–1894 | **1881**

*aureus* (Table 3, entries 10 and 11, respectively).[120] Compounds **128** and **129** (Fig. 12) showed antimycobacterial activity, with MIC$_{90}$ values of 5.61 to 45.41 μM, against *Mycobacterium tuberculosis* H37Rv (Table 3, entries 12 and 13, respectively).[118] Compound **128** was also active against *Enterococcus* species.[121] Torganol E (**130**), 6,7-*seco*-abietane (**131**) and compound **132** (Fig. 12) displayed antimycobacterial activity against *Mycobacterium tuberculosis* H37Rv (Table 3, entries 14–16, respectively).[122] Compound (**132**) was also active against *Staphylococcus aureus*, with an MIC value of 16 μg mL$^{-1}$.[122]

Ferruginol (**133**) (Fig. 12) had antimicrobial activity against *Staphylococcus aureus* including MRSA strains, but was devoid of antifungal activity.[115] Ferruginol (**133**) was also reported as an inhibitor of *Leishmania major* promastigotes, with an IC$_{50}$ value of 12.1 μg mL$^{-1}$ (Table 3, entry 17),[123] and *Leishmania donovani* promastigotes and *Leishmania amazonensis* amastigotes, although with low SI values.[115,117] Among the abietane diterpenoids isolated from the roots of *Salvia sahendica*, ferruginol (**133**) and Δ$^{6,7}$-ferruginol (**134**) (Fig. 12) were potent antimalarial agents against *Plasmodium falciparum* with moderate selectivity (Table 3, entry 18).[124,126] Miltiodiol (**135**) and 7α-ethoxyrosmanol (**136**) (Fig. 12) were active against *Trypanosoma brucei rhodesiense*, but inactive against *Trypanosoma cruzi* (Table 3, entries 19 and 20, respectively).[124] 6α-Hydroxysugiol (**137**) and 7,8-*seco* abietane (**138**) (Fig. 12), isolated from *Taxodium distichum*, were active against *Leishmania* species (Table 3, entries 21 and 22, respectively).[117] 6α-Hydroxysugiol (**137**) was also active against *Mycobacterium tuberculosis* H37v, with an MIC value of 16 μg mL$^{-1}$ and *Staphylococcus aureus*, with an MIC value of 4 μg mL$^{-1}$.[122] 12-Methoxycarnosic acid (**139**) (Fig. 12) inhibited the growth of axenic *Leishmania donovani* amastigotes with an IC$_{50}$ value of 0.75 μM and SI value of 23.2 (Table 3, entry 23).[127] Royleanones **140–142** (Fig. 12) completely (∼100%) inhibited the growth of both *Trypanosoma cruzi* epimastigotes and amastigotes at a concentration of 5 μg mL$^{-1}$ with low selectivity.[167] Leriifoliol (**143**) and leriifolione (**144**) (Fig. 12), two rearranged abietanes isolated from *Salvia leriifolia*, displayed good antiprotozoal properties (Table 3, entries 24 and 25, respectively).[128] Leriifoliol (**143**) was very effective against *Plasmodium falciparum*, with an IC$_{50}$ value of 0.4 μM and SI value of 84.[128] Mangiolide (**145**) and compound (**146**) (Fig. 12) were also potent antimalarial agents against both chloroquine-sensitive and -resistant *Plasmodium falciparum* strains (Table 3, entries 26 and 27, respectively).[129] In addition, **145** inhibited the growth of *Cryptococcus neoformans*, MRSA and vancomycin-resistant *Enterococcus* (VRE); however, its selectivity was poor.[129] Among the panel of compounds isolated from *Plectranthus barbatus* Andr., compound **147** (Fig. 12) was both a potent and selective antiprotozoal agent, especially against macrophages infected with *Trypanosoma brucei* amastigotes, where it displayed an IC$_{50}$ of 1.9 μM, with a high SI of 50.5 (Table 3, entry 28).[116] Abietanes **148–152** (Fig. 12 and 13) were moderate inhibitors of *Giardia lamblia* and *Entamoeba histolytica* (Table 3, entries 29–33, respectively).[130]

The three *ent*-abietanes (**153–155**) (Fig. 13), isolated from the leaves of *Croton cascarilloide*, were modest antimicrobial agents against only Gram-positive bacteria (Table 3, entries 34–36,
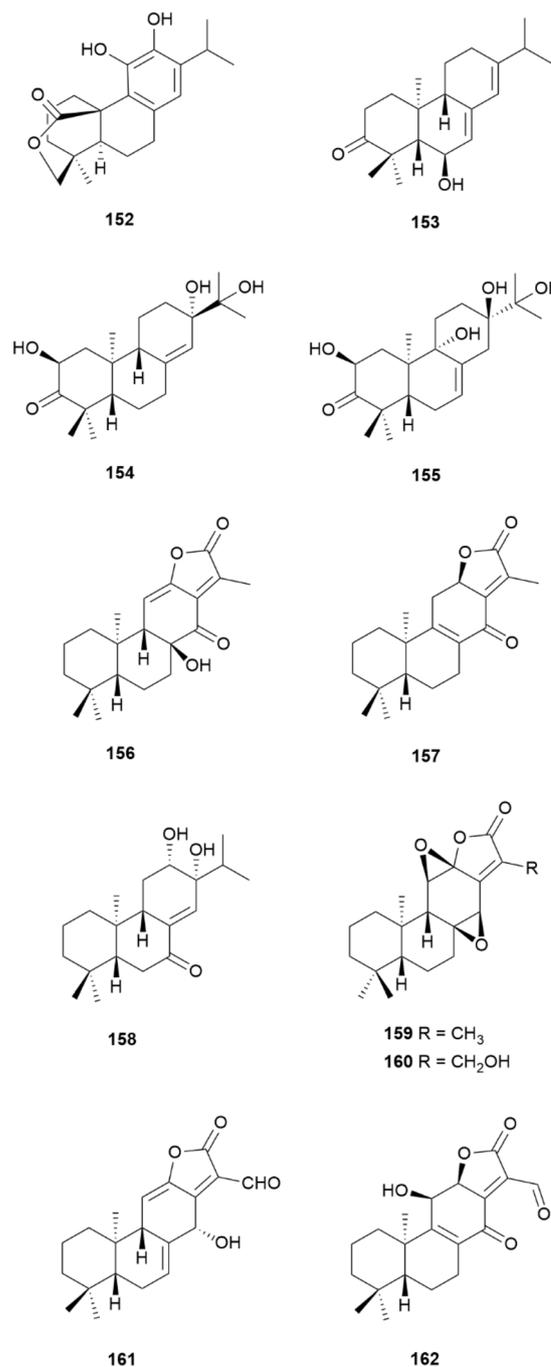


Fig. 13 Naturally occurring abietane-type diterpenoids (*Cont.*).

respectively).[131] Eupholides F (**156**), G (**157**), and H (**158**) (Fig. 13) were the only active compounds against *Mycobacterium tuberculosis*, among the 15 abietanes isolated from the roots of *Euphorbia fischeriana*, with MIC values of 50 μM (Table 3, entries 37–39, respectively).[132] The *ent*-abietane derivatives jolkinolide B (**159**) and 17-hydroxyjolkinolide (**160**) (Fig. 13), also isolated from *Euphorbia fischeriana*, were active against *Mycobacterium smegmatis* with MIC values of 25 and 1.5 μg mL$^{-1}$ (Table 3, entries 40 and 41),[133] whereas *ent*-abietanes **161** and **162** (Fig. 13), isolated from a different *Euphorbia* species, were only
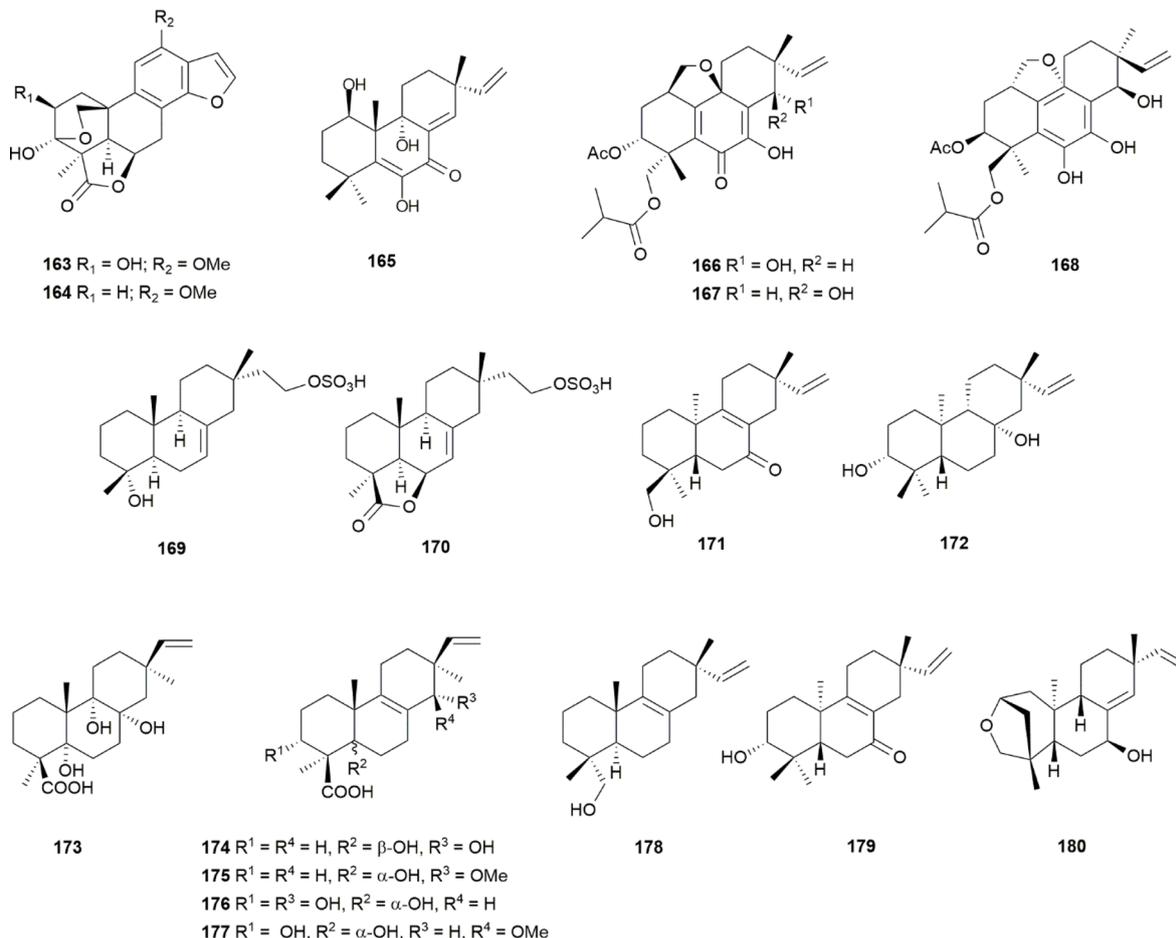
**1882** | *Nat. Prod. Rep.*, 2024, **41**, 1858–1894

This journal is © The Royal Society of Chemistry 2024

**Fig. 14** Naturally occurring pimarane-type diterpenoids.

active against Gram-positive bacteria (Table 3, entries 42 and 43), respectively.[134]

## 4.2 Naturally occurring pimarane-type diterpenoids

Icacinlactones H (163) and B (164) (Fig. 14) inhibited the growth of both standard and multi-drug resistant strains of *Helicobacter pylori*, with MIC values ranging from 8 to 16 μg mL$^{-1}$ (Table 3, entries 44 and 45, respectively).[135] Icancinlactone B (164) had an additive effect against this bacterium when used in combination with metronidazole or clarithromycin. Pimaranes 165 and 166 (Fig. 14), isolated from the arctic fungus *Eutypella* spp. D-1, were active against *Escherichia coli*, *Staphylococcus aureus*, *Bacillus subtilis* and *Vibrio vulnificus*, but cytotoxic (Table 3, entries 46 and 47, respectively).[136,137] Compound 166 also inhibited the growth of *Streptococcus agalactiae* and *Aeromonas hydrophila* and displayed antifungal activity against a panel of fungal strains (Table 3, entry 47). Eutypellenoid C (167) and Eutypenoid C (168) (Fig. 14) were overall less potent and devoid of antifungal activity (Table 3, entries 48 and 49, respectively).[137]

Isopimaranes 169 and 170 (Fig. 14), isolated from the fungus *Xylaria* spp., inhibited the growth of *Pleomorphomonas oryzae* with MIC values of 32 and 16 μg mL$^{-1}$ (Table 3, entries 50 and 51), respectively.[138] Both compounds also displayed antifungal activity.

*Ent*-pimarane 171 (Fig. 14) showed the best activity against *Plasmodium falciparum* compared to other protozoal parasites, with an IC$_{50}$ value of 3.8 μM and SI of >10 (Table 3, entry 52).[139] Compound 172 (Fig. 14), obtained by fungal biotransformation, was active against a panel of bacterial strains, with MIC values ranging from 8 to 25 μg mL$^{-1}$ (Table 3, entry 53).[140] Talascortenes C-G (173–177) (Fig. 14) from the endozoic fungus *Talaromyces scorteus* displayed antibacterial activity against several strains (Table 3, entries 54–58, respectively). Talascortene G (177) was active against the Gram-negative *Pseudomonas aeruginosa*, with an MIC value of 32 μg mL$^{-1}$.[70] Pimaranes 178–180 (Fig. 14) were modest antiprotozoal agents, with poor selectivity (Table 3, entries 59–61, respectively).[124,139]

## 4.3 Naturally occurring cassane-type diterpenoids

Compounds 181 and 182 (Fig. 15), isolated from the root bark of *Swartzia simplex*, could inhibit the growth of *Candida albicans*, with MIC values of 32 μg mL$^{-1}$, and limit its ability to form mature biofilms with MIC values of 50 and 25 μg mL$^{-1}$ (Table 3, entries 62 and 63, respectively).[141] Treatment of *Candida albicans* with 182 resulted in alterations and breakage zones of the plasma membrane, which were evident disorganisation of the cytoplasm and the nuclear membrane. This compound also hampered the budding ability of the fungus. The cassane-type
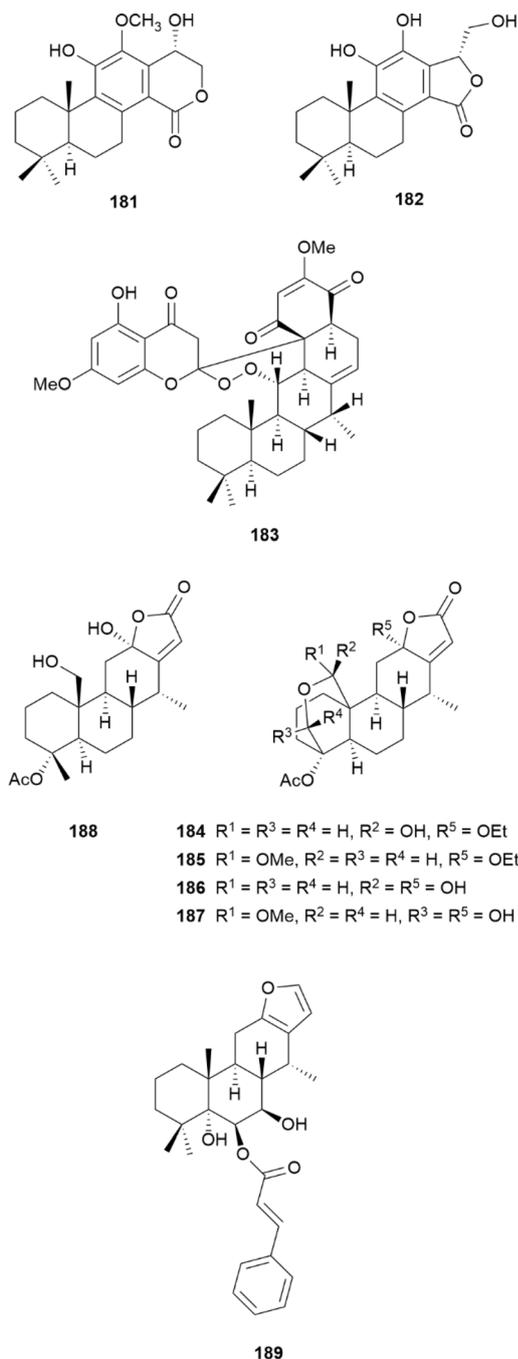
This journal is © The Royal Society of Chemistry 2024

*Nat. Prod. Rep.*, 2024, **41**, 1858–1894 | **1883**

181        182



183



188

184  $R^1 = R^3 = R^4 = H, R^2 = OH, R^5 = OEt$
185  $R^1 = OMe, R^2 = R^3 = R^4 = H, R^5 = OEt$
186  $R^1 = R^3 = R^4 = H, R^2 = R^5 = OH$
187  $R^1 = OMe, R^2 = R^4 = H, R^3 = R^5 = OH$



189

Fig. 15 Naturally occurring cassane-type diterpenoids.

diterpenoid bokkosin (183) (Fig. 15) was reported as a potent antiprotozoal agent targeting *Trypanosoma brucei*, *Trypanosoma congolense* and *Leishmania mexicana*, with low $EC_{50}$ values, and no cross-resistance to pentamidine or diminazene in the case of *Trypanosoma* species (Table 3, entry 64).[142] The best selectivity index (>200) was obtained for wild-type strains of *Trypanosoma brucei*. The effect of 183 was dose-dependent, leading to growth arrest and cell death, after exposure to 2- or 4-times the $EC_{50}$ value, after 2 h. Compounds 184–188 (Fig. 15), isolated from *Caesalpinia sappan*, were active against the chloroquine-resistant K1 strain of *Plasmodium falciparum*, with $IC_{50}$ values

ranging from 0.52 and 15.7 μM, and SI values above 10, with the exception of compound 185, which was poorly selective (Table 3, entries 65–69, respectively).[143] 6β-Cinnamoyl cassane (189) (Fig. 15), isolated from *Caesalpinia pulcherrima*, was moderately active against the promastigotes of *Leishmania major* (Table 3, entry 70).[144]

### 4.4 Semi-synthetic tricyclic diterpenoids

Several abietane-type derivatives have been prepared starting from the parent abietic (3) and dehydroabietic (4) acids (Fig. 2), dehydroabietylamine and ferruginol (133) (Fig. 12), given that they are available in greater amounts and high purity for chemical synthesis. The most accessible positions of the abietane scaffold for modification are the carboxylic acids attached to ring A, C7 on ring B, C12 on ring C, and C15 on the isopropyl side chain.

**4.4.1 Abietic acid derivatives.** The activity of the L-serine methyl ester derivative of abietic acid 190 (Fig. 16) was found to be limited to inhibit the growth of the bacteria *Staphylococcus epidermidis* and *Rothia mucilaginosa*, with $MIC_{90}$ values of 16 and 31 μg mL$^{-1}$, respectively (Table 4, entry 1).[104] The 7-formyl derivative 191 (Fig. 16) displayed good antifungal activity against *Candida albicans* and *Cryptococcus neoformans* var. *grubii*, with MIC values of 8 and 4 μg mL$^{-1}$, respectively (Table 4, entry 2).[145] This compound was active against *Staphylococcus aureus* at 32 μg mL$^{-1}$, but inactive against Gram-negative bacteria. VO(IV)-bis(abietate) complex 192 (Fig. 16) showed activity against *Candida albicans*, with an MIC value of 15.6 μM (Table 4, entry 3).[146]

**4.4.2 Dehydroabietic acid derivatives.** A series of *N*-sulfonaminoethyloxime, 7-*N*-acylaminoethyl/propyloxime and 12-oxime and *O*-oxime derivatives of dehydroabietic acid (4) was tested against *Staphylococcus aureus* Newman and a panel of multi-drug resistant *Staphylococcus aureus* strains (Table 4, entries 4–14).[110,111,147] Compounds 193–198 (Fig. 17) were potent
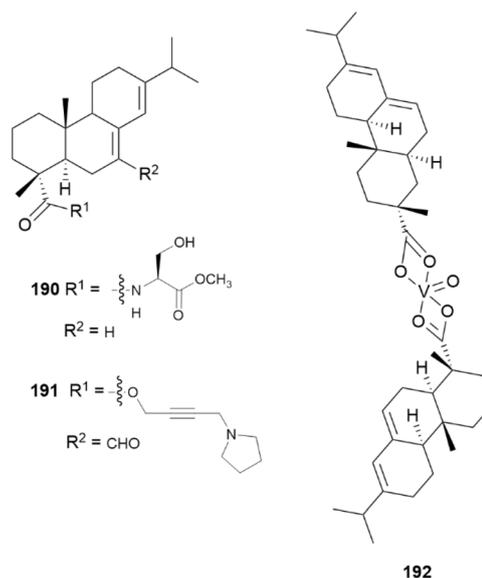


190  $R^1 = $               $R^2 = H$

191  $R^1 = $               $R^2 = CHO$

192

Fig. 16 Abietic acid derivatives.

1884 | *Nat. Prod. Rep.*, 2024, 41, 1858–1894

This journal is © The Royal Society of Chemistry 2024
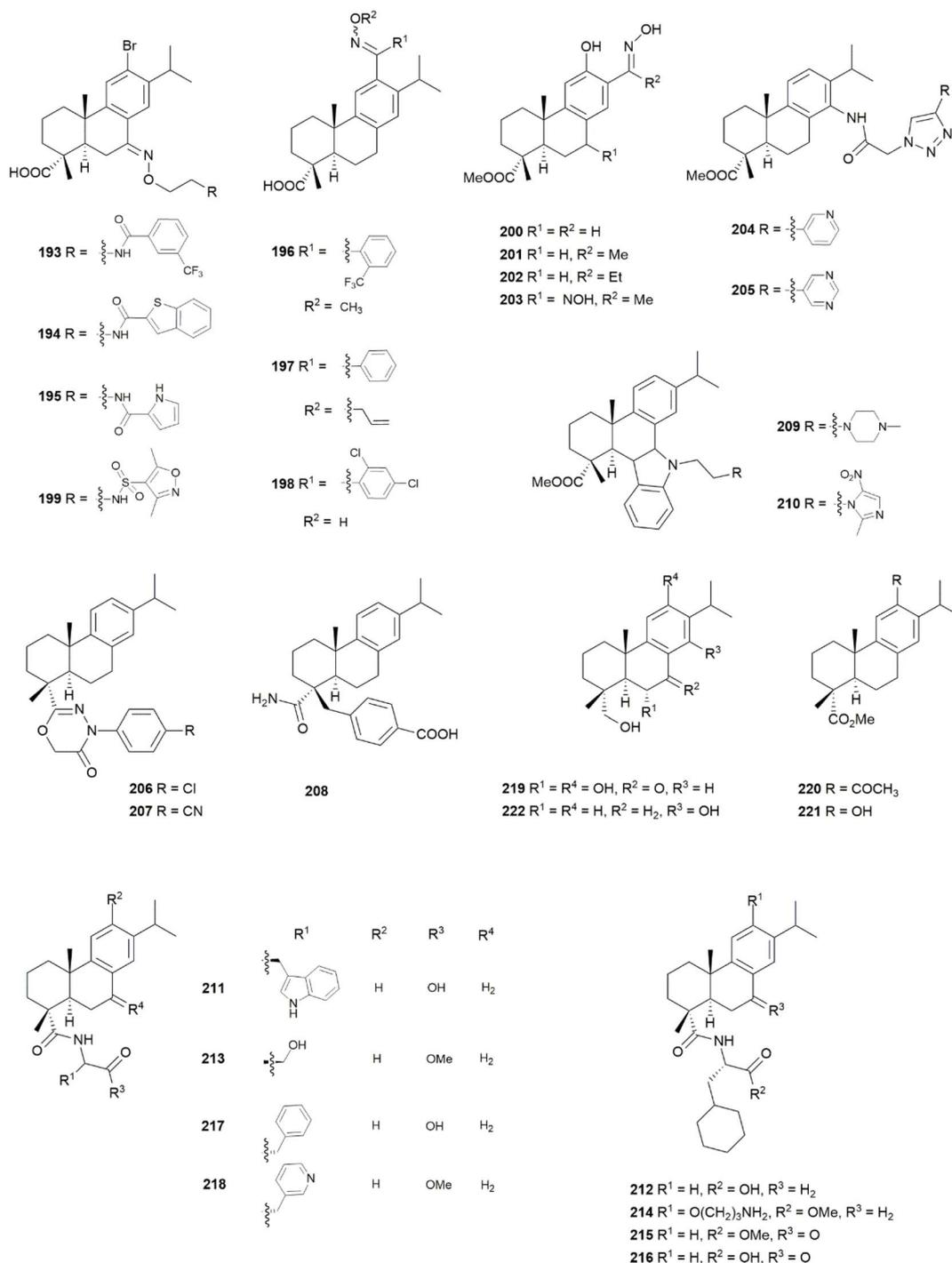
Fig. 17   Dehydroabietic acid derivatives.

antistaphylococcal agents with MIC values ranging from 1.25 to 6.25 µg mL$^{-1}$. Compound **199** (Fig. 17) was stable in plasma and devoid of significant toxicity against human cells. None of the N-sulfonaminoethyloxime or 7-N-acylaminoethyl/propyloxime derivatives studied displayed activity against the Gram-negative *Escherichia coli* even at a high concentration of 50 µg mL$^{-1}$.

The presence of an oxime on the isopropyl side chain alongside a hydroxyl group at C12 was also noted as important

for the activity of derivatives **200–203** (Fig. 17) against staphylococci (Table 4, entries 11–14, respectively).[168] The activity of compound **201** was particularly noteworthy, given that its MIC values on all strains, both drug-resistant and drug-sensitive, ranged from 7.8 to 15.6 µg mL$^{-1}$, with some values being lower than that of penicillin and gentamicin. Compound **201** was not cytotoxic at concentrations of up to 250 µg mL$^{-1}$ and no haemolysis was observed after treatment of peripheral

blood mononuclear cells (PBMC) with 4–16 times its MIC value.[168]

Among a library of 86 abietanes, compounds **204** and **205** (Fig. 17), bearing triazole rings substituted with pyridyl or pyrimidyl groups, displayed MIC values as low as 1.6 and 12.5 μg mL$^{-1}$ against both Gram-positive and Gram-negative bacteria (Table 4, entries 15 and 16, respectively), with low cytotoxicity against normal foreskin fibroblasts and liver cells.[106]

1,3,4-Oxadiazin-5(6$H$)-one derivatives **206** and **207** (Fig. 17) were active against both Gram-positive and Gram-negative bacteria, and fungi (Table 4, entries 17 and 18, respectively).[148] However, compound **206**, bearing a chlorine substituent, was cytotoxic, as opposed to **207**, bearing a cyano group. A C–H activation protocol allowed the functionalization of the otherwise difficult to modify C19 of abietanes.[149] Among a series of C-19 arylated derivatives of dehydroabietic acid (**4**), compound **208** (Fig. 17) displayed desirable antimicrobial activity against MRSA, with an MIC value of 32 μg mL$^{-1}$ (Table 4, entry 19).[149] The presence of a free carboxylic acid on the aryl moiety was relevant for the observed activity, and also for the solubility of the compound to allow the screening of its bioactivity.[149]

In a series of $N$-substituted 1$H$-dibenzo[$a,c$]carbazole derivatives of dehydroabietic acid (**4**), the compounds bearing piperazine or azole heterocyclic moieties bridged by flexible ethyl chains were active against *Bacillus subtilis*, *Staphylococcus aureus*, *Escherichia coli* and *Pseudomonas fluorescens*, with MIC values ranging from 0.9 to 15.6 μg mL$^{-1}$.[150]

Derivative **209** (Fig. 17), bearing an $N$-methyl piperazine and derivative **210**, with a 2-methyl-5-nitro-imizazole moiety, were the most active, with **210** being as potent against *Bacillus subtilis* as the reference drug amikacin (Table 4, entries 20 and 21, respectively). Compound **209** was also active against the fungi *Aspergillus niger*, *Candida albicans* and *Candida tropicalis*, with a low MIC value of 7.8 μg mL$^{-1}$.[150]

Among a panel of hybrid compounds bearing the dehydroabietic acid (**4**) scaffold and an amino acid side chain, compounds **211** and **212** (Fig. 17) displayed improved antimicrobial and antibiofilm activity against staphylococci compared to the parent compound (Table 4, entries 22 and 23, respectively).[108,163] Both compounds could affect pre-formed biofilms at concentrations only 3-fold higher than that required to limit biofilm formation by *Staphylococcus aureus*. Compound **212** was particularly active, displaying an MIC value of 15 μM against planktonic *Staphylococcus aureus* and reducing the viability and biomass of the cells in pre-formed biofilms by 50% at a concentration of 27.9 μM, an effect that could not be achieved with either penicillin G or vancomycin at a concentration of 400 μM. Moreover, it was deemed relatively safe given that no significant reduction in the viability of HL cells was observed after treatment with **212** at concentrations of up to 100 μM. Compound **212** has an unusual cyclohexyl -L-alanine side chain attached to ring A and a free carboxylic acid, which was found to be essential for the antibiofilm activity of the prepared hybrid compounds.[108] However, in the case of derivative **213**, it was observed to exhibit activity against several strains of bacteria including *Rothia mucilaginosa* (Table 4, entry 24), even if the methyl ester was not converted into a free carboxylic acid.[104]

Compound **214** (Fig. 17), also devoid of a free carboxylic acid, was highly potent against the virulent *Staphylococcus aureus* strain UAMS-1 and the MRSA strain Mu50, with MIC values of 7.4 μM (Table 4, entry 25).[151] Compound **212** and a few other hybrids namely, **215–218** (Fig. 17) were also potent antiprotozoal agents against *Trypanosoma cruzi* or *Leishmania donovani*, without significant general toxicity (Table 4, entries 26–29, respectively).[152] In the case of compounds **212** and **217**, inhibition of the growth of *Leishmania donovani* residing inside human macrophages was observed with IC$_{50}$ values of 5 and 9 μM and high SI values of 24 and 33, respectively. In the case of compound **218**, a 3-pyridyl-D-alanine methyl ester derivative, a 1.5-fold increase in potency was observed compared to the reference compound benznidazole for inhibiting the growth of *Trypanosoma cruzi* residing inside rat skeletal muscle myoblasts (L6 cells), with an SI of 17.[152] Derivative **219** (Fig. 17), synthesised from abietic acid (**3**), was 3 times more potent than benznidazole against the amastigote forms of *T cruzi*, with an IC$_{50}$ value of 7.1 μM and very low cytotoxicity (Table 4, entry 30).[153] When tested *in vivo* on BALB/c albino mice infected with the parasite for 5 consecutive days at a dose of 5 mg per kg per body mass per day, it could reduce the rate of infection by 80% after 5 days, being more efficient than benznidazole, and to reduce parasitemia and prevent reactivation of the infection. Among the plausible modes of action investigated, the activity of **219** on the parasite glucose metabolism and inhibition of the activity of superoxide dismutase (SOD) were notable. Incubation of **219** with the parasite epimastigotes revealed morphological disturbances such as swollen mitochondria, the presence of small vacuoles in the cytoplasm and a lack of ribosomes.[153] The oxidised derivatives of methyl dehydroabietate **220** and **221** (Fig. 17) were potent antiprotozoal agents against the promastigote forms of several *Leishmania* species (Table 4, entry 31 and 32, respectively), with IC$_{50}$ values in the low micromolar range, and being more potent than the reference drug miltefosine in some of the tested strains.[154] The hydroxyl group at position C12 in compound **221** had a remarkable effect on the SI of the compounds in the case of *Leishmania infantum*, where compound **220** was deemed exceptionally safe with an SI of 58.1 compared to that of **221**, which was 6.8. However, compound **220** was both less potent and more toxic when tested against the amastigote forms of both *Leishmania amazonensis* and *Leishmania infantum* (Table 4, entry 31).[154]

Modest antifungal activity was reported for 12-hydroxyabietane **222** (Fig. 17), with MIC values of 25 and 50 μg mL$^{-1}$ against *Aspergillus fumigatus* and *Aspergillus terreus*, respectively (Table 4, entry 33).[155]

**4.4.3 Ferruginol derivatives.** The 18-(phthalimide-2-yl) ferruginol derivative **223** (Fig. 18) was the most promising among a series of C18 or C19-functionalized abietane derivatives when tested against Colombina Zika virus (ZIKV) strains and CHIKV (Table 4, entry 34) (135).[156] It had been previously shown that **223** affected the post-infection stages in DENV-2 with an EC$_{50}$ of 1.4 μM, herpes virus type 2 (HHV-2) with an EC$_{50}$ of 19.2 μM and a Brazilian Zika clinical isolate (EC$_{50}$ of 7.7 μM).[169] This was also confirmed for infections with CHIKV, where **223** displayed a dose-dependent effect in the post-infection stages with an EC$_{50}$

**1886** | *Nat. Prod. Rep.*, 2024, **41**, 1858–1894

This journal is © The Royal Society of Chemistry 2024

of 6.3 μM after 72 h of treatment and with Colombian CHICK ($EC_{50}$ of 9.8 μM). The authors confirmed that compound **223** could inhibit the production of viral particles, the replication of viral genome and the production of viral proteins and concluded that successful antiviral activity for ferruginol derivatives was obtained with the presence of a C12 hydroxyl group and the C18 phthalimide group. Compound **223** was also studied against the Dengue Virus type 2 (DENV-2) and its effects were similar to the results described above against Zika and CHIKV, affecting the post-infection stages of infection with an $EC_{50}$ of 1.4 μM and high SI value of 57.7, and therefore deemed as a promising antiviral agent worth further investigation.[157] Following these observations on the promising antiviral properties of phthalimide derivatives of ferruginol, fluorinated analogues **224** and **225** (Fig. 18) were prepared and tested against the human coronavirus 229E.[170] Both could reduce the viral titer by approximately 2 log units, at a concentration of 6.7 μM.[170]

**4.4.4 Dehydroabietylamine derivatives.** Dehydroabietylamine derivative compound **226** (Fig. 19) was found to be a modest antimicrobial agent (Table 4, entry 35) with a great impact on membrane integrity, given that it could cause significant ATP efflux from *Staphylococcus aureus* cells after 1 h of exposure at a concentration of 100 μM.[158]

Compound **227** (Fig. 19), an amide of dehydroabietylamine and acrylic acid, was identified among a library of dehydroabietylamine derivatives as the most promising antiprotozoal agent against *Leishmania donovani* and *Trypanosoma cruzi* (Table 4, entry 36).[159] This compound displayed an $IC_{50}$ value of 0.37 μM against *Leishmania donovani* axenic amastigotes, with an outstanding SI of 63. It could inhibit the growth of intracellular amastigotes in *Leishmania donovani*-infected human macrophages, with a low $IC_{50}$ value of 0.06 μM. Compound **227** was 3-times more potent than the reference compound benznidazole in inhibiting the growth of
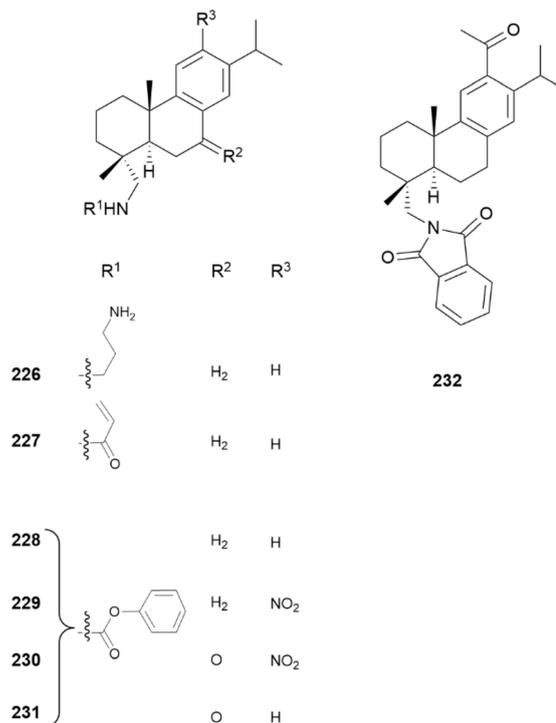


Fig. 19 Dehydroabietylamine derivatives.

*Trypanosoma cruzi* residing inside L6 cells, and no general toxicity was observed (SI of 58). A set of benzamide derivatives **228–231** (Fig. 19) had potent antiprotozoal activity against several species of *Leishmania* (Table 4, entries 37–40, respectively).[160] These compounds were more potent than the reference compound miltefosine when tested on *Leishmania infantum* and *Leishmania amazonensis* amastigotes and did not display significant cytotoxicity (Table 4, entries 37–40).[160]

18-Phthalimide derivative **232** (Fig. 19) was reported as a potent antimalarial agent, active against both chloroquine-sensitive and chloroquine-resistant strains of *Plasmodium falciparum*, with $EC_{50}$ values of 86 and 201 nM, respectively, and very high selectivity (Table 4, entry 41).[125] This study found that the presence of the phthalimide group was better than a free amino group at the same position, and that the presence of chlorine substituents on the phthalimide group was not advantageous for the activity of the compound.

**4.4.5 Other semi-synthetic tricyclic diterpenoids.** A set of royleanones, including compounds **233** and **234** (Fig. 20), was prepared and tested against a panel of bacterial strains (Table 4, entries 42 and 43, respectively).[121] Despite having low MIC values against a few of the strains, they were found to be cytotoxic. Compounds **235** and **236** (Fig. 20), prepared from levopimaric acid, displayed antifungal activity against *Cryptococcus neoformans* and *Candida albicans*, with MIC values of 16 and 32 μg mL$^{-1}$ (Table 4, entries 44 and 45), respectively.[161] The oxidation of the cassane-type diterpenoids from the roots of *Caesalpinia pulcherrima* gave compounds **237** and **238** (Fig. 20), which displayed activity against *Leishmania major* with $IC_{50}$ values of 9.18 and 23.32 μg mL$^{-1}$, but with low selectivity (Table



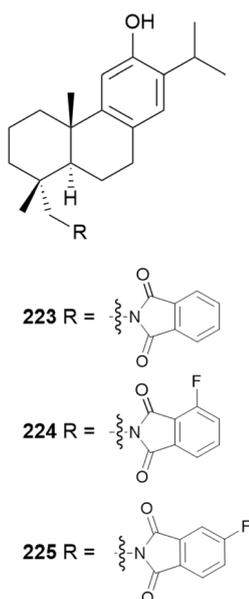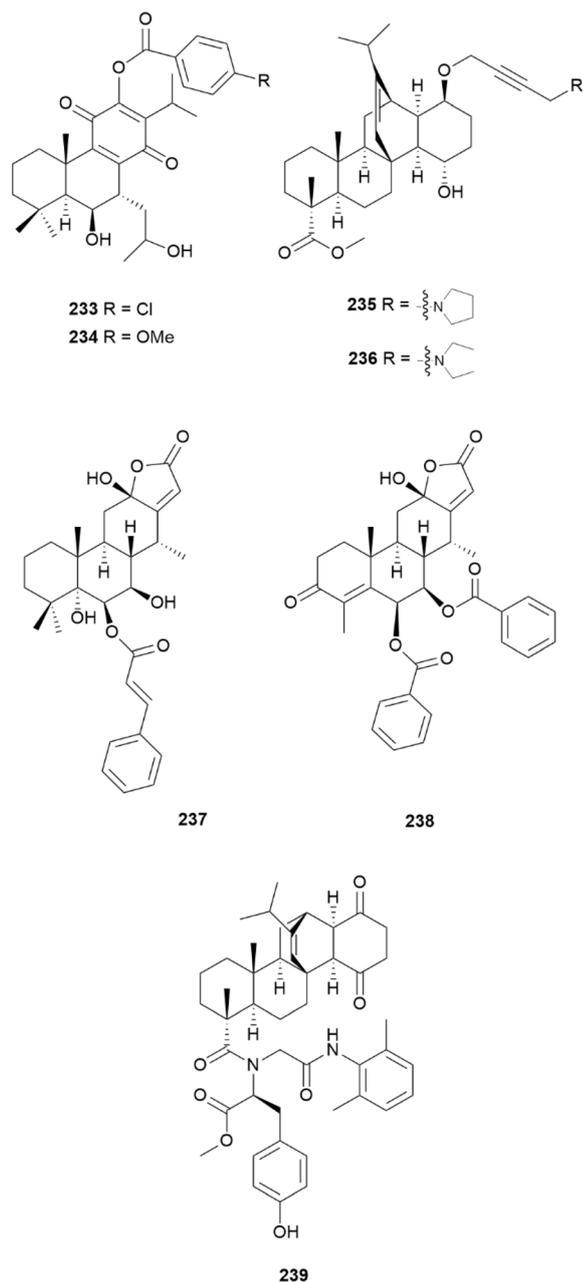Fig. 18 Ferruginol derivatives.

This journal is © The Royal Society of Chemistry 2024

*Nat. Prod. Rep.*, 2024, **41**, 1858–1894 | **1887**

**233** R = Cl
**234** R = OMe

**235** R = pyrrolidine

**236** R = pyrrolidine

**237**     **238**

**239**

Fig. 20  Other semi-synthetic tricyclic diterpenoids.

4, entries 46 and 47), respectively.[144] Maleopimaric acid derivative **239** (Fig. 20), bearing a L-tyrosine moiety, was particularly effective against influenza virus A/Puerto Rico/8/34 (H1N1), with an IC$_{50}$ value of 3.5 μM and very high SI of 200 (Table 4, entry 48).[162]

## 5.  Structure–activity considerations

The outstanding chemical diversity of the labdanes that stems from their biosynthetic origin is well portrayed across the naturally occurring anti-infective labdane-type diterpenoids. Semi-synthetic derivatives tested for anti-infective properties remain scarce, with the exception of a few derivatives of salvic (**13**), *ent*-

polyalthic (**57**) and *ent*-copalic (**14**) acids, where a modest improvement concerning bioactivity/selectivity has been achieved compared to their parent compounds. Among the anti-infective labdanes, stachyonic acid A (**42**) (Fig. 4), belonging to the "normal" series of labdanes, with the particular *E*-configuration on the diene side chain, has promising broad-spectrum antiviral properties worth further investigation, where chemical derivatization should establish important SAR in this field. Among the tricyclic diterpenoids, phthalimide derivative **223** (Fig. 18) showed the best potential to affect several viruses in the post-infection stage, and its hydroxyl group at position 12 was very important for this particular activity (Fig. 21).

Concerning antifungal compounds, the labdane-type diterpenoids produced by fungal biotransformation stand out as compounds among the diterpenoid classes portrayed herein with the most promising activity. The *ent*-labdane di-acids with acyclic side chains (**15**) and (**19**) (Fig. 4), 77 (Fig. 10) and derivative 78 (Fig. 10) were all active, but the presence of the additional hydroxymethyl groups introduced by biotransformation in 77 and 78 was particularly relevant for the antifungal activity. Biotransformation of labdanes with a furan ring on the side
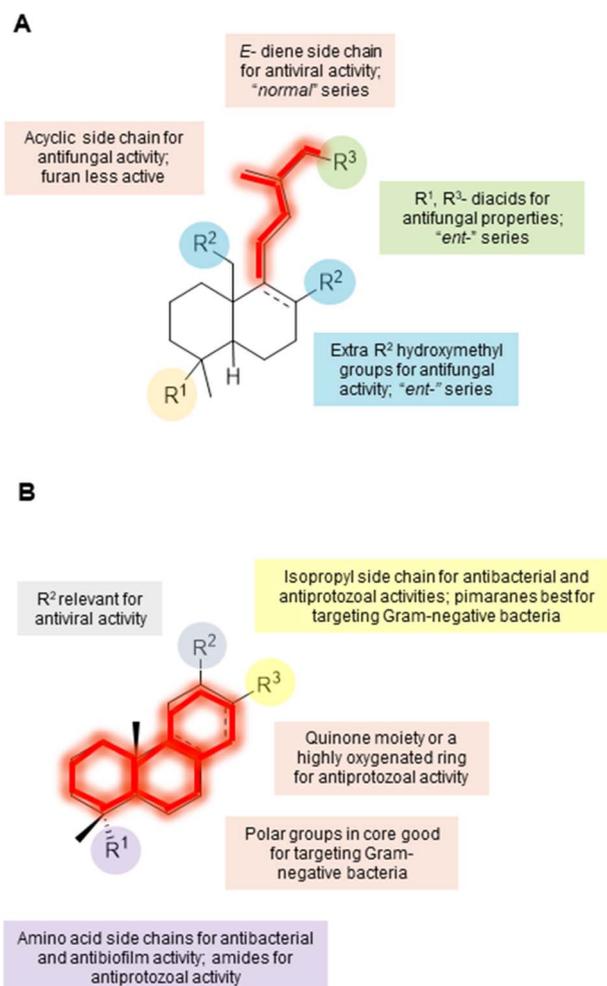


Fig. 21  Relevant SAR for labdane-type (A) and tricyclic (B) diterpenoids.

**1888** | *Nat. Prod. Rep.*, 2024, **41**, 1858–1894

This journal is © The Royal Society of Chemistry 2024

chain at C9 was not as beneficial, which is consistent with the more modest antifungal activity of the furan labdane *ent*-polyalthic acid (**57**).

Overall, both the naturally occurring labdanes and the tricyclic diterpenoids of all classes are mostly active against Gram-positive bacteria with the significant exception of the highly oxygenated pimaranes talascortenes (**173–177**) (Fig. 14), isolated not from plants but from fungal sources, which can target important Gram-negative pathogens including *Escherichia coli* and *Pseudomonas aeruginosa*. Their highly oxygenated structures suggest that a decrease in lipophilicity is advantageous when targeting Gram-negative bacteria because this facilitates permeation through the outer membrane *via* hydrophilic β-barrel protein pores,[171] which is consistent with the common knowledge in the antibiotics field. Despite the focus on Gram-positive bacteria, the activity of dehydroabietic acid (**4**) and of the semi-synthetic derivatives bearing amino acid side chains **211** and **212** (Fig. 17) to target bacterial biofilms has been well documented.[108,163] The ability to limit biofilm formation and/or to affect bacterial biofilms once they are fully established can be advantageous, for instance, when looking for synergistic effects to revive the action of traditional antibiotics. Finally, the presence of a lactone in both labdanes **65** and **66** (Fig. 7) and abietane **60** (Fig. 13) seems relevant for their activity against mycobacteria.

The tricyclic diterpenoids should be regarded as an indisputable source of potential leads for new antiprotozoal agents, especially among the abietanes. Several naturally occurring abietanes display potent activity against parasites causing malaria, Chagas disease and leishmaniasis, with very high selectivity indexes. The presence of a quinone moiety or a highly oxygenated ring as in **112**, **133–135**, **139**, **143** and **147** (Fig. 12) seems very important for this activity. In this regard, chemical derivatization work has already allowed the confirmation of the potential of abietanes to produce new leads for the treatment of diseases caused by protozoan parasites. Several amides prepared from dehydroabietic acid (**4**) and dehydroabietylamine, namely compounds **215–218** (Fig. 17) and **227–231** (Fig. 19), are very potent antiprotozoal agents, with outstanding selectivity, which can target parasites inside infected cells, *i.e.*, during the most relevant stages of the disease. In addition, phthalimide derivative **232** (Fig. 19) is an outstanding antimalarial agent.

# 6. Conclusions and future perspectives

This review clearly shows that new drug leads for infection can be found among the bi- and tricyclic diterpenoids of the classes covered herein. The road to the clinic is a long one, with the final goal still out of reach. In this regard, the economic burden of anti-infective drug development on major pharmaceutical companies, which fail to see return for their investment, is still a significant roadblock. As humanity becomes increasingly aware of the global impact of AMR on human health, we hope that this issue will be overcome. In fact, finding new molecules with original modes of action that can either act as self-standing agents or revive the action of clinically used anti-infectives

through synergy will be key for future breakthroughs to overcome resistance.

Therefore, additional work is needed for deconvolution of the primary targets of the most promising bi- and tricyclic diterpenoids, which will prompt medicinal chemistry optimisation campaigns to drive the compounds forward along the pipeline. It is also relevant to go beyond *in vitro* assessment of pathogen growth inhibition/death alone to report the actions of the compounds as broadly as possible, *i.e.*, including effects on biofilms, mixed species communities, synergy studies, and effects inside infected cells. New developments in pathogen biology, druggable targets, and infection models are currently emerging, especially in the case of bacteria, which are worth following closely, and will surely aid in improving the quality of future bioactivity data produced.

The overwhelming majority of the compounds reported herein originate from plant sources; however, the few originating from fungi, and especially that produced by biotransformation with fungi display very interesting anti-infective activity. This suggests that not only should the kingdom of fungi be investigated in more detail in search for novel bioactive compounds, but also exploited as an outstanding biotransformation factory to allow the unusual functionalization of diterpenoids of several classes and sources. Biotransformation is an important source of chemical diversity, which allows access to scaffold positions otherwise very difficult to modify *via* common synthetic chemistry, and the introduction of polar groups that make the compounds overall more hydrophilic. This hydrophilicity can be advantageous, for instance, in making the diterpenoids more "drug-like" in the long run, which is desirable for any anti-infective activity, with the goal of developing oral drugs. Designing novel bi- or tricyclic diterpenoids that are more hydrophilic should also not be overlooked for trying to shift their predominant antibacterial activity against Gram-positive bacteria towards a more broad-spectrum effect, given that the harder infections to treat at present are mostly caused by resistant Gram-negative bacteria.

We envision that interesting new diterpenoids will continue to be investigated during the next decade, with important disclosures on the more precise modes of antiprotozoal and antibacterial actions of the tricyclic diterpenoids, which should continue to steer research in this field. Among the natural sources portrayed in this review, half of the compounds reported were tested as antibacterials and one quarter as antiprotozoal agents, whereas their antifungal and antiviral activities remained far less exploited. We encourage all researchers in this field to bridge this gap and focus on all anti-infective activities when possible, harmonising the presentation of the results for the sake of producing data that is fully comparable, *i.e.*, including the reported activities in molar units, with reference to a positive control, and including the selectivity index.

# 7. Data availability

No primary research results, software or code has been included and no new data were generated or analysed as part of this review.

This journal is © The Royal Society of Chemistry 2024

*Nat. Prod. Rep.*, 2024, **41**, 1858–1894 | **1889**

## 8. Author contributions

## 9. Conflicts of interest

There are no conflicts to declare.

## 10. Acknowledgements

## 11. Notes and references

1 R. Li, S. L. Morris-Natschke and K.-H. Lee, *Nat. Prod. Rep.*, 2016, **33**, 1166–1226.

2 A. M. Roncero, I. E. Tobal, R. F. Moro, D. Díez and I. S. Marcos, *Nat. Prod. Rep.*, 2018, **35**, 955–991.

3 I. Chinou, *Curr. Med. Chem.*, 2005, **12**, 1295–1317.

4 M. Singh, M. Pal and R. P. Sharma, *Planta Med.*, 1999, **65**, 002–008.

5 C. Demetzos and K. S. Dimas, *Stud. Nat. Prod. Chem.*, 2001, **25**, 235–292.

6 R. J. Peters, *Nat. Prod. Rep.*, 2010, **27**, 1521.

7 P. Saha, F. I. Rahman, F. Hussain, S. M. A. Rahman and M. M. Rahman, *Front. Pharmacol.*, 2021, **12**, 820312.

8 K. O. Ndjoubi, R. Sharma and A. A. Hussein, *Curr. Pharm. Des.*, 2020, **26**, 2909–2932.

9 M. Hao, J. Xu, H. Wen, J. Du, S. Zhang, M. Lv and H. Xu, *Toxins*, 2022, **14**, 632.

10 M. A. González, *Nat. Prod. Rep.*, 2015, **32**, 684–704.

11 Institute for Health Metrics and Evaluation (IHME). *Global Burden of Disease*, GBD Results, IHME, University of Washington, Seattle, WA, 2019. **https://vizhub.healthdata.org/gbd-results**, (accessed April 2024).

12 G. B. D. A. R. Collaborators, *Lancet*, 2022, **400**, 2221–2248.

13 World Health Organization (WHO), The top 10 causes of death, Published online, 2020, **https://www.who.int/news-room/fact-sheets/detail/the-top-10-causes-of-death**, accessed April 2024.

14 Institute for Health Metrics and Evaluation (IHME), *Measuring Infectious Causes and Resistance Outcomes for Burden Estimation (MICROBE)*, IHME, University of Washington, Seattle, WA, 2022, **https://vizhub.healhtdata.org/microbe**, (accessed April 2024).

15 G. B. D. A. R. Collaborators, *Lancet*, 2022, **399**, 629–655.

16 M. Lyman, K. Forsberg, D. J. Sexton, N. A. Chow, S. R. Lockhart, B. R. Jackson and T. Chiller, *Ann. Intern. Med.*, 2023, **176**, 489–495.

17 Organisation for Economic Co-operation and Development (OECD), 17 Embracing a One Health Framework to Fight Antimicrobial Resistance, 2023. **https://www.oecd.org/els/embracing-a-one-health-framework-to-fight-antimicrobial-resistance-ce44c755-en.htm**.

18 World Health Organization (WHO), Prioritization of Pathogens To Guide Discovery, Research And Development of New Antibiotics For Drug-Resistant Bacterial Infections, Including Tuberculosis, World Health Organization, **https://www.who.int/publications/i/item/WHO-EMP-IAU-2017.12**.

19 M. C. Fisher and D. W. Denning, *Nat. Rev. Microbiol.*, 2023, **21**, 211–212.

20 World Health Organization (WHO), Fungal Priority Pathogens List to Guide Research, Development and Public Health Action, **https://www.who.int/publications/i/item/9789240060241**.

21 K. I. Kasozi, E. T. MacLeod and S. C. Welburn, *Pathogens*, 2022, **11**, 1100.

22 A. Ponte-Sucre, F. Gamarro, J.-C. Dujardin, M. P. Barrett, R. López-Vélez, R. García-Hernández, A. W. Pountain, R. Mwenechanya and B. Papadopoulou, *PLoS Neglected Trop. Dis.*, 2017, **11**, e0006052.

23 J. Hoefle-Bénard and S. Salloch, *BMJ Glob. Health*, 2024, **9**, e013439.

24 P. J. Rosenthal, V. Asua, J. A. Bailey, M. D. Conrad, D. S. Ishengoma, M. R. Kamya, C. Rasmussen, F. G. Tadesse, A. Uwimana and D. A. Fidock, *Lancet Infect. Dis.*, 2024, **9**, e591–e600.

25 R. J. Melander, A. K. Basak and C. Melander, *Nat. Prod. Rep.*, 2020, **37**, 1454–1477.

26 A. Uberoi, A. McCready-Vangi and E. A. Grice, *Nat. Rer. Microbiol.*, 2024, **8**, 507–521.

27 C. S. Thornton, M. Mellett, J. Jarand, L. Barss, S. K. Field and D. A. Fisher, *Eur. Respir. rev.*, 2021, **30**, 200299.

28 P. Chakraborty, S. Bajeli, D. Kaushal, B. D. Radotra and A. Kumar, *Nat. Commun.*, 2021, **12**, 1606.

29 M. Usui, Y. Yoshii, S. Thiriet-Rupert, J.-M. Ghigo and C. Beloin, *Commun. Biol.*, 2023, **6**, 275.

30 K. Abel, E. Agnew, J. Amos, N. Armstrong, D. Armstrong-James, T. Ashfield, S. Aston, J. K. Baillie, S. Baldwin, G. Barlow, V. Bartle, J. Bielicki, C. Brown, E. Carrol, M. Clements, G. Cooke and A. Dane, *Lancet Microbe*, 2024, **5**, e500–e507.

31 U. Theuretzbacher, K. Outterson, A. Engel and A. Karlén, *Nat. Rev. Microbiol.*, 2020, **18**, 275–285.

32 U. Theuretzbacher, K. Bush, S. Harbarth, M. Paul, J. H. Rex, E. Tacconelli and G. E. Thwaites, *Nat. Rev. Microbiol.*, 2020, **18**, 286–298.

33 U. Theuretzbacher, E. Baraldi, F. Ciabuschi and S. Callegari, *Clin. Microbiol. Infect.*, 2023, **29**, 610–615.

34 D. J. Newman and G. M. Cragg, *J. Nat. Prod.*, 2020, **83**, 770–803.

1890 | *Nat. Prod. Rep.*, 2024, **41**, 1858–1894

This journal is © The Royal Society of Chemistry 2024

35 J. Sucher, A. Thai, C. Tran, N. Mantena, A. Noronha and E. B. Chahine, *Am. J. Health-Syst. Pharm.*, 2022, **79**, 2208–2221.

36 T. P. McCarty, C. M. White and P. G. Pappas, *Infect. Dis. Clin. North Am.*, 2021, **35**, 389–413.

37 S. Krishna, L. Bustamante, R. K. Haynes and H. M. Staines, *Trends Pharmacol. Sci.*, 2008, **29**, 520–527.

38 J. Zi, S. Mafu and R. J. Peters, *Annu. Rev. Plant Biol.*, 2014, **65**, 259–286.

39 J. S. Dickschat, *Angew. Chem., Int. Ed.*, 2019, **58**, 15964–15976.

40 L. Zhao, W. Chang, Y. Xiao, H. Liu and P. Liu, *Annu. Rev. Biochem.*, 2013, **82**, 497–530.

41 M. Sapir-Mir, A. Mett, E. Belausov, S. Tal-Meshulam, A. Frydman, D. Gidoni and Y. Eyal, *Plant Physiol.*, 2008, **148**, 1219–1228.

42 R. C. Misra, A. Garg, S. Roy, C. S. Chanotiya, P. G. Vasudev and S. Ghosh, *Plant Sci.*, 2015, **240**, 50–64.

43 M. J. Smanski, R. M. Peterson and B. Shen, in *Methods in Enzymology*, ed. D. A. Hopwood, Academic Press, 2012, vol. 515, pp. 163–186.

44 S. Kugler, P. Ossowicz, K. Malarczyk-Matusiak and E. Wierzbicka, *Molecules*, 2019, **24**, 1651.

45 A. San Feliciano, M. Gordaliza, M. Salinero and J. del Corral, *Planta Med.*, 1993, **59**, 485–490.

46 Mordor Intelligence, Tall Oil Rosin Market Size & Share Analysis – Growth Trends & Forecasts (2024–2029), Source: **https://www.mordorintelligence.com/industry-reports/tall-oil-rosin-market**, (Acessed on July 22nd, 2024).

47 N. B. Cech and N. H. Oberlies, *Nat. Prod. Rep.*, 2023, **40**, 1153–1157.

48 A. M. Erlendsson, U. H. Olesen, M. Haedersdal and A. M. Rossi, *Adv. Drug Delivery Rev.*, 2020, **153**, 185–194.

49 S. Paukner and R. Riedl, *Cold Spring Harbor Perspect. Med.*, 2017, 7, a027110.

50 A. Kameyama, A. Saito, A. Haruyama, T. Komada, S. Sugiyama, T. Takahashi and T. Muramatsu, *Materials*, 2020, **13**, 1700.

51 A. Sipponen, O. Kuokkanen, R. Tiihonen, H. Kauppinen and J. J. Jokinen, *Int. J. Dermatol.*, 2012, **51**, 726–732.

52 Y. R. Lee and K. L. Jacobs, *Drugs*, 2019, **79**, 1867–1876.

53 A. San Feliciano, M. Gordaliza, M. Salinero and J. del Corral, *Planta Med.*, 1993, **59**, 485–490.

54 A. Fonseca, F. Estrela, T. Moraes, L. Carneiro, J. Bastos, R. Santos, S. Ambrósio, C. Martins and R. Veneziani, *Molecules*, 2013, **18**, 7865–7872.

55 A. Bisio, A. M. Schito, F. Pedrelli, O. Danton, J. K. Reinhardt, G. Poli, T. Tuccinardi, T. Bürgi, F. De Riccardis, M. Giacomini, D. Calzia, I. Panfoli, G. C. Schito, M. Hamburger and N. De Tommasi, *J. Nat. Prod.*, 2020, **83**, 1027–1042.

56 V. Iobbi, P. Brun, G. Bernabé, R. A. Dougué Kentsop, G. Donadio, B. Ruffoni, P. Fossa, A. Bisio and N. De Tommasi, *Molecules*, 2021, **26**, 6681.

57 C. Kim, J.-G. Kim and K.-Y. Kim, *J. Fungi*, 2023, **9**, 98.

58 J. Echeverría, A. Urzúa, L. Sanhueza and M. Wilkens, *Molecules*, 2017, **22**, 1039.

59 M. G. M. de Souza, L. F. Leandro, T. da S. Moraes, F. Abrão, R. C. S. Veneziani, S. R. Ambrosio and C. H. G. Martins, *Anaerobe*, 2018, **52**, 43–49.

60 M. Nakamura, E. Endo, J. P. de Sousa, D. Callejon, T. Ueda-Nakamura, B. Dias Filho, O. de Freitas, C. Nakamura and N. Lopes, *J. Braz. Chem. Soc.*, 2017, **28**, 08.

61 A. L. Pfeifer Barbosa, A. Wenzel-Storjohann, J. D. Barbosa, C. Zidorn, C. Peifer, D. Tasdemir and S. S. Çiçek, *J. Ethnopharmacol.*, 2019, **233**, 94–100.

62 Y. Qiao, Y. Liu, X. Duan, C. Chen, J. Liu, H. Zhu, Y. Xue and Y. Zhang, *Tetrahedron*, 2018, **74**, 3852–3857.

63 I. P. Sousa, M. V. De Sousa Teixeira, J. A. Freitas, A. G. Ferreira, L. M. Pires, R. A. Santos, V. C. G. Heleno and N. A. J. C. Furtado, *Chem. Biodiversity*, 2022, **19**, e202100757.

64 P. Chawengrum, J. Boonsombat, P. Kittakoop, C. Mahidol, S. Ruchirawat and S. Thongnest, *Phytochem. Lett.*, 2018, **24**, 140–144.

65 M. K. Langat, A. Helfenstein, C. Horner, P. Tammela, H. Hokkanen, D. Izotov and D. A. Mulholland, *Chem. Biodiversity*, 2018, **15**, e1800056.

66 J. Yu, Z. Yu, D. Wu, X. Yan, Y. Wang and H. Zhang, *Chem. Biodiversity*, 2019, **16**, e1900317.

67 Y. Sivasothy, H. Ibrahim, A. S. Paliany, S. A. Alias and K. Awang, *Bioorg. Med. Chem. Lett.*, 2013, **23**, 6280–6285.

68 I. M. Hulley, S. F. van Vuuren, N. J. Sadgrove and B.-E. van Wyk, *J. Ethnopharmacol.*, 2019, **228**, 92–98.

69 N. Corlay, M. Lecsö-Bornet, E. Leborgne, F. Blanchard, X. Cachet, J. Bignon, F. Roussi, M.-J. Butel, K. Awang and M. Litaudon, *J. Nat. Prod.*, 2015, **78**, 1348–1356.

70 L.-H. Meng, X.-M. Li, F.-Z. Zhang, Y.-N. Wang and B.-G. Wang, *J. Nat. Prod.*, 2020, **83**, 2528–2536.

71 R. R. Kulkarni, K. Shurpali, V. G. Puranik, D. Sarkar and S. P. Joshi, *J. Nat. Prod.*, 2013, **76**, 1836–1841.

72 S. Ghosh, K. Indukuri, S. Bondalapati, A. K. Saikia and L. Rangan, *Eur. J. Med. Chem.*, 2013, **66**, 101–105.

73 D. Daniel-Jambun, J. Dwiyanto, Y. Y. Lim, J. B. L. Tan, A. Muhamad, S. W. Yap and S. M. Lee, *J. Appl. Microbiol.*, 2017, **123**, 810–818.

74 M. Farimani, A. Taleghani, A. Aliabadi, A. Aliahmadi, M. Esmaeili, N. Namazi Sarvestani, H. Khavasi, M. Smieško, M. Hamburger and S. Nejad Ebrahimi, *Planta Med.*, 2016, **82**, 1279–1285.

75 M. Afolayan, R. Srivedavyasasri, O. T. Asekun, O. B. Familoni, A. Orishadipe, F. Zulfiqar, M. A. Ibrahim and S. A. Ross, *Med. Chem. Res.*, 2018, **27**, 2325–2330.

76 K. Mahadeo, G. Herbette, I. Grondin, O. Jansen, H. Kodja, J. Soulange, S. Jhaumeer-Laulloo, P. Clerc, A. Gauvin-Bialecki and M. Frederich, *J. Nat. Prod.*, 2019, **82**, 1361–1366.

77 Y. P. Tan, S. D. Houston, N. Modhiran, A. I. Savchenko, G. M. Boyle, P. R. Young, D. Watterson and C. M. Williams, *Chem.–Eur. J.*, 2019, **25**, 5664–5667.

78 Y. P. Tan, Y. Xue, A. I. Savchenko, S. D. Houston, N. Modhiran, C. L. D. McMillan, G. M. Boyle, P. V. Bernhardt, P. R. Young, D. Watterson and C. M. Williams, *J. Nat. Prod.*, 2019, **82**, 2828–2834.

This journal is © The Royal Society of Chemistry 2024

*Nat. Prod. Rep.*, 2024, **41**, 1858–1894 | **1891**

79 K.-L. Xiang, R.-X. Liu, L. Zhao, Z.-P. Xie, S.-M. Zhang and S.-J. Dai, *Phytochemistry*, 2020, **173**, 112298.

80 L. Zhao, K.-L. Xiang, R.-X. Liu, Z.-P. Xie, S.-M. Zhang and S.-J. Dai, *Bioorg. Chem.*, 2020, **96**, 103651.

81 F. Abrão, J. A. Alves, G. Andrade, P. F. de Oliveira, S. R. Ambrósio, R. C. S. Veneziani, D. C. Tavares, J. K. Bastos and C. H. G. Martins, *Front. Microbiol.*, 2018, **9**, 201.

82 M. B. Santiago, V. C. O. dos Santos, S. C. Teixeira, N. B. S. Silva, P. F. de Oliveira, S. D. Ozelin, R. A. Furtado, D. C. Tavares, S. R. Ambrósio, R. C. S. Veneziani, E. A. V. Ferro, J. K. Bastos and C. H. G. Martins, *Pharmaceuticals*, 2023, **16**, 1357.

83 S. C. Teixeira, A. M. Rosini, G. de Souza, A. F. Martínez, R. J. Silva, S. R. Ambrósio, R. C. Veneziani, J. K. Bastos, C. H. Martins, B. F. Barbosa and E. A. Ferro, *Exp. Parasitol.*, 2023, **250**, 108534.

84 I. Pontes de Sousa, A. G. Ferreira, A. E. Miller Crotti, R. Alves dos Santos, J. Kiermaier, B. Kraus, J. Heilmann and N. A. Jacometti Cardoso Furtado, *Bioorg. Chem.*, 2020, **95**, 103560.

85 C. S. Mizuno, A. B. Souza, B. L. Tekwani, S. R. Ambrósio and R. C. S. Veneziani, *Bioorg. Med. Chem. Lett.*, 2015, **25**, 5529–5531.

86 S. Songsri and N. Nuntawong, *Molecules*, 2016, **21**, 749.

87 N. Intakhan, W. Chanmol, P. Somboon, M. D. Bates, V. Yardley, P. A. Bates and N. Jariyapan, *Pathogens*, 2020, **9**, 49.

88 M. Banerjee, D. Parai, P. Dhar, M. Roy, R. Barik, S. Chattopadhyay and S. K. Mukherjee, *Acta Trop.*, 2017, **176**, 58–67.

89 P. Wintachai, P. Kaur, R. C. H. Lee, S. Ramphan, A. Kuadkitkan, N. Wikan, S. Ubol, S. Roytrakul, J. J. H. Chu and D. R. Smith, *Sci. Rep.*, 2015, **5**, 14179.

90 J. Lee, C. Tseng, K. Young, H. Sun, S. Wang, W. Chen, C. Lin and Y. Wu, *Br. J. Pharmacol.*, 2014, **171**, 237–252.

91 P. Panraksa, S. Ramphan, S. Khongwichit and D. R. Smith, *Antiviral Res.*, 2017, **139**, 69–78.

92 E. F. Martínez-Pérez, E. Burgueño-Tapia, S. Roa-Flores, A. E. Bendaña-Piñeiro, E. Sánchez-Arreola, H. Bach and L. R. Hernández, *Nat. Prod. Res.*, 2022, **36**, 71–78.

93 A. Paemanee, A. Hitakarun, P. Wintachai, S. Roytrakul and D. R. Smith, *Biomed. Pharmacother.*, 2019, **109**, 322–332.

94 K. Du, M. De Mieri, M. Neuburger, P. C. Zietsman, A. Marston, S. F. van Vuuren, D. Ferreira, M. Hamburger and J. H. van der Westhuizen, *J. Nat. Prod.*, 2015, **78**, 2494–2504.

95 N. Tiwari, J. Thakur, D. Saikia and M. M. Gupta, *Phytomedicine*, 2013, **20**, 605–610.

96 W. Li, L. Zhao, L.-T. Sun, Z.-P. Xie, S.-M. Zhang, X.-D. Yue and S.-J. Dai, *RSC Adv.*, 2021, **11**, 29684–29689.

97 H. Ikeda, K. Shin-ya, T. Nagamitsu and H. Tomoda, *J. Ind. Microbiol. Biotechnol.*, 2016, **43**, 325–342.

98 A. Endale, D. Bisrat, A. Animut, F. Bucar and K. Asres, *Phytother. Res.*, 2013, **27**, 1805–1809.

99 M. Argentin, F. Cruz, A. Souza, E. D'Aurea, J. Bastos, S. Ambrósio, R. Veneziani, I. Camargo and C. Mizuno, *Antibiotics*, 2023, **12**, 1202.

100 P. Matos, B. Mahoney, Y. Chan, D. Day, M. Cabral, C. Martins, R. Santos, J. Bastos, P. Page and V. Heleno, *Molecules*, 2015, **20**, 18264–18278.

101 A. K. Maurya, N. Baliyan, R. Kumar and V. K. Agnihotri, *J. Nat. Prod.*, 2022, **85**, 1691–1696.

102 Q. T. N. Tran, R. C. H. Lee, H. J. Liu, D. Ran, V. Z. L. Low, D. Q. To, J. J. H. Chu and C. L. L. Chai, *Eur. J. Med. Chem.*, 2022, **230**, 114110.

103 M. G. de Lima Silva, L. Y. S. da Silva, T. S. de Freitas, J. E. Rocha, R. L. S. Pereira, S. R. Tintino, M. R. C. de Oliveira, A. O. B. P. Bezerra Martins, M. C. P. Lima, G. C. Alverni da Hora, C. L. G. Ramalho, H. D. M. Coutinho and I. R. A. de Menezes, *Process Biochem.*, 2022, **122**, 363–372.

104 A. Helfenstein, M. Vahermo, D. A. Nawrot, F. Demirci, G. İşcan, S. Krogerus, J. Yli-Kauhaluoma, V. M. Moreira and P. Tammela, *Bioorg. Med. Chem.*, 2017, **25**, 132–137.

105 Y. Ito, T. Ito, K. Yamashiro, F. Mineshiba, K. Hirai, K. Omori, T. Yamamoto and S. Takashiba, *Odontology*, 2020, **108**, 57–65.

106 W. Hou, G. Zhang, Z. Luo, D. Li, H. Ruan, B. H. Ruan, L. Su and H. Xu, *Bioorg. Med. Chem. Lett.*, 2017, **27**, 5382–5386.

107 A. Fallarero, M. Skogman, J. Kujala, M. Rajaratnam, V. Moreira, J. Yli-Kauhaluoma and P. Vuorela, *Int. J. Mol. Sci.*, 2013, **14**, 12054–12072.

108 S. Manner, M. Vahermo, M. E. Skogman, S. Krogerus, P. M. Vuorela, J. Yli-Kauhaluoma, A. Fallarero and V. M. Moreira, *Eur. J. Med. Chem.*, 2015, **102**, 68–79.

109 I. Neto, E. M. Domínguez-Martín, E. Ntungwe, C. P. Reis, M. Pesic, C. Faustino and P. Rijo, *Pharmaceutics*, 2021, **13**, 825.

110 W.-M. Zhang, T. Yang, X.-Y. Pan, X.-L. Liu, H.-X. Lin, Z.-B. Gao, C.-G. Yang and Y.-M. Cui, *Eur. J. Med. Chem.*, 2017, **127**, 917–927.

111 M.-L. Liu, X.-Y. Pan, T. Yang, W.-M. Zhang, T.-Q. Wang, H.-Y. Wang, H.-X. Lin, C.-G. Yang and Y.-M. Cui, *Bioorg. Med. Chem. Lett.*, 2016, **26**, 5492–5496.

112 E. Buommino, A. Vollaro, F. P. Nocera, F. Lembo, M. DellaGreca, L. De Martino and M. R. Catania, *Antibiotics*, 2021, **10**, 80.

113 B. Sadowska, Ł. Kuźma, B. Micota, A. Budzyńska, H. Wysokińska, A. Kłys, M. Więckowska-Szakiel and B. Różalska, *Microb. Pathog.*, 2016, **98**, 132–139.

114 Ł. Kuźma, M. Kaiser and H. Wysokińska, *Prep. Biochem. Biotechnol.*, 2017, **47**, 58–66.

115 J. Búfalo, C. Cantrell, M. Jacob, K. Schrader, B. Tekwani, T. Kustova, A. Ali and C. Boaro, *Planta Med.*, 2015, **82**, 131–137.

116 R. Mothana, M. Al-Said, N. Al-Musayeib, A. Gamal, S. Al-Massarani, A. Al-Rehaily, M. Abdulkader and L. Maes, *Int. J. Mol. Sci.*, 2014, **15**, 8360–8371.

117 C. B. Naman, A. D. Gromovsky, C. M. Vela, J. N. Fletcher, G. Gupta, S. Varikuti, X. Zhu, E. M. Zywot, H. Chai,

**1892** | *Nat. Prod. Rep.*, 2024, **41**, 1858–1894

This journal is © The Royal Society of Chemistry 2024

K. A. Werbovetz, A. R. Satoskar and A. D. Kinghorn, *J. Nat. Prod.*, 2016, **79**, 598–606.

118 K. O. Ndjoubi, R. Sharma, J. A. Badmus, A. Jacobs, A. Jordaan, J. Marnewick, D. F. Warner and A. A. Hussein, *Plants*, 2021, **10**, 175.

119 R. Nzogong, B. Nganou, A. Tedonkeu, M. Awouafack, M. Tene, T. Ito, P. Tane and H. Morita, *Planta Med.*, 2018, **84**, 59–64.

120 J. Boonsombat, C. Mahidol, P. Chawengrum, N. Reuk-Ngam, N. Chimnoi, S. Techasakul, S. Ruchirawat and S. Thongnest, *Phytochemistry*, 2017, **143**, 36–44.

121 P. Rijo, A. Duarte, A. P. Francisco, T. Semedo-Lemsaddek and M. F. Simões, *Phytother. Res.*, 2014, **28**, 76–81.

122 J.-J. Cui, W.-J. Li, C.-L. Wang, Y.-Q. Huang, W. Lin, B. Zhou and J.-M. Yue, *Phytochemistry*, 2022, **201**, 113278.

123 S. Zare, G. Hatam, O. Firuzi, A. Bagheri, J. N. Chandran, B. Schneider, C. Paetz, S. Pirhadi and A. R. Jassbi, *J. Mol. Struct.*, 2021, **1228**, 129447.

124 M. Tabefam, M. Farimani, O. Danton, J. Ramseyer, M. Kaiser, S. Ebrahimi, P. Salehi, H. Batooli, O. Potterat and M. Hamburger, *Planta Med.*, 2018, **84**, 913–919.

125 M. A. González, J. Clark, M. Connelly and F. Rivas, *Bioorg. Med. Chem. Lett.*, 2014, **24**, 5234–5237.

126 S. Ebrahimi, S. Zimmermann, J. Zaugg, M. Smiesko, R. Brun and M. Hamburger, *Planta Med.*, 2013, **79**, 150–156.

127 T. A. Mokoka, X. K. Peter, G. Fouche, N. Moodley, M. Adams, M. Hamburger, M. Kaiser, R. Brun, V. Maharaj and N. Koorbanally, *S. Afr. J. Bot.*, 2014, **90**, 93–95.

128 M. M. Farimani, B. Khodaei, H. Moradi, A. Aliabadi, S. N. Ebrahimi, M. De Mieri, M. Kaiser and M. Hamburger, *J. Nat. Prod.*, 2018, **81**, 1384–1390.

129 J. Obegi Matundura, J. O. Midiwo, A. Yenesew, L. K. Omosa, M. Kumarihamy, J. Zhao, M. Wang, S. Tripathi, S. Khan, V. M. Masila, V.-A. Nchiozem-Ngnitedem and I. Muhammad, *Nat. Prod. Res.*, 2023, **37**, 4008–4012.

130 C. Bustos-Brito, P. Joseph-Nathan, E. Burgueño-Tapia, D. Martínez-Otero, A. Nieto-Camacho, F. Calzada, L. Yépez-Mulia, B. Esquivel and L. Quijano, *J. Nat. Prod.*, 2019, **82**, 1207–1216.

131 W. Wang and L.-B. Dong, *J. Asian Nat. Prod. Res.*, 2023, **25**, 68–74.

132 D.-W. Li, X.-P. Deng, X. He, X.-Y. Han, Y.-F. Ma, H.-L. Huang, Z.-L. Yu, L. Feng, C. Wang and X.-C. Ma, *Phytochemistry*, 2021, **183**, 112593.

133 C.-J. Wang, Q.-L. Yan, Y.-F. Ma, C.-P. Sun, C.-M. Chen, X.-G. Tian, X.-Y. Han, C. Wang, S. Deng and X.-C. Ma, *J. Nat. Prod.*, 2017, **80**, 1248–1254.

134 H. Li, P. Yang, E.-H. Zhang, L.-M. Kong and C.-Y. Meng, *J. Asian Nat. Prod. Res.*, 2021, **23**, 652–659.

135 M.-M. Xu, J. Zhou, L. Zeng, J. Xu, M. M. Onakpa, J.-A. Duan, C.-T. Che, H. Bi and M. Zhao, *Org. Chem. Front.*, 2021, **8**, 3014–3022.

136 X. Wang, K. Sun and B. Wang, *Chem. Biodiversity*, 2018, **15**, 7.

137 H.-B. Yu, X.-L. Wang, W.-H. Xu, Y.-X. Zhang, Y.-S. Qian, J.-P. Zhang, X.-L. Lu and X.-Y. Liu, *Mar. Drugs*, 2018, **16**, 284.

138 S.-H. Wu, J. He, X.-N. Li, R. Huang, F. Song, Y.-W. Chen and C.-P. Miao, *Phytochemistry*, 2014, **105**, 197–204.

139 M. Nogueira, F. Da Costa, R. Brun, M. Kaiser and T. Schmidt, *Molecules*, 2016, **21**, 1237.

140 T. S. Porto, M. R. Simão, L. Z. Carlos, C. H. G. Martins, N. A. J. C. Furtado, S. Said, N. S. Arakawa, R. A. dos Santos, R. C. S. Veneziani and S. R. Ambrósio, *Phytother. Res.*, 2013, **27**, 1502–1507.

141 Q. Favre-Godal, S. Dorsaz, E. F. Queiroz, L. Marcourt, S. N. Ebrahimi, P.-M. Allard, F. Voinesco, M. Hamburger, M. P. Gupta, K. Gindro, D. Sanglard and J.-L. Wolfender, *J. Nat. Prod.*, 2015, **78**, 2994–3004.

142 J. B. Nvau, S. Alenezi, M. A. Ungogo, I. A. M. Alfayez, M. J. Natto, A. I. Gray, V. A. Ferro, D. G. Watson, H. P. de Koning and J. O. Igoli, *Front. Chem.*, 2020, **8**, 574103.

143 G. Ma, H. Wu, D. Chen, N. Zhu, Y. Zhu, Z. Sun, P. Li, J. Yang, J. Yuan and X. Xu, *J. Nat. Prod.*, 2015, **78**, 2364–2371.

144 O. Erharuyi, A. Adhikari, A. Falodun, R. Imad and M. I. Choudhary, *Tetrahedron Lett.*, 2016, **57**, 2201–2206.

145 E. V. Tret'yakova, G. F. Zakirova, E. V. Salimova, O. S. Kukovinets, V. N. Odinokov and L. V. Parfenova, *Med. Chem. Res.*, 2018, **27**, 2199–2213.

146 A. B. Schons, J. S. Correa, P. Appelt, D. Meneguzzi, M. A. A. Cunha, C. Bittencourt, H. E. Toma and F. J. Anaissi, *Molecules*, 2022, **27**, 6679.

147 W.-M. Zhang, Y. Yao, T. Yang, X.-Y. Wang, Z.-Y. Zhu, W.-T. Xu, H.-X. Lin, Z.-B. Gao, H. Zhou, C.-G. Yang and Y.-M. Cui, *Bioorg. Med. Chem. Lett.*, 2018, **28**, 1943–1948.

148 X. Jin, K. Zhang, H. Chen, T. Miao, S. Wang and W. Gu, *J. Chin. Chem. Soc.*, 2018, **65**, 538–547.

149 M. Berger, A. Roller and N. Maulide, *Eur. J. Med. Chem.*, 2017, **126**, 937–943.

150 W. Gu, C. Qiao, S.-F. Wang, Y. Hao and T.-T. Miao, *Bioorg. Med. Chem. Lett.*, 2014, **24**, 328–331.

151 G. Hassan, N. Forsman, X. Wan, L. Keurulainen, L. M. Bimbo, S. Stehl, F. van Charante, M. Chrubasik, A. S. Prakash, L.-S. Johansson, D. C. Mullen, B. F. Johnston, R. Zimmermann, C. Werner, J. Yli-Kauhaluoma, T. Coenye, P. E. J. Saris, M. Österberg and V. M. Moreira, *ACS Appl. Bio Mater.*, 2020, **3**, 4095–4108.

152 M. Vahermo, S. Krogerus, A. Nasereddin, M. Kaiser, R. Brun, C. L. Jaffe, J. Yli-Kauhaluoma and V. M. Moreira, *Medchemcomm*, 2016, **7**, 457–463.

153 F. Olmo, J. J. Guardia, C. Marin, I. Messouri, M. J. Rosales, K. Urbanová, I. Chayboun, R. Chahboun, E. J. Alvarez-Manzaneda and M. Sánchez-Moreno, *Eur. J. Med. Chem.*, 2015, **89**, 683–690.

154 D. Hamulić, M. Stadler, S. Hering, J. M. Padrón, R. Bassett, F. Rivas, M. A. Loza-Mejía, M. A. Dea-Ayuela and M. A. González-Cardenete, *J. Nat. Prod.*, 2019, **82**, 823–831.

155 B. Zapata, M. Rojas, L. Betancur-Galvis, A. C. Mesa-Arango, D. Pérez-Guaita and M. A. González, *Medchemcomm*, 2013, **4**, 1239.

156 M. A. González-Cardenete, D. Hamulić, F. J. Miquel-Leal, N. González-Zapata, O. J. Jimenez-Jarava, Y. M. Brand, L. C. Restrepo-Mendez, M. Martinez-Gutierrez,

This journal is © The Royal Society of Chemistry 2024

*Nat. Prod. Rep.*, 2024, **41**, 1858–1894 | 1893

L. A. Betancur-Galvis and M. L. Marín, *J. Nat. Prod.*, 2022, **85**, 2044–2051.

157 V. C. Roa-Linares, Y. M. Brand, L. S. Agudelo-Gomez, V. Tangarife-Castaño, L. A. Betancur-Galvis, J. C. Gallego-Gomez and M. A. González, *Eur. J. Med. Chem.*, 2016, **108**, 79–88.

158 G. Hassan, N. Forsman, X. Wan, L. Keurulainen, L. M. Bimbo, L.-S. Johansson, N. Sipari, J. Yli-Kauhaluoma, R. Zimmermann, S. Stehl, C. Werner, P. E. J. Saris, M. Österberg and V. M. Moreira, *ACS Sustain. Chem. Eng.*, 2019, **7**, 5002–5009.

159 M. Pirttimaa, A. Nasereddin, D. Kopelyanskiy, M. Kaiser, J. Yli-Kauhaluoma, K.-M. Oksman-Caldentey, R. Brun, C. L. Jaffe, V. M. Moreira and S. Alakurtti, *J. Nat. Prod.*, 2016, **79**, 362–368.

160 M. A. Dea-Ayuela, P. Bilbao-Ramos, F. Bolás-Fernández and M. A. González-Cardenete, *Eur. J. Med. Chem.*, 2016, **121**, 445–450.

161 E. V. Tret'yakova, E. V. Salimova and L. V. Parfenova, *Nat. Prod. Res.*, 2022, **36**, 79–86.

162 E. V. Tretyakova, X. Ma, O. B. Kazakova, A. A. Shtro, G. D. Petukhova, A. A. Smirnova, H. Xu and S. Xiao, *Nat. Prod. Res.*, 2023, **37**, 1954–1960.

163 World Intellectual Property Organization, *WO pat.* 2016/051013A1, 2016.

164 R. C. S. Veneziani, S. R. Ambrosio and C. H. G. Martins, *J. Med. Microbiol.*, 2014, **63**, 1649–1653.

165 E. Saruul, T. Murata, E. Selenge, K. Sasaki, F. Yoshizaki and J. Batkhuu, *Bioorg. Med. Chem. Lett.*, 2015, **25**, 2555–2558.

166 N. Abdissa, M. Frese and N. Sewald, *Molecules*, 2017, **22**, 1919.

167 S. Alegre-Gómez, P. Sainz, M. Simões, P. Rijo, C. Moiteiro, A. González-Coloma and R. Martínez-Díaz, *Planta Med.*, 2016, **83**, 306–311.

168 M. F. Chabán, A. I Antoniou, C. Karagianni, D. Toumpa, M. B. Joray, J. L. Bocco, C. Sola, C. M Athanassopoulos and M. C. Carpinella, *Future Med. Chem.*, 2019, **11**, 3109–3124.

169 F. T. G. Sousa, C. Nunes, C. M. Romano, E. C. Sabino and M. A. González-Cardenete, *Rev. Inst. Med. Trop. Sao Paulo*, 2020, **7**(62), e97.

170 M. Varbanov, S. Philippot and M. A. González-Cardenete, *Viruses*, 2023, **15**, 1342.

171 D. Saxena, R. Maitra, R. Bormon, M. Czekanska, J. Meiers, A. Titz, S. Verma and S. Chopra, *npj Antimicrob. Resist.*, 2023, **1**, 17.

**1894** | *Nat. Prod. Rep.*, 2024, **41**, 1858–1894

This journal is © The Royal Society of Chemistry 2024